Summer 9-11-2017

Investigations of Electronic Cigarette Chemistry: 1. Formation Pathways for Degradation Products Using Isotopic Labeling; and 2. Gas/Particle Partitioning of Nicotine and Flavor Related Chemicals in Electronic Cigarette Fluids

Kilsun Kim
Portland State University

Investigations of Electronic Cigarette Chemistry: 1. Formation Pathways for Degradation Products Using Isotopic Labeling; and 2. Gas/Particle Partitioning of Nicotine and Flavor Related Chemicals in Electronic Cigarette Fluids

by

Kilsun Kim

A thesis submitted in partial fulfillment of the
requirements for the degree of

Master of Science
In
Chemistry

Thesis Committee:
James F. Pankow, Chair
David H. Peyton
Robert M. Strongin

Portland State University
2017

Abstract

Use of electronic cigarettes (e-cigarettes) is rapidly growing around the world. E-cigarettes are commonly used as an alternative nicotine delivery system, and have been advocated as generating lower levels of harmful chemicals compared to conventional cigarettes. Cigarette smoke-like aerosols are generated when e-cigarettes heat e-liquids. The main components of e-cigarette liquids are propylene glycol (PG) and glycerol (GL) in a varying ratio, plus nicotine and flavor chemicals. Both PG and GL are considered safe to ingest in foods and beverages, but the toxicity of these chemicals in aerosols is unknown. Current studies of e-cigarettes have mainly focused on dehydration and oxidation products of PG and GL. In this study, the other degradation products that can be generated during the vaping process are discussed. In addition, the gas/particle partitioning of chemicals in vaping aerosols is determined.

This work finds that the formation of benzene in electronic cigarettes depends on the wattage, types of coils, and devices. To simulate commerical e-cigarette liquids, mixtures containing equal parts of PG and GL by volume were made with the following added components: benzoic acid (BA), benzoic acid with nicotine (Nic), benzaldehyde (BZ), band enzaldehyde with nicotine. PG only, GL only, and PG and GL mixtures were also made for comparison. The data presented here demonstrate that more benzene is generated as the wattage of a device increases. The results also seem to support the importance of ventilation in the generation of benzene. More benzene is generated from the mixtures containing benzoic acid when using the EVOD device with a smaller vent.

However, benzaldehyde yields more benzene when using the Subtank Nano device with a larger vent. Findings also indicate that more benzene is produced from GL rather than PG.

This thesis also addresses the chemical formation pathways of degradation compounds found in the aerosols formed from isotopically labeled e-cigarette liquids. Mixtures of both ^{13}C-labeled and unlabeled PG as well as GL were made. The mixtures were vaped and gas-phase samples were collected to determine which chemicals were in the gas-phase portion of the aerosols. With the use of GC/MS methods, these isotopic labeling experiments provided evidence that the majority of the benzene, acetaldehyde, 2,3-butanedione, toluene, xylene, acrolein, and furan found in e-cigarette aerosols originates from GL in the PG plus GL mixtures. It was also shown that the majority of propanal is derived from PG: while hydroxyacetone can be formed from both PG and GL. Possible mechanisms for the formation of acetaldehyde, benzene, 2,3-butanedione, toluene, and xylene formation are proposed.

Last, this study investigated the gas/particle partitioning of nicotine and flavor-related chemicals in e-cigarette fluids. The gas/particle partitioning behavior of chemicals in e-cigarettes fluids is highly dependent on the chemical volatility. A total of 37 compounds were examined. The target compounds were divided into 3 groups based on their vapor pressures: high, medium, and low. Headspace gas samples were collected and analyzed to determine the concentration of a compound in equilibrium with the liquid phase. The gas

and liquid concentrations were used to calculate the gas/particle partitioning constant (K_p) for each compound. In an e-cigarette aerosol, volatile compounds have smaller K_p values and tend to be found in greater proportion in the gas-phase, whereas the less volatile compounds are likely to stay in the particle phase. General agreement with theory was found for compounds with known activity coefficients in PG and GL, indicating that theory can be used to predict K_p values for other compounds.

ACKNOWLEDGEMENT

I would like to first thank my advisor Professor James Pankow, at Portland State University. He guided me through the long and difficult journey of obtaining my master's degree, and watched over me with incredible patience every time I needed help.

I would also like to thank Wentai Luo, who helped me passionately in every step of the process. Without him, I could not have completed my research with the same quality as I do now.

I would also like to thank my graduate committee, Dr. David Peyton and Dr. Robert Strongin. They were always willing to give me valuable comments and opinions on my thesis, and they did not hesitate to help me when I needed it the most.

I would also like to thank Dr. David Stuart, Dr. Dean Atkinson, and Dr. Dirk Iwata-Reuyl, who were constantly providing me with the support that I needed to finish writing my thesis.

My lab mates Amy DeVita-McBride, Chris Motti, and Kevin McWhirter cheered me on through the process and helped me stay positive despite the difficult work
.
My dear friend ChunJa Ha kept my life from falling apart when I was busy from working in the lab.

My family cheered and supported me with endless love and stood by my side during my worst times. My son, Daniel Kim gave me the motivation to continue working and encouraged me when I wanted to give up. This accomplishment could not have been possible without him. Thank you.

Table of Contents

List of Tables

List of Figures

List of Schemes

1. Benzene Formation in Electronic Cigarettes

1.1. Introduction

Use of electronic cigarettes (e-cigarettes) has grown rapidly as an alternative to conventional cigarettes. E- cigarettes can be used as a tool for smoking cessation aid, and as an alternative nicotine delivery system with a possibly reduced intake of harmful chemicals (Mcrobbie et al., 2014). E-cigarettes are advertised as "healthy" alternatives to conventional cigarettes, and a large population of cigarette users have switched to e-cigarettes (Zhao et al., 2016; Farsalinos et al., 2013). According to a Centers for Disease Control and Prevention (CDC) report, e-cigarettes were the most commonly used tobacco product in 7.7% of middle school and 25.0% of high school students among an estimated 4.7 million middle and high school tobacco product users in 2015 (Singh et al., 2016). Among middle school students, the number of e-cigarette users increased from 1.4% to 5.3% during 2011-2015. During this time, the number of high school users increased from 1.5% to 16.0% (Corey et al., 2013; Singh et al 2016). This is a sharp escalation of e-cigarette use among students in grades 6 through 12. A similar trend is also seen among adult e-cigarette users based on the National Youth Tobacco Survey (NATS) in 2015 (Singh et al., 2016; NATS, 2015).

The ingredients in e-cigarettes liquids are primarily propylene glycol, glycerol, nicotine, and flavor chemical addivtives. The variety of flavors in e-cigarettes appeals to many cigarette users especially to younger people (Pepper et al., 2016; Harrell et al., 2017). It

seems possible that people believe the flavorants in e-liquids are safe because flavors like chocolate, strawberry, cotton candy, and creme are commonly used in food and many are recognized as “food-safe”. However, just because the flavors resemble those in safe edibles does not mean that flavored e-cigarette aerosols are safe to inhale when vaping. Also, e-cigarettes are not free of toxic degradation products. Sleiman et al., in a Berkeley lab, detected significant levels of 31 toxic chemicals, including benzene, in the aerosol produced by vaping e-cigarettes (Sleiman et al., 2016). Benzene is classfied as Group 1 carcinogenic chemical by the World Health Organization (WHO). Understanding what types of chemicals are produced and how these chemicals are formed in e-cigarettes is important. In this chapter, the formation of benzene and the levels of benzene generated with varying coils, devices, and wattages is discussed.

1.2. Materials and Methods

1.2.1. Electronic Cigarettes

The e-cigarette was invented by a Chinese pharmacist, Hon Lik, in 2003 (Ridley, 2015). His idea was to create an electronic "cig-a-like" nicotine delivery device, which could produce cigarette smoke-like vapor to help consumers quit smoking. Modern e-cigarettes can be divided into three groups: disposable cig-a-likes, vape pens, and personal vaporizers. The disposable cig-a-likes are mostly for newer vapers, while vape pens and vaporizers are used mostly by experienced vapers. Personal vaporizers can be used to control the levels of nicotine and flavor chemicals, and have a relatively longer battery life. Three different types of devices were used in this work: JUUL™ , KangerTech™ EVOD bottom coil clearomizer (BCC), and KangerTech™ Subtank Nano.

1.2.2. JUUL™

1.2.2.1. JUUL™ Pods and Device

The JUUL™ is an e-cigarette that is targeted at new e-cigarette users who want to try an alternative to conventional cigarettes in terms of size and weight (https://www.juulvapor.com/shop-juul-device/). The device does not provide power buttons or switches. A colored refill cartridge ("pod") is inserted into the device. This part becomes the mouthpiece. The JUUL™ device does not have customizable options

for users such as different coils (varying the resistance), control over the wattage, or various concentrations of nicotine. JUUL™ pods come in four different flavors: tobacco, mint, fruit, and crème brulee. According to the JUUL™ website, each JUUL™ pod contains 0.7 mL of fluid that is 5% nicotine by weight, and is equivalent to 1 pack of cigarettes.

1.2.2.2. Sampling Procedure

Blanks were collected before collecting the puffs through the JUUL™ cartridges disconnected from the battery portion.

The vaping procedure for the JUUL™ system was different from that of the other e-cigarette devices. The JUUL™ cartridge activates upon an inhalation draw. In order to collect gas-phase sample from JUUL pod e-liquid, a unique experimental setup was required to maintain electrical contact between components during sampling. The experimental setup is shown in Figure 1. Flow was sequentially drawn from the e-cigarette through the following elements: 1) glass fiber/cellulose acetate (GF/CA), 0.45 µm pore size, 28 mm diameter filter (Phenomenex Inc., Torrance, CA) to remove the aerosol droplets from the sample stream; 2) single ATD (adsorption and thermal desorption) gas sampling cartridge (for adsorbing benzene) containing 100 mg of 35/60 mesh Tenax TA followed by 200 mg of 60/80 mesh Carbograph 1 TD (Camsco Inc., Houston, TX); and 3) a plastic syringe with a maximum capacity of 60 mL, 2 mL

graduation, and 0.17 inch diameter nozzle, which was used to simulate human lung inhalation during vaping. The lengths of connections between the components were minimized using short pieces of flexible 0.125 inch internal diameter (i.d.) polyvinyl chloride (PVC) tubing. The trials were carried out using 4 different flavors: Tobacco, Brulee, Fruit, and Mint. Each cartridge sample was purchased online in May 2016 and provided a set of six 50 mL puffs and a total of 3 sets of 6 puffs were collected for each cartridge sample. To eliminate carryover, the PVC pieces were replaced between each sample collection.

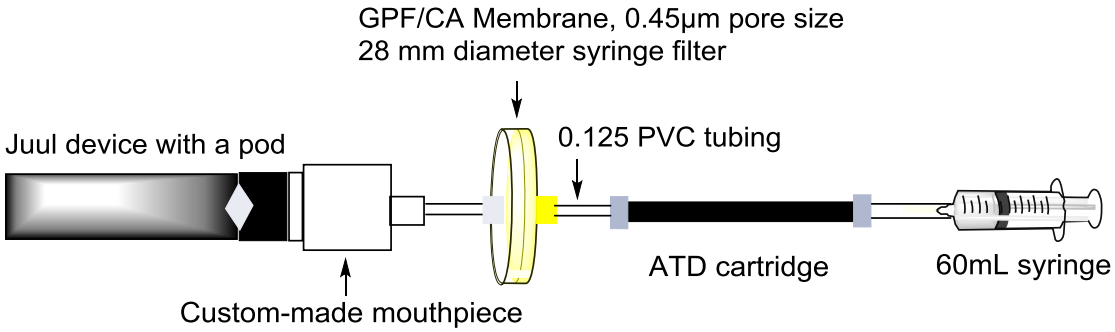

Figure 1. *Vaping Aerosol Sample Collection Apparatus for JUUL™*

1.2.2.3. Determination of Nicotine and Benzoic Acid Concentrations in JUUL™ Pods Fluids by High-Performance Liquid Chromatography with Ultraviolet Detector (HPLC/UV)

Four standard solutions of nicotine and benzoic acid in methanol ranging in concentration from 0.2 to 1 mg/mL were made. Four different flavor versions of JUUL™ pods were

opened to acquire aliquots to determine the levels of benzoic acid and nicotine in each fluid. 10 or 100 µL of e-liquid was obtained from each pod and diluted with methanol to make a 1:1000 or 1:100 mixture. The dilutions were filtered by a syringe-mounted PVDF (polyvinylidene fluoride) filter having a 13 mm diameter with 0.22 µm pore size, purchased from Thermo Fisher Scientific, Inc. (Waltham, MA). 20 µL of each dilution was analyzed with high performance liquid chromatography (HPLC) using a Waters Corp. (Milford, MA) Model 1525 binary solvent delivery module with Rheodyne 7725i injector, Discovery™ C-18 column (250 × 4.6 mm × 5µm, Supelco Inc.) and a Waters Model 2996 photodiode array detector at 40 °C. The mobile phase A composition was water with 0.1% trifluoroacetic acid, and mobile phase B was methanol. The ratio between mobile phase A and B was held 60:40 using an isocratic flow rate of mobile phase A of 0.5 mL/min, and mobile phase B of 0.4 mL/min. The wavelength of the UV absorption detector was 227.9 nm for benzoic acid, and 259 nm for nicotine. The calibration range for the benzoic acid standards was 0 to 1 mg/mL, while 0 to 0.1 mg/mL was used for nicotine. Two GC/MS injections occurred for each flavor and standard (2 trials/sample).

1.2.3. Kangertech™ EVOD and Subtank Nano Experiments

1.2.3.1. Solution Preparation

Electronic cigarette liquids (e-liquids) are mixtures of propylene glycol

(PG), Glycerol (GL), nicotine, and flavor chemicals. PG and GL mixtures of various composition are the base solvents of e-liquids used to dilute nicotine and additives to generate aerosols that resemble cigarette smoke when they are vaped.

PG, GL, benzoic acid, benzaldehyde, and nicotine were purchased from Sigma-Aldrich Inc (St. Louis, MO). The following mixtures containing equal parts PG and GL by mass were made: benzoic acid (BA), benzoic acid with nicotine (Nic), benzaldehyde (BZ), benzaldehyde with nicotine (Table 1).

Table 1. *Combinations of sample mixtures*

Mixtures	PG (g)	GL (g)	Nicotine (g)	Benzoic Acid (g)	Benzaldehyde (g)
1	10	10			
2	10	10		0.2	
3	10	10	0.24	0.2	
4	10	10			0.2
5	10	10	0.24		0.2

1.2.3.2. Electronic Cigarette Sample Collection for Analysis by Gas Chromatography Mass Spectrometry (GC/MS)

It has been estimated that an average smoker smoking a conventional cigarette completes one puff in 2.4 seconds with the range of standard deviation from 0.5 to 0.8 seconds (Hua et al., 2013; Zaho et al., 2016). In contrast, the average time taken to complete one puff of

e-cigarette has been measured to be 4.3 seconds ± 1.6 seconds (S.D) for men and 4.0 seconds ± 0.8 seconds for women (Hua et al., 2013; Zaho et al., 2016). The puff interval (time between puffs) in one group has been measured to average 52.4 seconds (Robinson et al., 2015). For these experiments, the selected puff duration was 5 seconds, the puff interval was 55 seconds, and the puff period (puff duration plus puff interval) was 60 seconds.

Three blank samples were collected using two different e-cigarette devices prior to gas each gas-phase sample collection event. Blanks were collected without applying power, and each blank sample was collected using six 50 mL "puffs" for a 300 mL sample volume. The sample collection method for the blanks was the same used when vaping. A schematic of the gas-phase sample collection apparatus is shown in Figure 2. The Kangertech EVOD Protank BCC atomizers employed a 1.8 ohm single horizontal coil, with a silica wick. The Kangertech Subtank Nano atomizer employed a 1.2 ohm single vertical coil with an organic cotton wick. A new coil was used for each vaping sampling. Prior to actual sampling, the coil was "aged" using 6 puffs at 6 watts for the EVOD and at 13 watts for the Subtank Nano device. For each sampling, the atomizer was connected to a syringe pump (Model NE-1010, New Era Pump Systems Inc., Farmingdale, NY) via a 28mm diameter (Phenomenex Inc., Torrance, CA) glass fiber/ cellulose acetate (GF/CA) (0.45 μm pore size), non-sterile luer lock syringe filter, followed by an ATD cartridge which contained 100mg of 35/60 mesh Tenax TA and 200mg of 60/80 mesh Carbograph 1 TD (Camsco Inc., Houston, TX). The GF/CA syringe filter was used to

collect the aerosol droplets. The ATD cartridge collected the target gas-phase analytes. Flexible polyvinyl chloride (PVC) tubing (0.125 inch) was used to connect between the filter and the atomizers. In order to minimize the sorptive loss of benzene to the tubing, a minimum amount of tubing was used. A 1 L Tedlar bag (Model 24633 Supelco Inc., Bellefonte, PA) was connected to a three-way "T" valve to confirm that the gas volume sampled by the syringe pump was accurate. Three or four vaping replicates were obtained for each e-liquid test mixture.

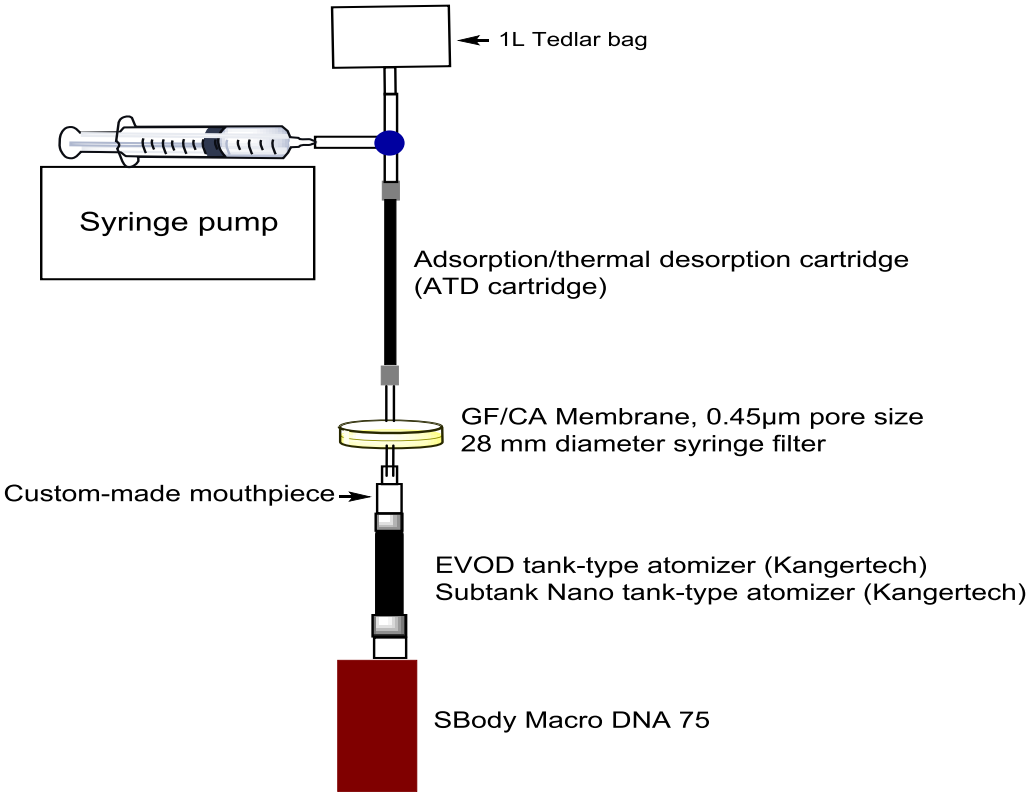

Figure 2. *Vaping collection apparatus for EVOD and Subtank Nano*

1.3. Results and Discussion

1.3.1. JUUL™

1.3.1.1. The Concentrations of Benzoic Acid and Nicotine in JUUL™ E-Liquids

The concentrations of nicotine and benzoic acid in the JUUL™ pods were found to be 59.9 ± 1.4 mg/mL and 44.2 ± 0.6 mg/mL respectively as shown in Table 2. Example HPLC-UV chromatograms are provided in Figures 3 and 4. For these levels, the molar ratio between nicotine and benzoic acid is 1:0.97. Pankow et al. (2017) estimated that among commercial refill e-liquids that contained benzoic acid, the concentration of benzoic acid in 14 out of 150 e-liquids ranged from 0.02 to 2 mg/mL (Pankow et al., 2017). JUUL™ pods contain at least 20 times more benzoic acid than other commercial e-liquids, as reported by Pankow et al. (2017).

Table 2. *Average concentrations of nicotine and benzoic acid in JUUL™ pod e-liquids.*

E-liquids Flavor	Average Concentration of Nicotine (mg/mL)	Average Concentration of Benzoic Acid (mg/mL)
"mint"	61.0	44.1
"fruit"	61.2	45.0
"brulee"	59.1	43.6
"tobacco"	58.3	44.2
Average	**59.9**	**44.2**
S.D	**1.4**	**0.6**

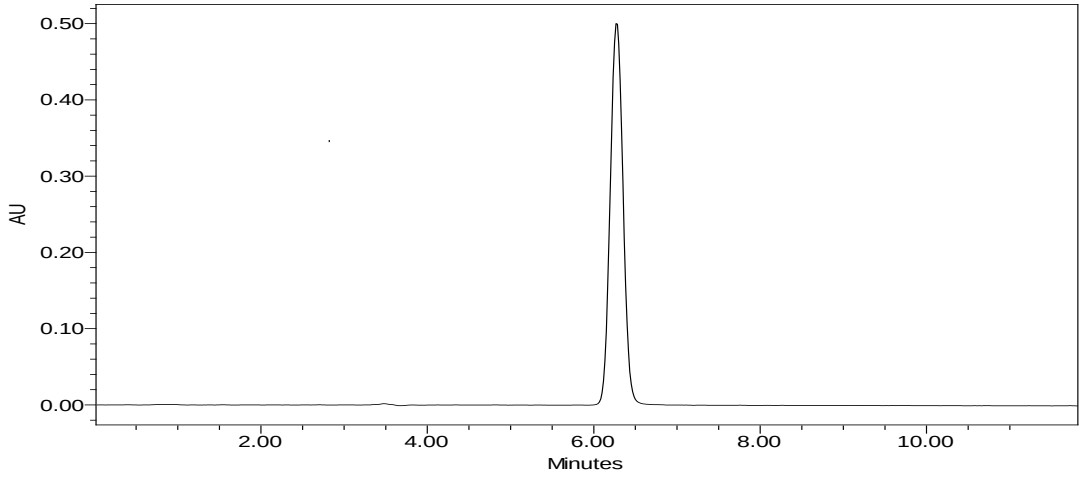

Figure 3. *HPLC-UV chromatogram for benzoic acid (227.9 nm). 20 μL of the benzoic acid standard (1mg/mL) was injected.*

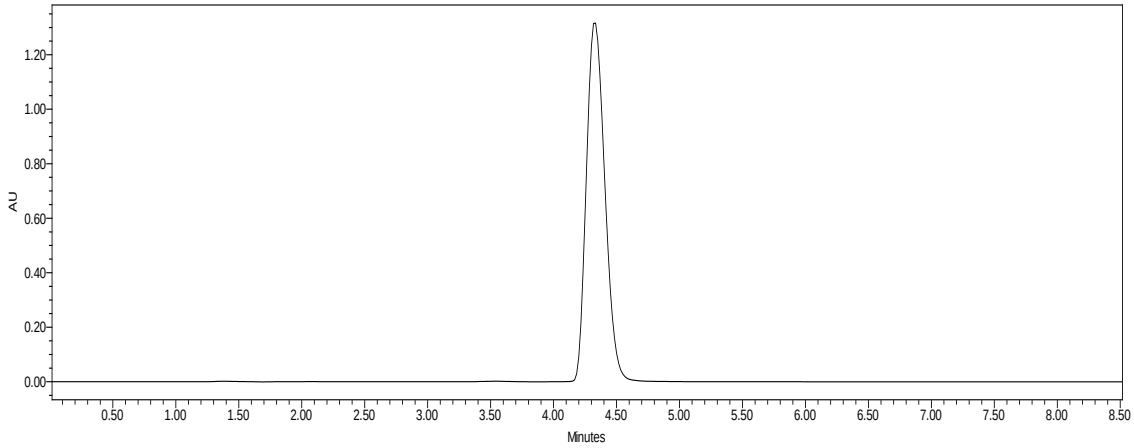

Figure 4. *HPLC-UV chromatogram for nicotine (259 nm). 20 μL of the nicotine standard (1mg/mL) was injected*

1.3.1.2. The Gas-Phase Concentration of Benzene in the Aerosols with the JUUL™ System

The concentrations of benzoic acid in the four different flavored JUUL™ pods were found to be similar to one other, averaging 44.2 ± 0.6 mg/mL. Benzene could potentially be generated by decarboxylation of benzoic acid. The concentrations of gaseous benzene found when vaping using the JUUL™ system were 1.2 ng/L for the "tobacco" flavor, 1.7 ng/L for "brulee", 4.8 ng/L for "fruit", and 3.8 ng/L for "mint" (Table 3).

Table 3. *Gaseous benzene concentrations and the log TPM values when vaping using the JUUL™ system.*

Flavor	Average Concentration (ng/L)	S.D	Average Log TPM (μg/m³)	S.D
"tobacco"	1.2	1.9	7.8	0.0
"brulee"	1.7	3.8	7.9	0.1
"fruit"	4.8	1.9	7.8	0.1
"mint"	3.8	4.3	7.9	0.1

1.3.2. Benzene Formation in Electronic Cigarettes: EVOD and Subtank Nano

1.3.2.1. The Pathways of Benzene Formation

As shown in schemes 1, 2, and 3, possible pathways for benzene formation in e-cigarettes are: 1) decarboxylation of benzoic acid, 2) oxidation of benzaldehyde to benzoic acid followed by decarboxylation, and 3) disproportionation (Cannizzaro reaction) of benzaldehyde followed by the decarboxylation of the resulting benzoic acid (Pankow et

al., 2017). Gas-phase samples were collected from Kangertech EOVD and Subtank Nano devices. Structurally, the two devices are slightly different. There is a bigger vent in the Subtank Nano, which allows more air to enter the device during vaping as compared to the EVOD device.

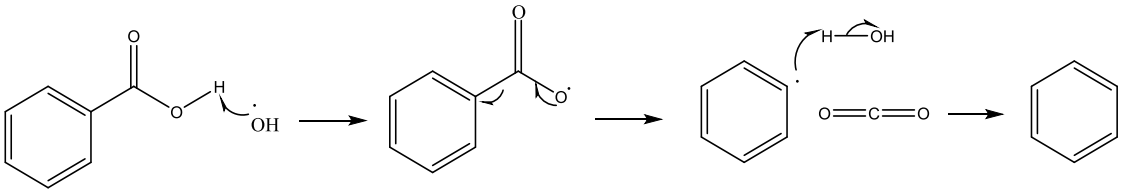

Scheme 1. *Decarboxylation of benzoic acid*

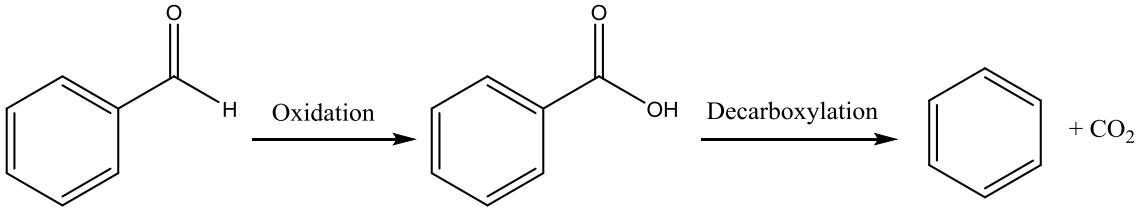

Scheme 2. *Oxidation and decarboxylation of benzaldehyde*

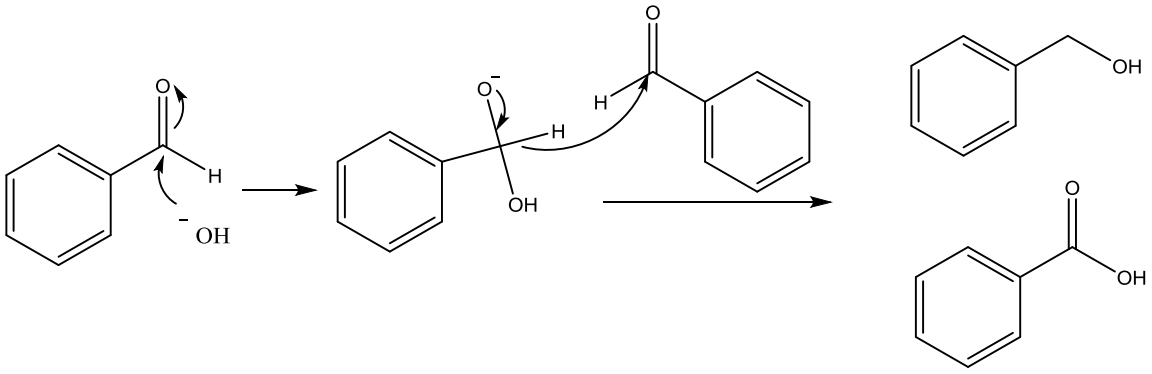

Scheme 3. *Cannizzaro reaction of benzaldehyde*

Possible mechanisms for forming benzene from PG and GL are shown in Schemes 4-7. Vinyl alcohol is a known degradation product of PG and GL (Jensen et al., 2016). Polyacetylene is generated by dehydration of polyvinyl alcohol (PVA) (Prosanov et al., 2012). There are two possible pathways to form benzene from vinyl alcohol: one is cyclotrimerization of acetylene, a dehydration product of vinyl alcohol; the other is cyclotrimerization of vinyl alcohol itself as shown in Schemes 5 and 6. Benzene can also be formed from propargyl radicals which can form from propyne (a dehydration product of PG). Propyne can decompose (with heat) to form propargyl radicals, a known precursor of benzene (Scheme 7).

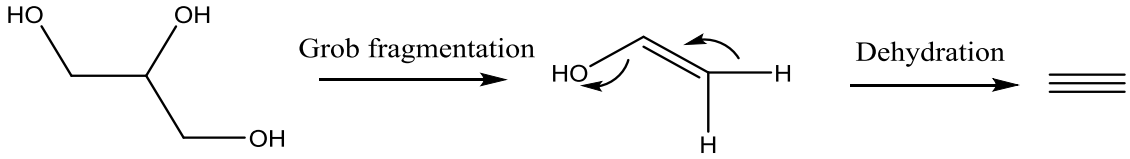

Scheme 4. *Reaction mechanism of formation of acetylene*

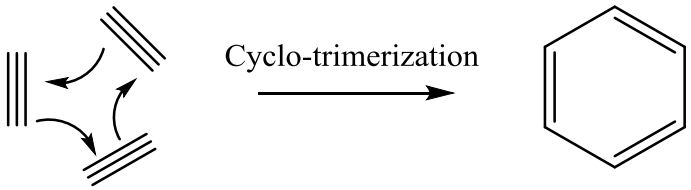

Scheme 5. *Formation of benzene from acetylene*

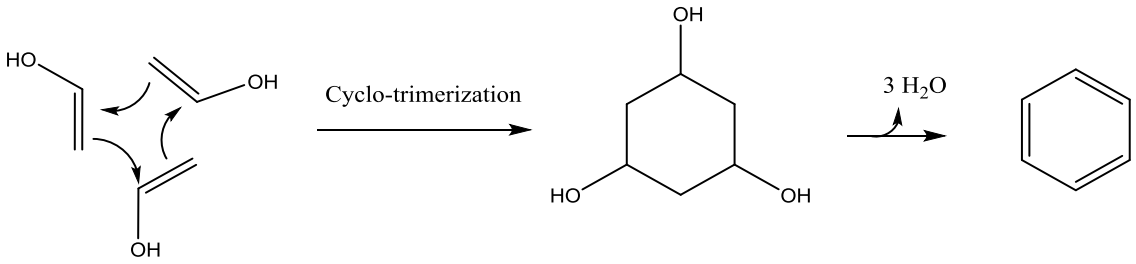

Scheme 6. *Formation of benzene from vinyl alcohol*

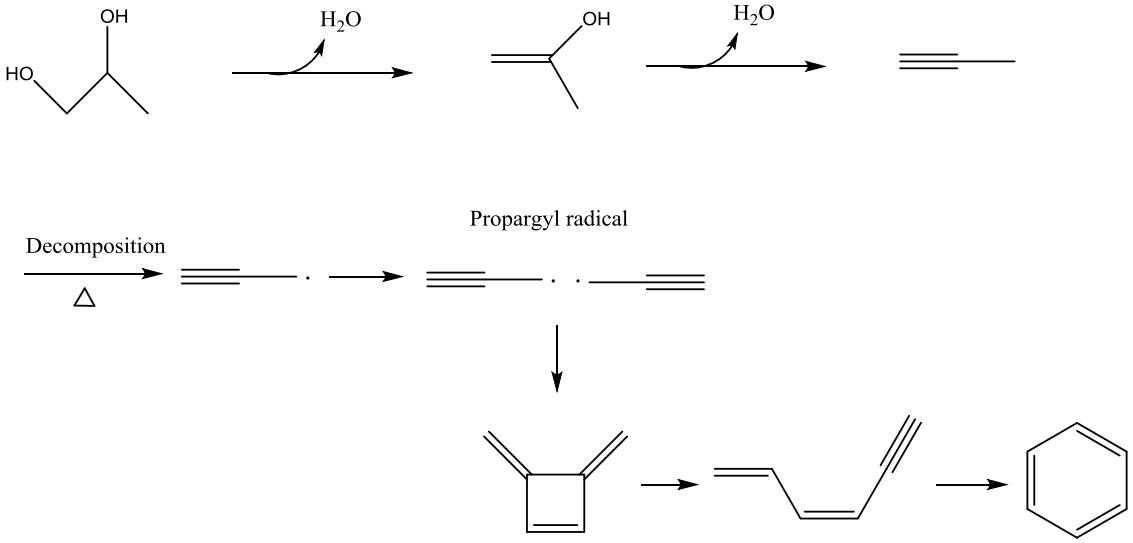

Scheme 7. *Reaction mechanism for formation of benzene from PG*

1.3.2.2. Benzene Concentrations in the Gas-Phase Samples Produced from Vaping Mixtures using the EVOD and Subtank Nano Devices

Benzene concentrations using the EVOD device at 6 watts (the manufacturer-recommended wattage) and 13 watts are compared in Figures 5 and 6. At 6 watts, benzene was detected when vaping the PG/GL/BA/Nic and PG/GL/BZ mixtures. The concentrations of benzene produced by these mixtures were 9.7±14 and 21±2.2 ng/L

respectively. At 13 watts, benzene was detected when vaping all of the mixtures tested, at concentrations that were much higher than at 6 watts. At 13 watts, the mixtures with benzoic acid generated more benzene than the mixtures with benzaldehyde (Figure 6). In the vaping samples from the Subtank Nano, no gas-phase benzene was detected at 6 watts. Even at high wattages, no benzene was detected when vaping mixtures of PG/GL and PG/GL/BA (Figure 7 and Appendix B). Only the mixtures with benzaldehyde yield benzene at 13 watts. Overall the benzene concentrations in the samples collected using the Subtank Nano device are lower than the benzene concentrations from EVOD.

At 13 watts, the concentration of benzene generated from GL alone is much higher than from PG alone; possible reasons will be discussed in the next chapter.

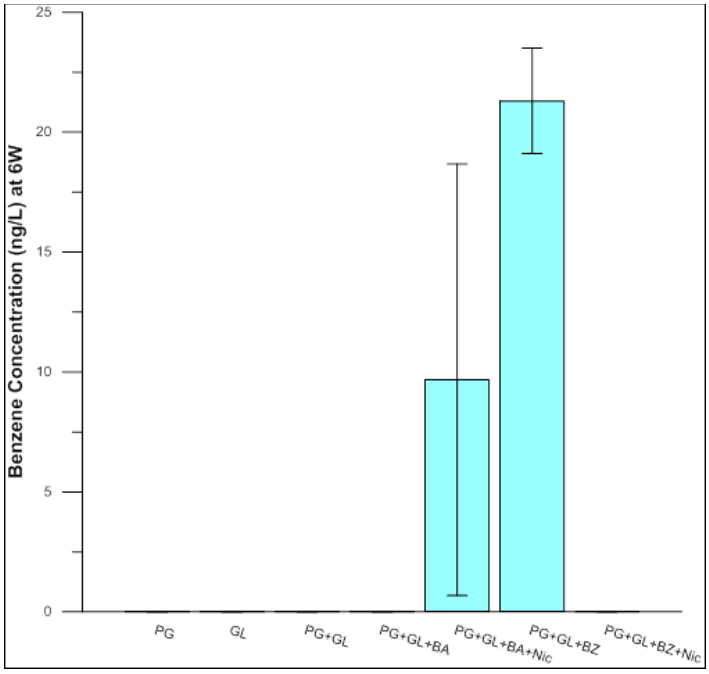

Figure 5. *Benzene concentration (ng/L) at 6 watts for EVOD*

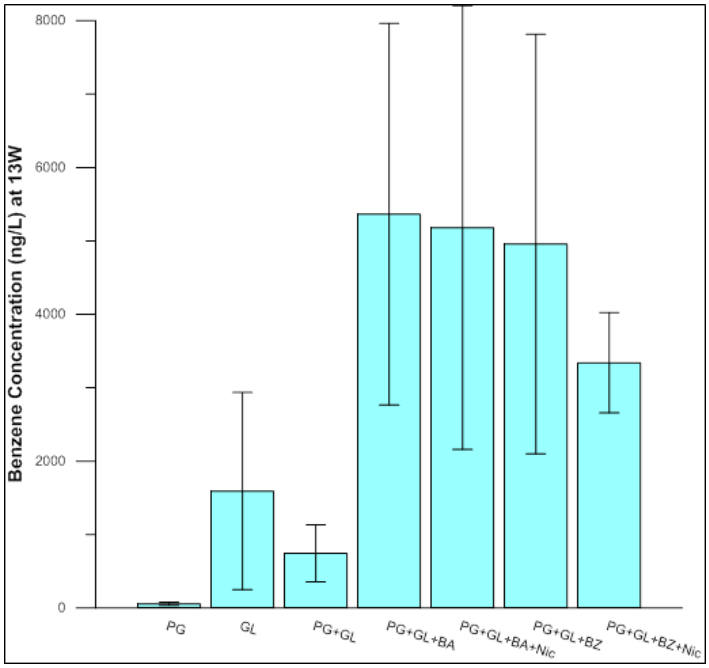

Figure 6. *Benzene concentration (ng/L) at 13 watts for EVOD*

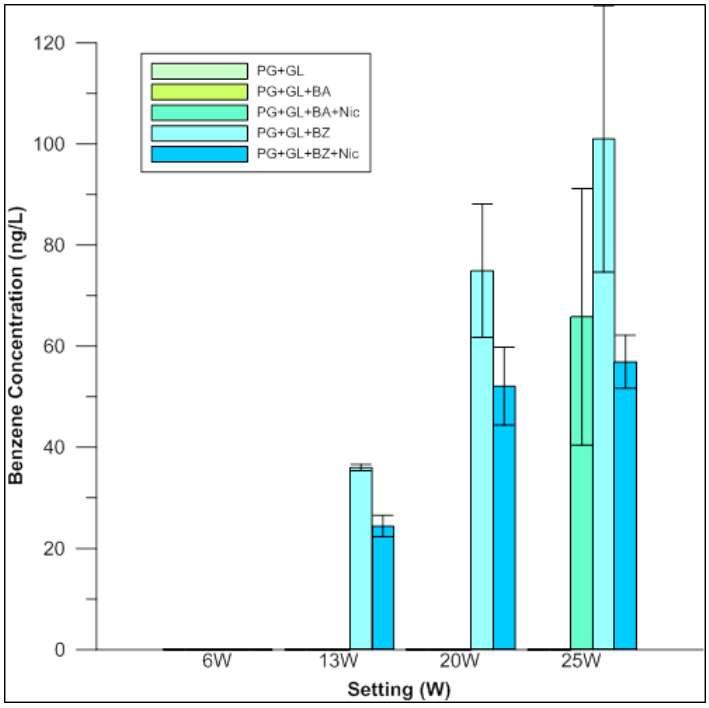

Figure 7. *Benzene concentration (ng/L) using Subtank Nano*

1.3.2.3. Benzene Mass per Gram of E-liquid Vaped

Benzene formation in the samples collected from the EVOD device were found to be much higher than in the samples collected with the Subtank Nano device. With the EVOD device, more benzene was produced at 13 watts vs. 6 watts (Figure 8). With the EVOD device, the mixtures with benzoic acid resulted in more benzene than those with benzaldehyde. With the Subtank Nano device, benzene was formed only from benzaldehyde mixtures at 13 and 20 watts (Figure 9); at 25 watts, the mixture of benzoic acid and nicotine produced benzene whereas e-liquid containing only benzoic acid did not.

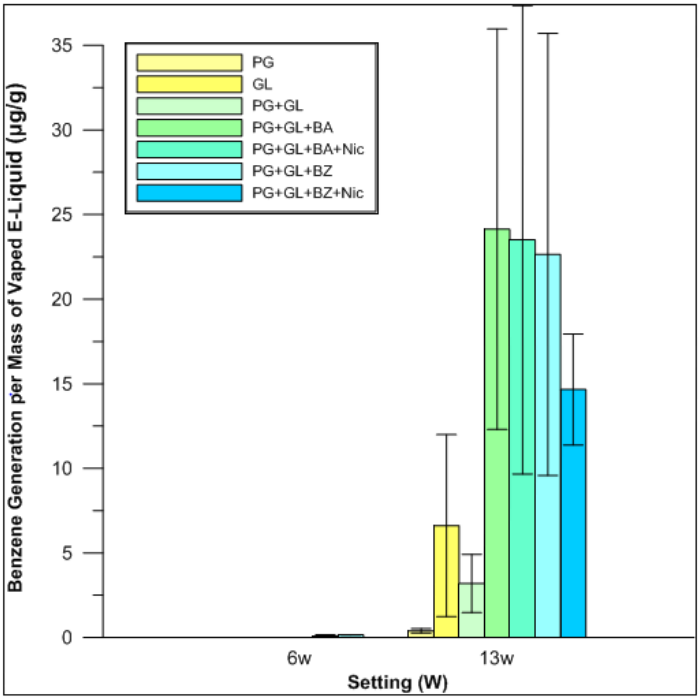

Figure 8. *Benzene generation per mass of vaped e-liquid using the EVOD device (µg/g)*

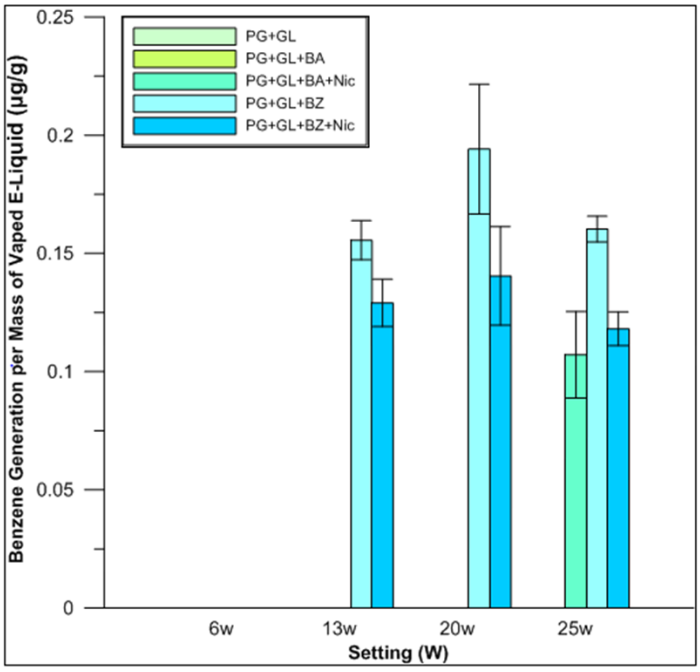

Figure 9. *Benzene generation per mass of vaped e-liquid using the Subtank Nano device (µg/g)*

1.3.2.4. The Amount of E-liquid Used Per Puff

The average amount of e-liquid used per puff by the EVOD device was approximately 6.6 mg and 11 mg for the samples taken at 6 watts and 13 watts (Appendix A). As the wattage increased from 6 to 13 watts, the amount of e-liquid used almost doubled (Figure 10). At a particular wattage, the consumption of e-liquid was nearly constant among the mixtures for EVOD, but not with the Subtank Nano device (Figure 11).

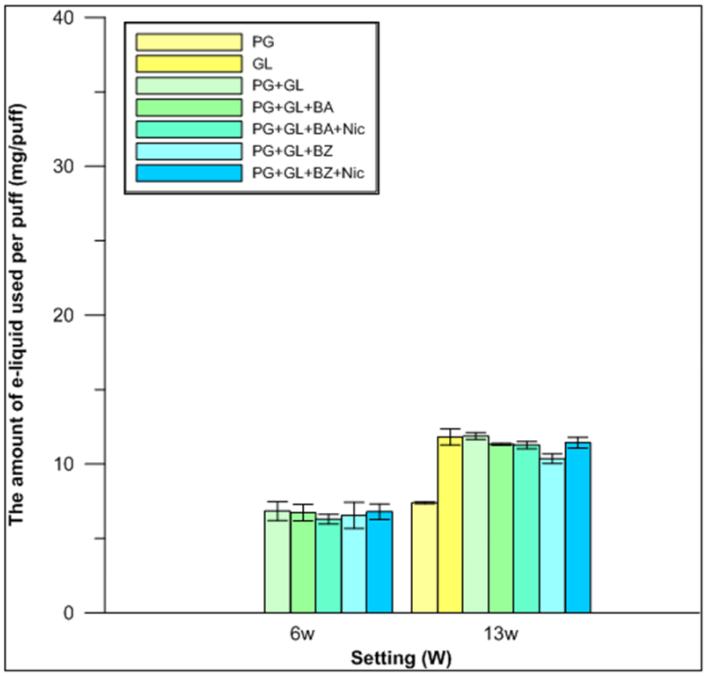

Figure 10. *The amount of e-liquid used per puff using the EVOD device (mg/puff)*

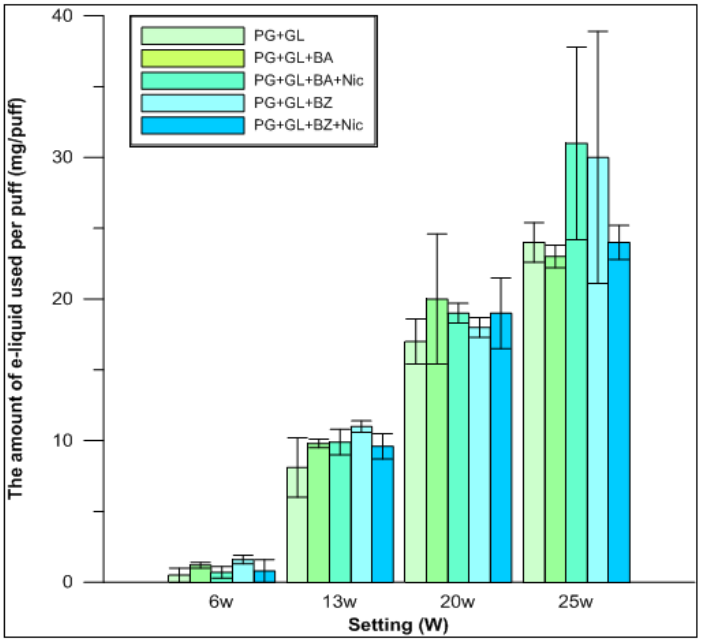

Figure 11. *The amount of e-liquid used per puff using the Subtank Nano device (mg/puff)*

1.4. Conclusions

The level of emissions of toxic chemicals (benzene) in e-cigarettes depends on the device and the power used. Regardless of device, the highest benzene emissions were found at the highest wattages. GL generates more benzene than PG. The reason for this will be addressed in the next chapter.

To prevent the inhalation of toxic chemicals (benzene), an e-cigarette device should be used at low wattages.

2. Investigation of the Chemical Pathways for Formation of Acetaldehyde, Diacetyl, Benzene, Toluene, and Xylene Using Isotopic Labeling

2.1. Introduction

Chemicals that can form in e-cigarette systems from PG or GL include 2,3-butanedione, benzene, toluene, and xylene. Understanding how these chemicals are formed during the vaping of e-cigarette liquids is important. In this chapter, chemical pathways for formation of benzene, acetaldehyde, 2,3-butanedione, toluene, and xylene are proposed. This is the first study to use carbon isotopic labeling to investigate reaction mechanisms for degradation reactions in e-cigarettes.

2.1.1. Physical Characteristics of Chemicals in Emissions of E-cigarettes

2.1.1.1. Physical Characteristics of Benzene

Benzene (a volatile, aromatic compound) is a clear, colorless, and highly flammable liquid (at room temperature) with a sweet gasoline-like odor. It is a commonly used in the synthesis of other chemicals such as drugs, pesticides, detergents, and plastics (American Cancer Society 2017; NIH 2017; Runion 1975). Benzene is classified as a group 1 carcinogen by the International Agency for Research on Cancer (IRAC). Major sources of benzene exposure are tobacco smoke, car emissions, pumping gasoline, painting, furniture wax, and other commonly used household products (Wallace1 1989; CDC, 2017). Short-term health effects of benzene exposures include headaches, vomiting,

dizziness, and confusion. Exposure to high levels of benzene can cause loss of consciousness or death. The long-term benzene exposure leads to mutation of blood cells and reduction of red blood cells (Duarte-Davidson, 2001; CDC 2017)

2.1.1.2. Physical Characteristics of Acetaldehyde

Acetaldehyde is a volatile organic compound associated with vinification and originates from yeast metabolism during fermentation of ethanol (Margalith, 1981; Orborne et al., 2000; Liu et al., 2000). Acetaldehyde is a natural the oxidation product of ethanol in humans (Lachenmeier et al., 2009). It is listed as a group 1 carcinogen by the International Agency for Research on Cancer (IARC) (U.S. Department of Health and Human Sevices, 2011). In the US, acetaldehyde is listed (along with formaldehyde, carbon tetrachloride, and benzene) as an air toxins that results in a cancer risk greater than one in a million at concentrations exceeding ambient levels (Zhou et al., 2015; National Air Toxics Assessment, 2011).

2.1.1.3. Physical Characteristics of 2,3-Butanedione

Diacetyl (or 2,3-butanedione) is a natural by-product of the fermentation of alcoholic beverages. Diacetyl is a yellowish liquid associated with a buttery aroma. Diacetyl became infamous in the 2000s when eight workers who inhaled diacetyl while working in a microwave popcorn factory developed severe bronchiolitis obliterans (an irreversible condition now known as “popcorn worker’s lung”) (Kreiss et al., 2002; Fedan et al.,

2006). The research carried out by Kreiss et al. states that there was a strong correlation between the severity of respiratory disease and the frequency of diacetyl exposure.

Diacetyl was detected in 39 of the 51 flavored e-cigarette liquids tested by Allen et al. (2016). The researchers point out that diacetyl is used not only in butter or popcorn flavored e-cigarette liquids but also in fruit, candy, and menthol-flavored e-cigarette liquids. It has been argued that when individuals vape e-cigarette liquids containing high levels of diacetyl, there is a risk of developing bronchiolitis obliterans (Kreiss et al., 2002; Fedan et al., 2006).

2.1.1.4. Physical Characteristics of Toluene and Xylene

Toluene is a clear, colorless, volatile liquid also known as methylbenzene. Toluene occurs naturally in crude oils and is used to make paint and paint thinner as well as many other commercial products. It also a commonly used organic solvent. The toxicity of toluene is much lower than that of benzene or diacetyl, but inhalation of toluene can cause liver and kidney damage and affect the central nervous system (CNS) (Luttrell and Ngendahimana 2012).

Xylene is an aromatic hydrocarbon There are three structural isomers of xylene: ortho-xylene, meta-xylene, and para-xylene. Xylene is used as a solvent in the printing, rubber, and leather industries. Xylene is also used as a cleaning agent, and paint thinner (ATSDR, 1993; Fay, 2007; Kandyala et al., 2010). The main effect of inhaling xylene

vapor is the depression of the central nervous system. The symptoms are vomiting, headache, dizziness, and nausea.

2.2. Materials and Methods

2.2.1. Solution Preparation

Fully ^{13}C-labeled PG and fully ^{13}C-labeled GL were purchased from Cambridge Isopotes Laboratory (Tewksbury, MA). Non-labeled PG and GL were purchased from Sigma-Aldrich Inc (St. Louis, MO). Investigation of the origin of benzene, diacetyl, toluene, and xylene in the mainstream aerosols of e-cigarettes was carried out by analyzing the gas-phase of e-cigarette aerosols using cartridge-based adsorption/thermal desorption (ATD) followed by gas-chromatography and mass spectrometry (GC/MS). The 50:50 (by mass) Fully ^{13}C-labeled and fully ^{13}C-labeled GL and non-labeled PG and GL mixtures were made with the quantities shown in Table 4. A total of four different mixtures were created by combining the ^{13}C-labeled and non-labeled compounds. For clarity, these 50:50 mixtures of propylene glycol and glycerol will be refered to as follows: Mixture 1 = non-labeled PG + non-labeled GL, Mixture 2 = fully ^{13}C-labeled PG + fully ^{13}C-labeled GL, Mixture 3 = fully ^{13}C-labeled PG + non-labeled GL, Mixture 4 = non-labeled PG + fully ^{13}C-labeled GL.

Table 4. *Sample combinations of ^{13}C-labeled PG and ^{13}C-labeled GL in "mix and match" experiments with non-labeled PG and GL.*

Mixture Number	$^{13}C_3$-labeled PG	$^{13}C_3$-labeled GL	Non-labeled PG	Non-labeled GL
2	0.3596 g	0.3549 g		
3	0.2537 g			0.2556 g
4		0.2456 g	0.2582 g	

2.2.2. Sample collection

All experiments in this series used the EVOD device. Prior to vaping sample collection, three sample blanks were taken with three 50 mL "puffs" each through the selected e-cigarette device, but without applying power. For vaping samples, gas-phase samples were collected in an ATD cartridge. Three replicates were collected for each sample. Each vaping sample consisted of three 50 mL puffs at 13 watts. The puff duration was 5 seconds, puff interval was 55 seconds giving a puff period of 60 seconds. The selection basis for these values involved existing studies of vaping topography. First, Hua et al. (2013) examined 64 different e-cigarette users on YouTube and reported an average puff duration for men of 4.3 seconds ± 1.6 seconds and 4.0 seconds ± 0.8 seconds for women. The average puff duration reported by Zhao et al. (2016) (4.2 seconds ± 0.7 seconds) does not differ from the values of Hua et al. A puff duration of 5 seconds was chosen for this experiment. Robinson et al. (2015) found that e-cigarette users have an average puff period of 52.4 seconds. A 60 second puff period was selected because it is similar to the value of Robinson et al. (2015) and long enough to mitigate the probability of "dry puffs".

A schematic of the gas collection equipment is shown below in Figure 12. For gas phase e-cigarette sampling, the EVOD Protank BCC atomizer (1.8 ohm resistance coil) was connected to a syringe pump (Model NE-1010, New Era Pump Systems Inc., Farmingdale, NY) through a 28 mm diameter (Phenomenex Inc., Torrance, CA) glass fiber/ cellulose acetate(GF/CA) (0.45 μm pore size), non-sterile luer lock syringe filter,

followed by an ATD cartridge which contained100 mg of 35/60 mesh Tenax TA and 200 mg of 60/80 mesh Carbograph 1 TD (Camsco Inc., Houston, TX). GF/CA syringe filters were used to remove the aerosol droplets. Gas phase analytes were collected on the ATD cartridge. A 0.125 inch piece of flexible polyvinyl chloride (PVC) tubing was used to connect the filter to the EVOD atomizer. The smallest feasible amount of PVC tubing was used to prevent the potential loss of benzene to the tubing. A 1L Tedlar bag (Model 24633 Supelco Inc., Bellefonte, PA) was connected to a three way "T" stopcock between the ATD cartridge and syringe pump to allow collection of exhausted gas from the syringe pump in order to verify each total sample volume.

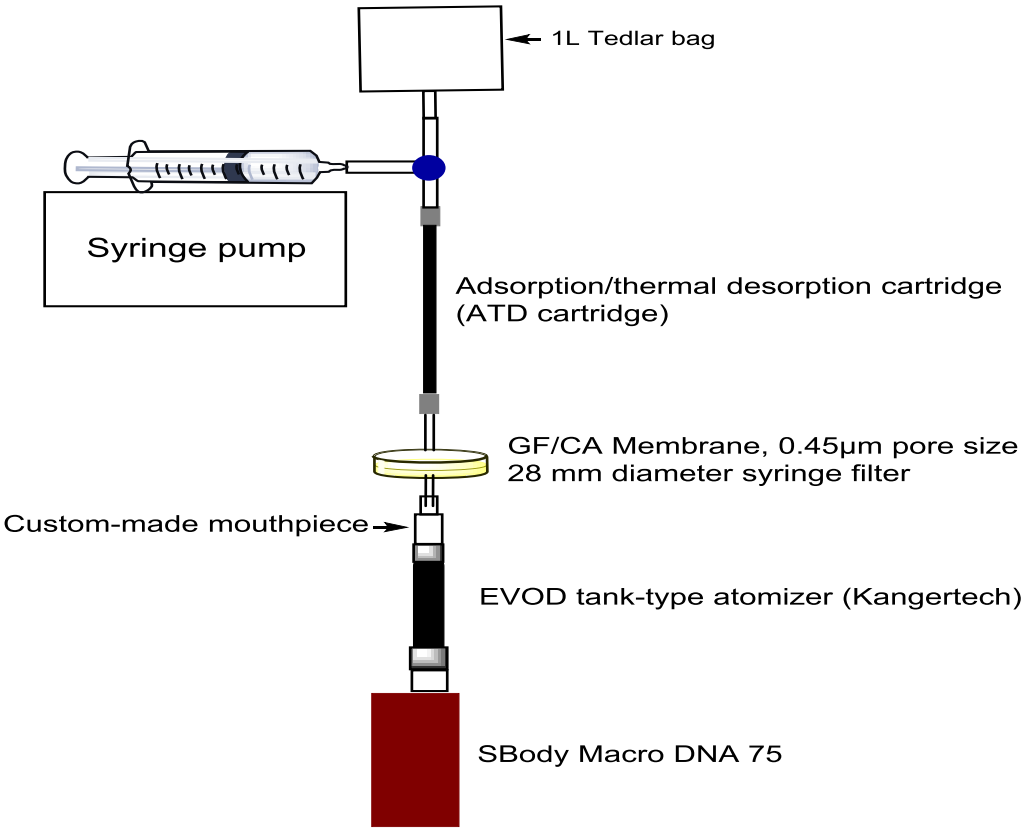

Figure 12. *Vaping gas sample collection apparatus for the EVOD device.*

2.2.3. Gas-Phase Sample in Adsorption and Thermal Desorption (ATD) Cartridges Analyses by GC/MS

Each ATD cartridge was purged for 10 minutes with a 50 mL/min flow of nitrogen gas and thermally desorbed in a TurboMatrix 650 ATD unit (PerkinElmer, Waltham, MA). Each cartridge were thermally desorbed for 10 minutes at 285 °C with helium gas at 40 mL/min and a split flow of 20 mL/min. The desorption stream was trapped at -10 °C on an intermediate "Tenax trap". The trap were then thermally desorbed at 295 °C and 25 psi

constant pressure helium with a split flow of 8 mL/min for 4 minutes. The non-split portion of the desorption gas stream passed onto the GC column in an Agilent 7890A GC (Santa Clara, CA) interfaced to an Agilent 5975C MS operated in electron impact ionization mode. The MS scan range was 34 to 400 amu. The electron multiplier voltage was 1400 V. The fused silica capillary GC column was a model Rxi-624Sil MS (Restek Inc., Bellefonte, PA) of 30 m length, 0.25 mm i.d., and 1.4 μm film thickness. For calibration, benzene standard solutions in methanol with concentrations ranging from 1 to 100 ng/μL were prepared. A 2 or 4 μL volume of a standard solution was spiked onto the inlet end of a cartridge to give a final mass of 4 to 200 ng of benzene on the cartridge. Prior to the thermal desorption, both sample and standard ATD cartridges were amended with 20 ng of an internal standard fluorobenzene (500 μL of a 40 ng/mL standard in nitrogen).

2.2.4. Blank Correction and Tracking the Mass of E-liquid Vaped for Total Particulate Matter (TPM)

Three blank samples were averaged to create a blank correction. This average concentration was then subtracted from the sample values. The mass of e-liquid vaporized per puff was recorded throughout the experiment to evaluate the concentration of total particulate matter (TPM) based on the change in e-liquid mass after vaping.

2.2.5. Calculation of Isotopic Distribution of Products

Benzene is a 6 carbon molecule. When benzene is formed from the mixtures of fully ^{13}C labeled PG and non-labeled GL or non-labeled PG and fully ^{13}C labeled GL mixtures, there are 7 possibile combinations of benzene that can be generated: all ^{12}C benzene, $^{13}C_1+^{12}C_5$, $^{13}C_2+^{12}C_4$, $^{13}C_3+^{12}C_3$, $^{13}C_4+^{12}C_2$, $^{13}C_5+^{12}C_1$, and all ^{13}C benzene. In order to determinethe peak areas of each isotopic product, relative peak sizes were calculated based on the intensity of each mass of a compound in a pure standard as shown in Appendix C to I, as corrected for satellite ions in the mass spectrum. The peak areas of major ions of the isotopic compounds were calculaed from the extracted ion chromatorgrams which are ion chromatogram plots derived froma GC series of MS spectra. The mathematics involve comparing peak areas of isotopic products. Least squares analysis in MATLAB was used to determine the contribution of the different ^{12}C-^{13}C compound combinations.

2.3. Results and Discussion

2.3.1. Identification of the Source of Benzene through Carbon Tagging

2.3.1.1. Investigation of the Origin of Benzene by Calculating Isotopic Distuributions for Benzene

Initially it was hypothesized that benzene could be formed by 1) decarboxylation of benzoic acid, 2) oxidation of benzaldehyde and then decarboxylation, and 3) disproportionation of benzaldehyde (Cannizzaro reaction) followed by the decarboxylation in e-cigarette liquids (Pankow et al., 2017). Indeed, benzene was found to be generated from benzoic acid and benzaldehyde (see preceding chapter). However, measurable levels of benzene were also detected in the aerosols from the experiment with the PG and GL only mixtures. Thus, it seemed that benzene can be formed during the heating of PG and/or GL.

The benzene concentrations generated from vaping Mixutures 2 and 4 are shown in Table 5. Calculations for the percentage of non-labeled benzene, three ^{13}C-labeled benzene, and fully ^{13}C-labeled benzene are shown in Table 6. The results show that 97.3% of fully ^{13}C-labeled benzene was produced in the samples from vaporization of Mixture 2 (fully ^{13}C-labeled PG and fully ^{13}C-labeled GL) the remainder of the benzene (which was non-labeled) was collected from ambient lab air. Samples produced by vaping Mixture 3 (fully ^{13}C-labeled PG and non-labeled GL) generated benzene that was 68.2% non-labeled and 12.6% fully ^{13}C-labeled. This means that approximately two thirds of the observed benzene originated from non-labeled GL in this mixture, i.e. more benzene is

formed from GL than from PG. This is supported by the result from Mixture 4 (non-labeled PG and fully ^{13}C-labeled GL), since 65.2% of fully ^{13}C-labeled benzene was produced while only 15.4% of non-labeled benzene was produced.

Table 5. *Benzene concentrations and standard deviations.*

Mixture Number	Non-labeled benzene		$^{13}C_3$-labeled benzene		Fully ^{13}C-labeled benzene	
	Concentration (ng/L)	SD	Concentration (ng/L)	SD	Concentration (ng/L)	SD
2	N.D		N.D		27.1	8.4
3	41.0	10.6	15.6	3.5	7.7	2.6
4	17.0	0.1	22.5	11.4	72.9	10.5

* Subscript on ^{13}C denotes the number of ^{13}C labels present in the compound.

Table 6. *Average percent generation of benzene*

Mixture Number	Non-labeled benzene		$^{13}C_3$-labeled benzene		Fully ^{13}C-labeled benzene	
	% Generation	SD	% Generation	SD	% Generation	SD
2	2.7	3.1	0.0	0.0	97.3	3.9
3	68.2	1.2	19.2	0.4	12.6	0.8
4	15.4	2.9	19.4	6.3	65.2	3.4

* Subscript on ^{13}C denotes the number of ^{13}C labels present in the compound.

2.3.1.2. Investigation of the Origins of Benzene by GC/MS analysis of Aerosols Formed by Vaping Mixtures of Isotopically Labeled Propylene Glycol and Glycerol

Figures 13 and 14 compare the extracted ion chromatograph for non-labeled benzene and fully ^{13}C-labeled benzene in the gas phase of aerosols generated from vaping Mixtures 3 and 4. The peak of non-labeled benzene, shown in Figure 13, is approximately six times greater than that of the fully ^{13}C-labeled benzene produced from the vaped samples of Mixture 3. In comparison, the relative quantity of fully ^{13}C-labeled benzene in the vaped samples of Mixture 4 is almost six times greater than non-labeled benzene (Figure 14).

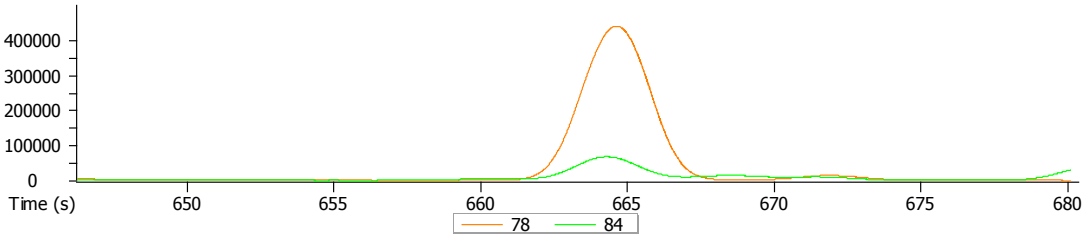

Figure 13. *Extracted ion chromatograph of benzene from GC/MS analysis of vaped Mixture 3. Mass 78 is fully ^{12}C benzene. Mass 84 is fully ^{13}C benzene.*

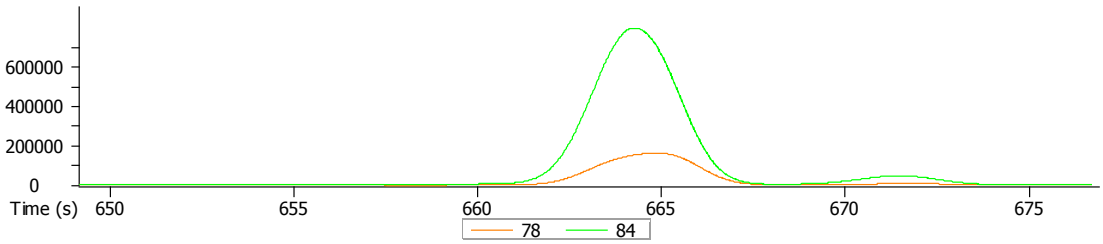

Figure 14. *Extracted ion chromatograph of benzene from GC/MS analysis of vaped Mixture 4. Mass 78 is fully ^{12}C benzene. Mass 84 is fully ^{13}C benzene.*

The mass spectra shown in Figure 15 shows parent ions and base peaks that are consistent with those in the NIST library spectrum for non-labeled benzene. The molecular ion of fully ^{13}C-labeled benzene has an m/z of 84. The highest m/z value in the mass spectrum for benzene produced from vaporization of Mixture 3 is 78 (Figure 15c), and 84 for the mass spectrum from the vaped Mixture 4 (Figure 15d). For Mixture 2, there is a peak corresponding to fully ^{13}C-labeled benzene (Figure 15b), and a peak corresponding to non-labeled benzene, the latter possibly due to benzene in the ambient laboratory air (sample blank) drawn through the device during the sample collections. These results indicate that majority of the benzene produced by vaping the PG and GL mixture originates from GL.

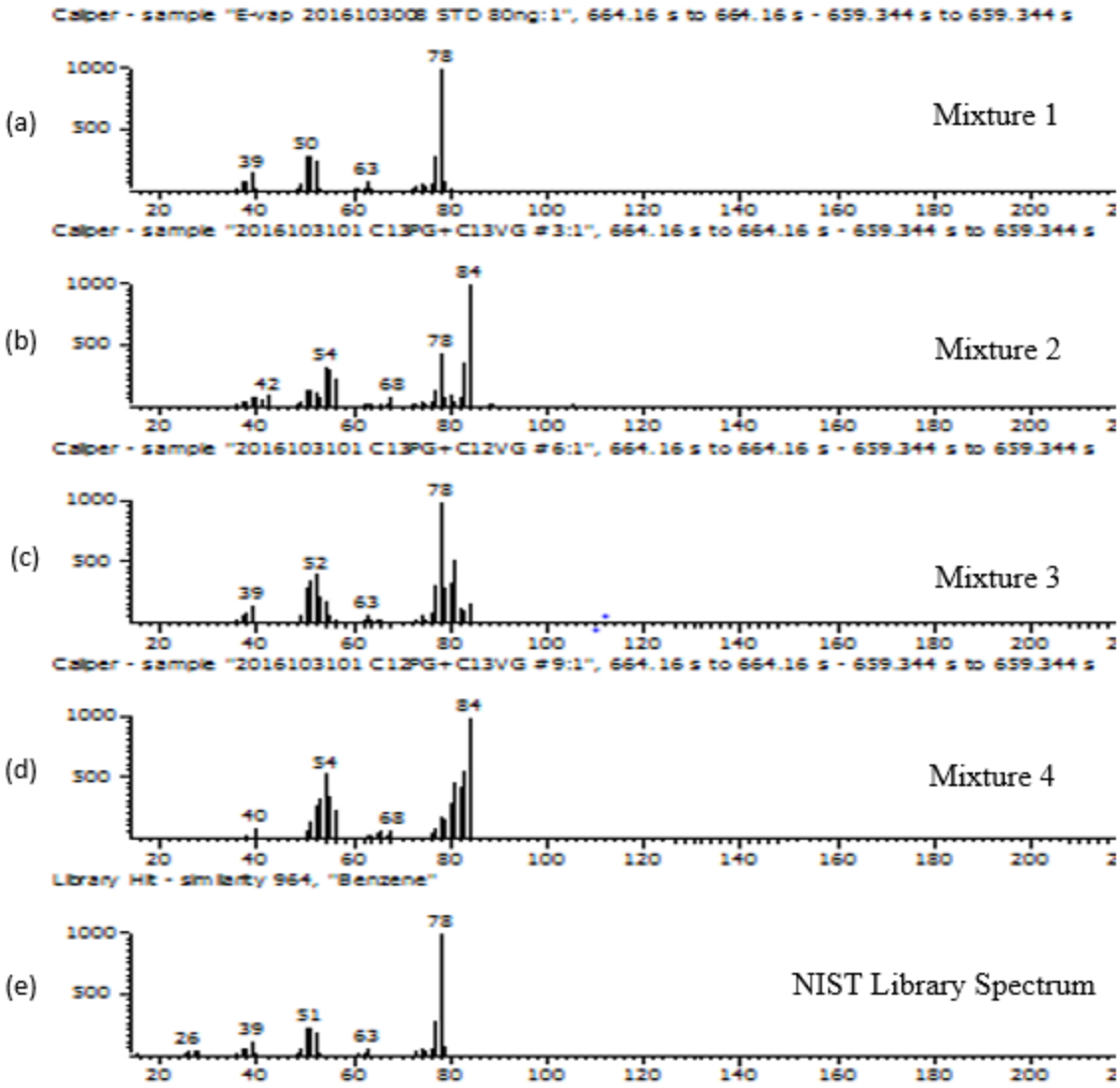

Figure 15. *The mass spectra of benzene produced from vaped mixtures (a) 1, (b) 2, (C) 3, and (d) 4. The NIST library spectrum for non-labeled benzene is shown in (e). A mass of 78 represents non-labeled benzene and a mass of 84 is fully* ^{13}*C-labeled benzene.*

2.3.1.3. Proposed Mechanisms of Benzene Formation from Glycerol

Vinyl alcohol (ethenol) is a thermal decomposition product of glycerol that can be transformed into acetaldehyde by tautomerization (Nimlos et al., 2006; Paine et al., 2017; Laine et al., 2011; Jensen et al., 2016). Acetylene can be formed by the dehydration reaction of vinyl alcohol shown in Scheme 8 (Prosanov et al., 2012). Research has shown that benzene, toluene, and other aromatic hydrocarbons are products of the polymerization and condensation of acetylene at above 400 °C (Robertson et al., 1958; Sanchez et al., 2013). Benzene can also be formed by cyclotrimerization of vinyl alcohols followed by a dehydration reaction as shown in Scheme 10. The trimerization reaction is a 2+2+2 cyclization reaction, which can form aromatic compounds in the presence of a metal catalyst. Research published by Sakurai et al. in 1985 suggested this type of mechanism for benzene formation by intermolecular cyclotrimerization of macrocyclic and acyclic trienes in the presence of group 6 metals. The mechanism is shown in Scheme 9 below. A recent study showed that e-liquid aerosols contain a range of metals such as cadmium, chromium, lead, manganese, and nickel, which are released during coil heating in e-cigarettes (Catherine et al., 2017). The high temperatures achieved in e-cigarettes could favor the E1 elimination reaction of 1,3,5-cyclohexatriol which would generate benzene.

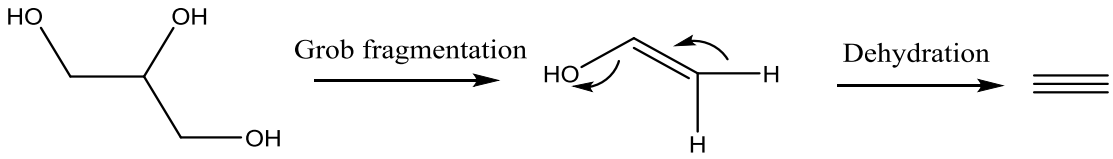

Scheme 8. *Reaction mechanism of formation of acetylene*

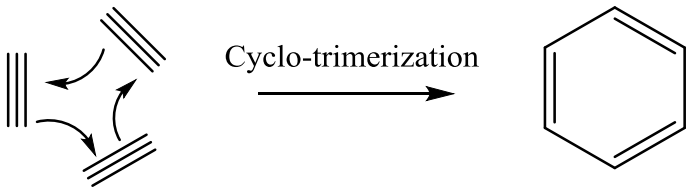

Scheme 9. *Formation of benzene from acetylene*

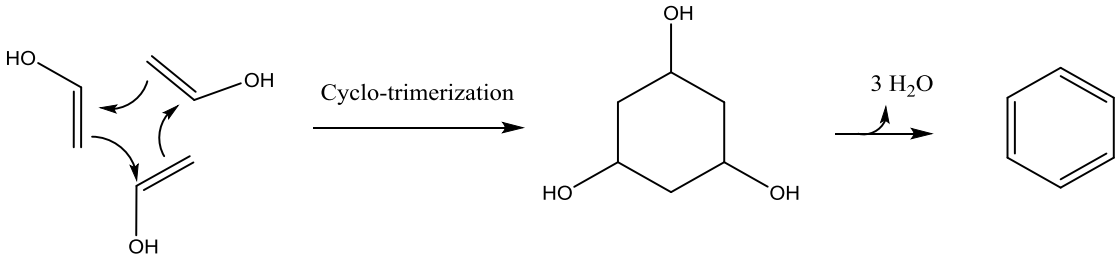

Scheme 10. *Formation of benzene from vinyl alcohol*

Another possible mechanism for benzene formation from GL is via the combination of propargyl (C_3H_3) radicals (Scheme 2.4). Based on the results discussed in Section 3.1.2, most of the benzene in the PG and GL mixture originates from GL. Moreover, the percent generation results (see Appendix D) indicate that benzene containing three ^{13}C-labeles is more abundant than benzene with two or four ^{13}C labels. Benzene generation

by propargyl radical formation and recombination may be the most likely pathway for benzene formation from GL. There are three possibilities for generation of propargyl radicals from GL: radical reaction (Scheme 11), acid-base reaction followed by dehydration (Scheme 11), and dehydration of GL followed by catalytic conversion to PG (Scheme 12). It is well-documented that radical reactions are dominant at high temperatures. The temperature of the heating coil while vaping e-cigarette liquids has been measured to vary from 130 °C to 300 °C, with dependence on the coil resistance and power setting (Geiss et al, 2016; Zhao et al., 2016). Thus, it is reasonable to hypothesize the formation of propargyl radicals from GL under these conditions. In addition, research carried out by Rossiter et al. (1985) states that aqueous GL and PG generate acidic degradation products by thermal oxidation leading to a pH decrease in aqueous solutions. Acid catalyzed dehydration is also a well-known principle in organic chemistry, thus forming a propyne cation via acid-base reaction and dehydration in vaporized e-liquids is plausible (see Scheme 11).

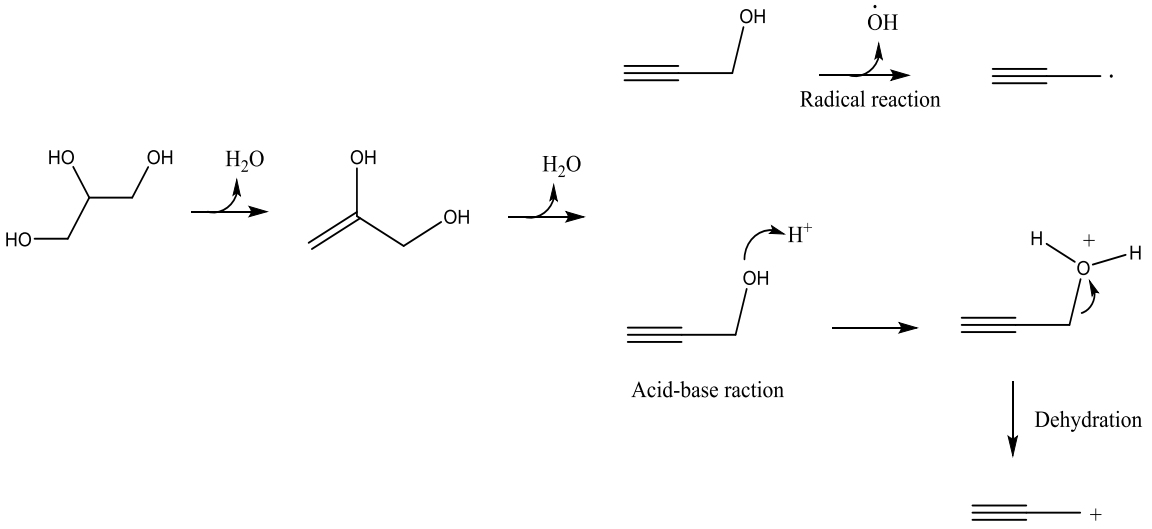

Scheme 11. *Formation of propargyl radical from glycerol*

The final proposed pathway to generate propargyl radicals from GL is through conversion of GL to PG by hydrogenolysis as illustrated by reaction Scheme 12 (Tuck et al., 2006; Chin et al., 2008; Tanielyan et al., 2014). PG can then form from the propyne intermediate via dehydration (Scheme 13). The conversion of GL to PG is an important mechanism in biodiesel production because of the simplicity of the conversion steps and cost efficiency compared to petroleum-based PG production (Ding et al., 2013). Although this is a well-documented mechanism, its application to e-cigarette chemistry is still purely hypothetical. This hydrogenolysis reaction happens only in the presence of H_2 and a metal catalyst. According to Carrero et al., glycerol can produce H_2 gas by steam reforming process under Ni-(Cu, Co, Cr) catalyst but the temperature for the glycerol steam reforming process is typically between 500 °C and 700 °C. The device used in the experiment did not have a temperature control feature, so the possibility of such temperatures cannot be excluded at this time.

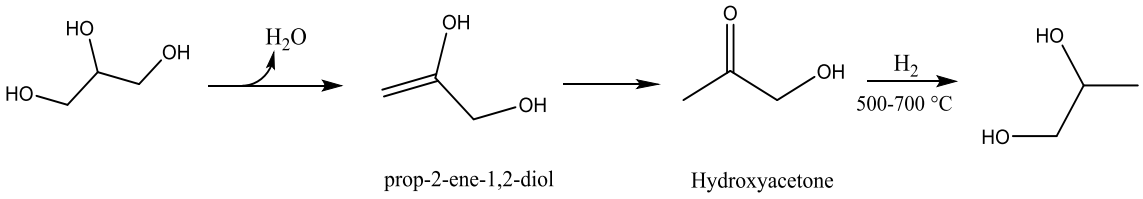

***Scheme 12**. The conversion of glycerol to propylene glycol by hydrogenolysis*

2.3.1.4. Proposed Mechanisms of Benzene Formation from Propylene Glycol

Propyne can be formed by the dehydration of propylene glycol as shown in Scheme 13. Propargyl radicals are then formed by a decomposition reaction of propyne at high

temperature (Blitz et al., 2000). The propargyl radical has been shown to be a precursor of benzene formation during combustion (Blitz et al., 2000; Tang et al., 2005; Tang et al., 2006). The proposed mechanism for the combination of propargyl radicals to form benzene is shown in Scheme 14. Thus, the overall chemical pathway to form benzene from propylene glycol is summarized in Schemes 13 and 14.

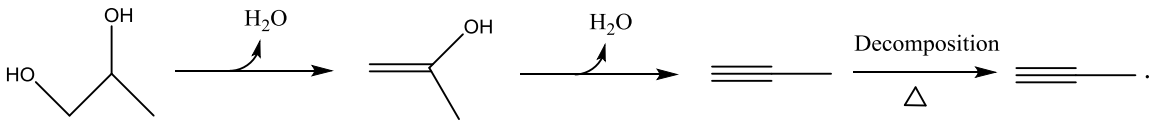

Scheme 13*. Mechanism for formation of propyne from propylene glycol*

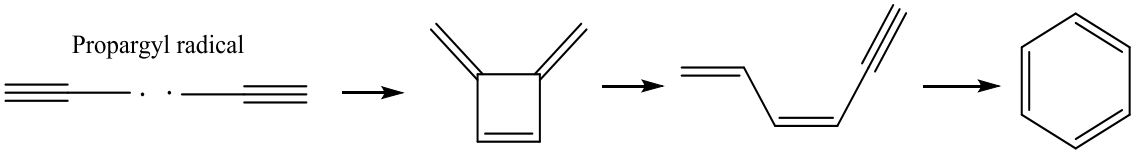

Scheme 14. *Formation of benzene from propargyl radicals*

2.3.2. Identification of the of Acetaldehyde through Isotopic Labeling

2.3.2.1. Investigation of the Origin of Acetaldehyde by Calculating Percent Compositions of Acetaldehyde Produced from the Thermolysis of the Mixtures

The percent compositions of non-labeled and fully ^{13}C-labeled acetaldehyde produced during vaping are shown in Table 7. Based on this data, for the samples

collected from vaping Mixture 3, the majority of acetaldehyde was non-labeled (61.3 %), while 37.5 % was fully ^{13}C-labeled. The opposite results were observed in the samples produced by vaping Mixture 4: 63.2% fully ^{13}C-labeled and 36.8% of non-labeled acetaldehyde. These results indicate that GL was the dominant precursor of acetaldehyde rather than PG.

Table 7. *Percent generation of non-labeled acetaldehyde and ^{13}C-labeled acetaldehyde*

Mixture Number	Non-labeled Acetaldehyde		$^{13}C_1$-labeled Acetaldehyde		Fully ^{13}C-labeled Acetaldehyde	
	% Generation	S.D	% Generation	S.D	% Generation	S.D
3	61.3	3.2	1.1	0.4	37.5	3.5
4	36.8	4.4	0.0	0.0	63.2	4.4

* Subscript on ^{13}C denotes the number of ^{13}C labels present in the compound.

2.3.2.2. Investigation of the Origin of Acetaldehyde by GC/MS Analysis of Samples Produced from the Vaped Propylene Glycol and Glycerol Mixtures

Extracted ion chromatrograph peaks corresponding to acetaldehyde produced from vaping Mixtures 3 and 4 can be seen in Figures 16 and 17, respectively. The peak of non-labeled acetaldehyde is larger than that of ^{13}C-labeled acetaldehyde in Figure 16, whereas ^{13}C-labeled acetaldehyde has a larger peak compared to the non-labeled acetaldehyde in samples from vaping Mixture 4 shown in Figure 17. Based on these results, it is concluded that a greater quantity of acetaldehyde is produced by GL compared to PG.

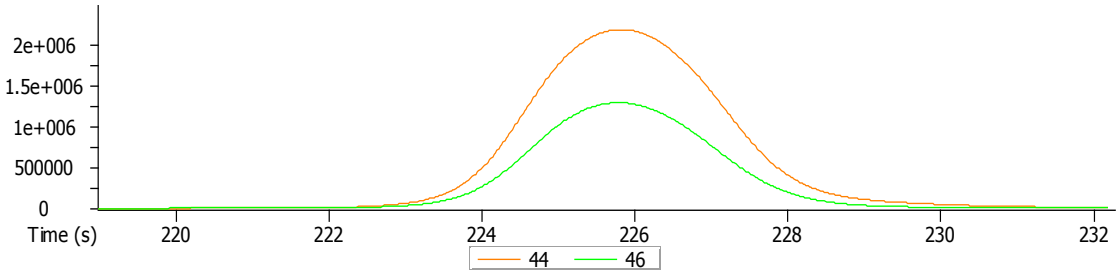

Figure 16. *Extracted ion chromatograph of acetaldehyde from GC/MS analysis of vaped Mixture 3. Mass 44 is fully ^{12}C acetaldehyde. Mass 46 is fully ^{13}C acetaldehyde.*

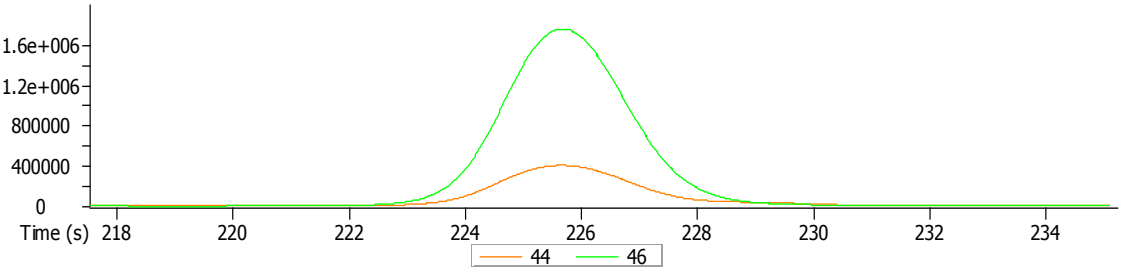

Figure 17. *Extracted ion chromatograph of acetaldehyde from GC/MS analysis of vaped Mixture 4. Mass 44 is fully ^{12}C acetaldehyde. Mass 46 is fully ^{13}C acetaldehyde.*

The mass spectra shown in Figure 18 provide further evidence for the origin of acetaldehyde. The parent ion peak of non-labeled acetaldehyde with 100% abundance is mass 44, in accordance with the NIST library spectrum (Figure 18e). The molecular ion of fully ^{13}C-labeled acetaldehyde had an m/z of 46. The highest m/z value in the mass spectrum of the vaped product from Mixture 3 (Figure 18c) is 44, and 46 for the mass spectrum of the vaped product from Mixture 4 (Figure 18d). This indicates that acetaldehyde originates primarily from GL, rather than PG. The mass spectrum for the products formed from the vaped product of Mixture 2 (Figure 18b), shows that this mixture produces only fully ^{13}C-labeled acetaldehyde.

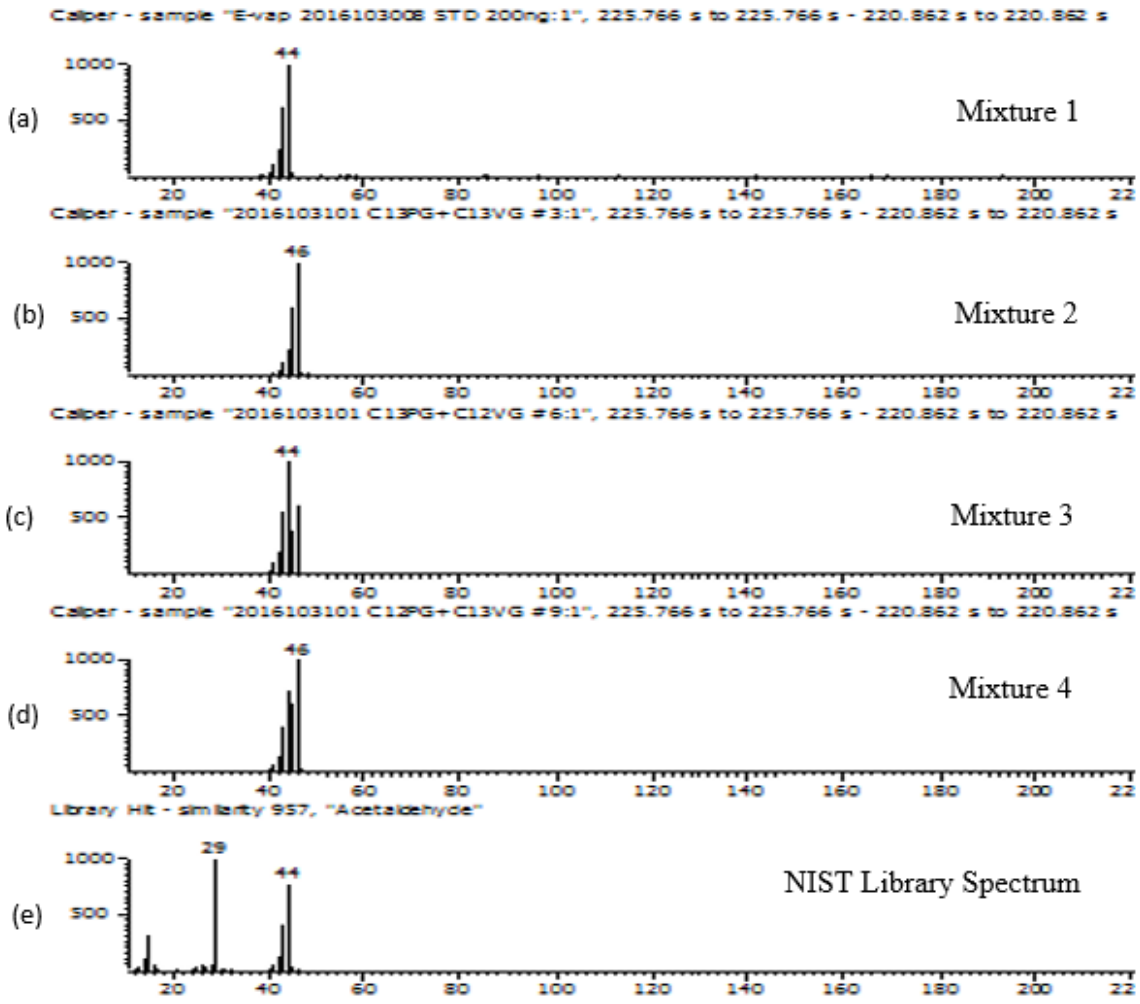

Figure 18. *The mass spectra of acetaldehyde produced from vaped mixtures (a) 1, (b) 2, (C) 3, and (d) 4. The NIST library spectrum for non-labeled acetaldehyde is shown in (e). A mass of 44 represents non-labeled acetaldehyde and a mass of 46 is fully ^{13}C-labeled acetaldehyde.*

2.3.2.3. Proposed Mechanism for Acetaldehyde Formation in Samples Produced from Vaping Mixtures of Propylene Glycol and Glycerol

Acetaldehyde is a thermal degradation product of PG and GL. Glycerol decomposition pathways were first described almost a century ago. According to previous research, 3-

hydroxypropanal, glycidol, and hydroxyacetone are primary glycerol dehydration products (Jensen et al., 2016). Acrolein, formaldehyde, and acetaldehyde have been determined to be decomposition products of glycerol (Scheme 19) (Nimlos et al., 2006; Paine et al., 2017; Laine et al., 2011; Jensen et al., 2016). This section will focus on acetaldehyde in particular as it is suggested to be an important percursor to yield 2,3-butanedione (discussed in Section 2.3.3).

The glycerol decomposition pathway in Scheme 15 was discussed by Laine et al. (2011) and Jensen et al. (2016). Vinyl alcohol, one of the glycerol degradation products, is converted to acetaldehyde by tautomerization. Paine et al. (2007) proposed a new pathway to form acetaldehyde from glycerol by intermolecular hydrogen bonding between two terminal hydroxyl groups (Scheme 16), which was supported by an isotope labeling experiment. Scheme 17 shows the H-abstraction and C-C bond cleavage of propylene glycol to form acetaldehyde .

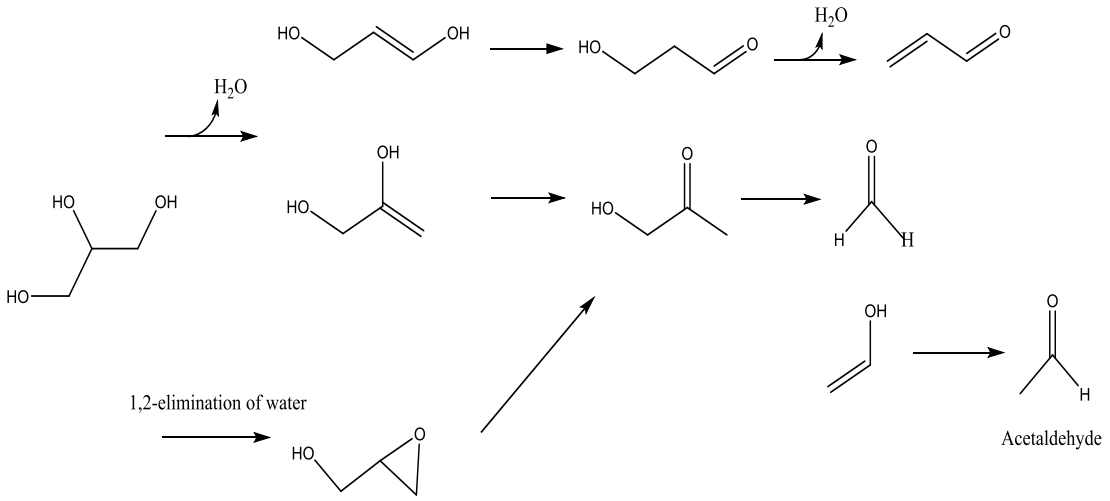

Scheme 15. *A decomposition pathway of glycerol (Laine et al., 2011; Jensen et al., 2016)*

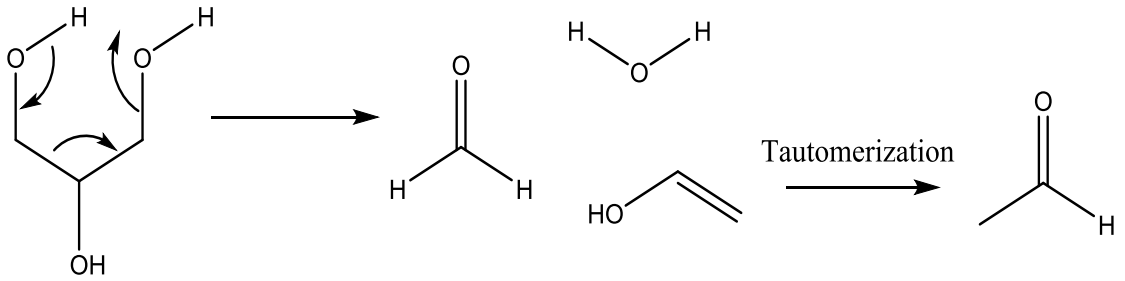

Scheme 16*. Cyclic grob fragmentation of glycerol*

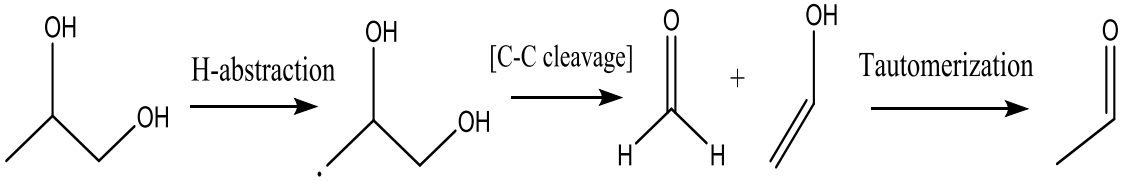

Scheme 17*. Thermal decomposition of propylene glycol (Jensen et al., 2016)*

2.3.3. Identification of the Source of 2,3-Butanedione through Isotopic Labeling

2.3.3.1. Investigation of the Origin of Diacetyl

The percent generation of 2,3-butanedione (diacetyl) in different mixtures are shown in Table 8. For the samples collected from vaping Mixture 3, the majority of the diacetyl is non-labeled (58.7%), while only 11.5% was fully ^{13}C-labeled. The results of the samples collected from vaping Mixture 4 showed the opposite trend: the majority of the diacetyl was fully ^{13}C-labeled (68.2%) and only 4.6% was non-labeled. These results confirm that the majority of diacetyl originates from GL, rather than PG.

Table 8. *Percent generation of non-labeled diacetyl and ^{13}C-labeled diacetyl.*

Mixture Number	Non-labeled diacetyl		$^{13}C_1$-labeled diacetyl		$^{13}C_2$-labeled diacetyl		$^{13}C_3$-labeled diacetyl		Fully ^{13}C-labeled diacetyl	
	%	S.D	%	S.D	%	S.D	%	S.D	%	S.D
3	58.7	5.6	5.2	0.5	6.1	0.7	18.5	1.9	11.5	3.2
4	4.6	1.1	15.6	2.7	4.2	0.8	7.3	1.7	68.2	4.9

* Subscript on ^{13}C denotes the number of ^{13}C labels present in the compound.

2.3.3.2 GC/MS Analysis of Diacetyl in Samples Produced from Vaped Propylene Glycol and Glycerol Mixtures

Non-labeled diacetyl is more abundant than fully ^{13}C-labeled diacetyl in samples from vaping Mixture 3 (see Figure 19). This means that most of the diacetyl in this mixture comes from the non-labeled GL. This idea is supported by the extracted ion chromatograph of diacetyl in a vaped sample of Mixture 4 (Figure 20). The peak arising from the fully ^{13}C-labeled diacetyl (mass of 90) is much larger than the peak representing the non-labeled diactyl (mass of 86) in this mixture.

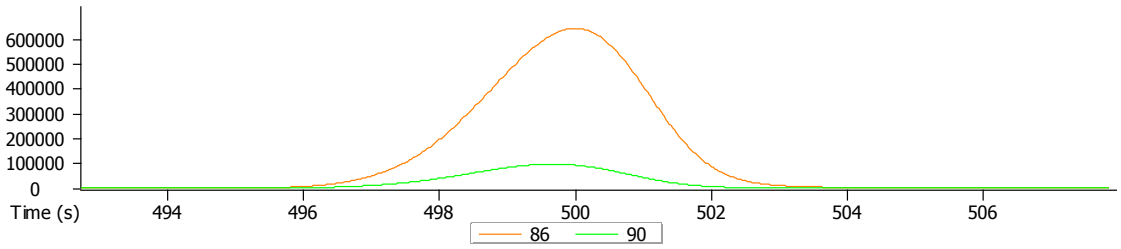

Figure 19. *Extracted ion chromatograph of diacetyl from GC/MS analysis of vaped Mixture 3. Mass 86 is fully ^{12}C diacetyl. Mass 90 is fully ^{13}C diacetyl.*

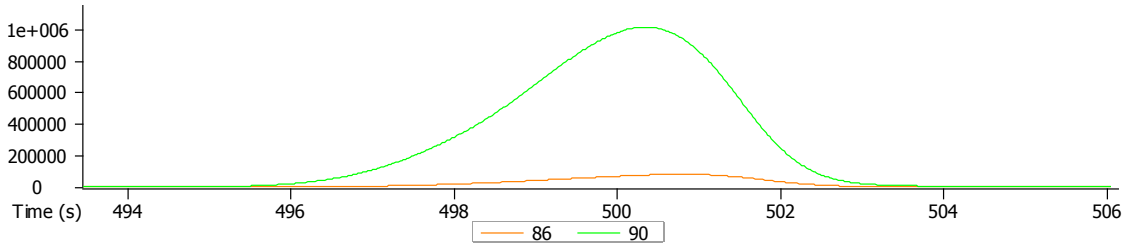

Figure 20. *Extracted ion chromatograph of diacetyl from GC/MS analysis of vaped Mixture 4. Mass 86 is fully ^{12}C diacetyl. Mass 90 is fully ^{13}C diacetyl.*

The base peak of non-labeled diacetyl has an m/z of 43. Scheme 18 illustrates how the cation with an m/z of 43 is formed by alpha cleavage of diacetyl. The base peak representing the ^{13}C-labeled cation has an m/z of 45. As shown in Figure 21, the base peak with an m/z of 43 was generated by vaping Mixture 3 (fully ^{13}C-labeled PG and non-labeled GL) and was seen in the NIST library spectrum for diacetyl. The base peaks for the ^{13}C-labeled cation are seen in both Mixtures 2 (fully ^{13}C-labeled PG and fully ^{13}C-labeled GL) and 4 (non-labeled PG and fully ^{13}C-labeled. GL). These results show that diacetyl is mainly created from GL, rather than PG, during e-liquid vaporization in an e-cigarette.

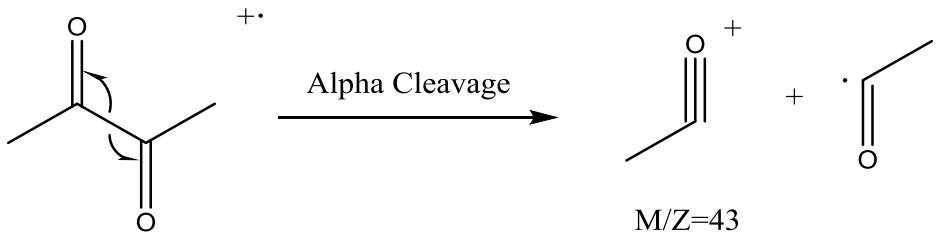

Scheme 18. *Acetaldehyde alpha cleavage mechanism*

Molecular ion peaks also support this idea. The highest m/z value for non-labeled diacetyl is 86, and the peak with an m/z of 90 represents the ^{13}C-labeled diacetyl. The largest peak observed in the samples produced by vaping Mixtures 1 (Figure 21a) and 3 (Figure 21c) is m/z = 86. In contrast, the samples produced by vaping Mixtures 2 (Figure 21b) and 4 (Figure 21d) resulted in the peak with an m/z of 90 being dominant. The combination of these results further support the case that diacetyl is primarily created from GL, rather than PG.

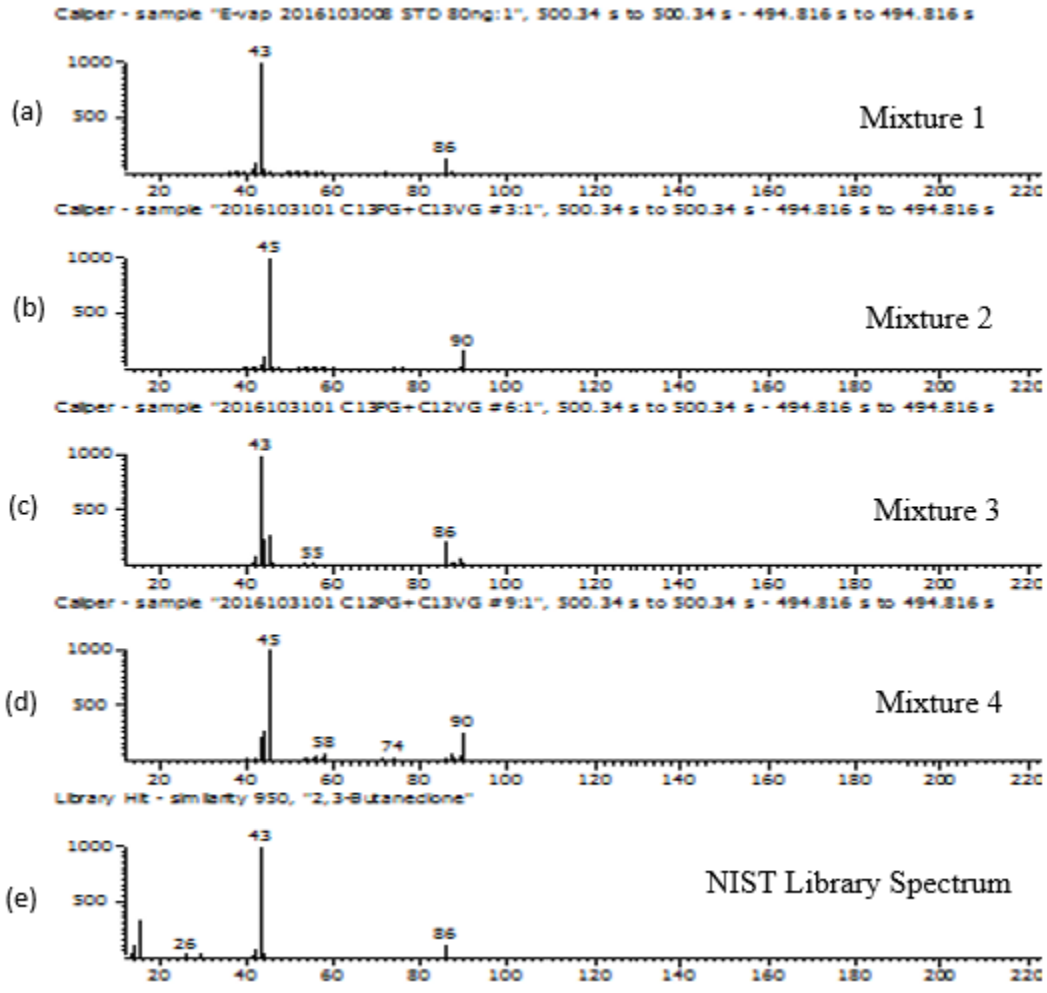

Figure 21. *The mass spectra of diacetyl (2,3-butanedione) produced from vaped mixtures (a) 1, (b) 2, (C) 3, and (d) 4. The NIST library spectrum for non-labeled diacetyl is shown in (e). A mass of 86 represents non-labeled diacetyl and a mass of 90 is fully ^{13}C-labeled diacetyl.*

2.3.3.3. Proposed Mechanism of Diacetyl Formation in the Samples Produced from Vaping Propylene Glycol and Glycerol Mixtures

Acetaldehyde is a decomposition product of PG and GL (Schemes 15, 16, and 17). Acetaldehyde is the key intermediate in the pyrolysis reaction for the formation of diacetyl. Scheme 19 shows that acetyl (CH_3CO) radicals are formed by acetaldehyde pyrolysis (Laidler et al., 1967; Liu et al., 1968). The research carried out by C. E. H Bawn claims that diacetyl is created by dimerization of acetyl radicals (Scheme 20) (Bawn, 1938). This set of chain reactions might occur in e-cigarettes at high temperatures leading to formation of diacetyl.

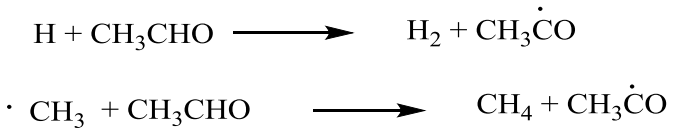

Scheme 19. *Acetaldehyde pyrolysis*

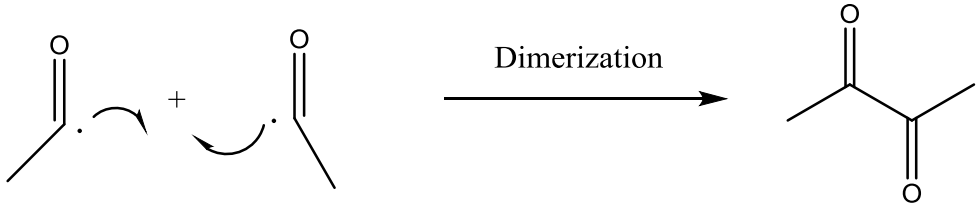

Scheme 20. *Formation of diacetyl by dimerization of acetyl radicals*

2.3.4. Identification of the Source of Toluene and Xylene through Isotopic Labeling

2.3.4.1. Investigation of the Origin of Toluene by Calculating the Isotopic Distributions

Table 9 shows the percent generation of toluene produced during the vaping of the isotopically labled mixtures. In the samples produced from vaporization of Mixture 3, non-labeled toluene (mass of 91) accounted for 55.2% of the total toluene, while fully ^{13}C-labeled toluene (mass of 98) accounted for only 7.3%. In samples from the vaping of Mixture 4, the result shows the opposite trend. The gas-phase samples produced from vaping Mixture 4 generated toluene that was 4.6 % non-labeled and 52.7 % fully ^{13}C-labeled.

Table 9. *Percent generation of non-labeled toluene and fully ^{13}C-labeled toluene*

Mixture Number	Non-labeled toluene		$^{13}C_1$-labeled toluene		$^{13}C_3$-labeled toluene		$^{13}C_4$-labeled toluene		$^{13}C_6$-labeled toluene		Fully ^{13}C-labeled toluene	
	%	S.D	%	S.D	%	S.D	%	S.D	%	S.D	%	S.D
3	55.2	6.7	4.7	1.4	11.9	3.5	4.8	1.4	3.5	0.6	7.3	1.2
4	4.6	1.2	3.0	0.6	4.4	1.9	12.9	4.4	11.5	1.9	52.7	10.2

2.3.4.2. Investigation of the Origin of Toluene by GC/MS Analysis of Samples Produced by Vaping the Propylene Glycol and Glycerol Mixtures

The extracted ion chromatographs show toluene produced in the vaped samples of Mixtures 3 and 4. The peak for non-labeled toluene is larger than that for the fully ^{13}C-

labeled toluene in the sample produced from vaping Mixture 3 (Figure 22). In the gas-phase samples formed from vaporization of Mixture 4, the peak of fully ^{13}C-labeled toluene is much larger than the peak of non-labeled toluene (Figure 23). These results provide clear evidence that the primary origin of toluene is GL rather than PG.

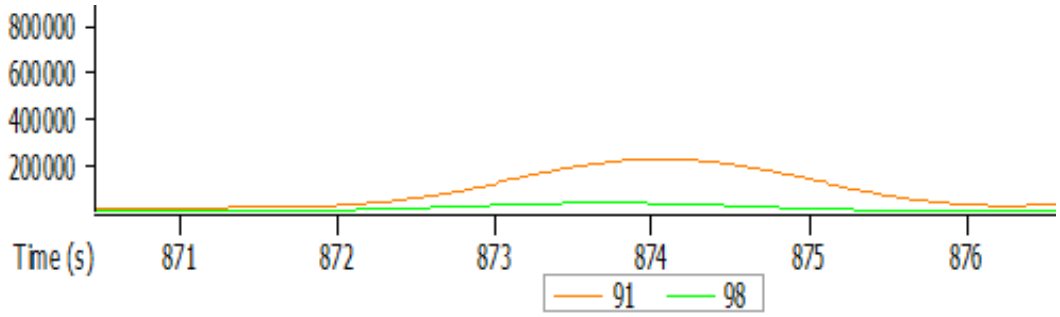

Figure 22. *Extracted ion chromatograph of toluene from GC/MS analysis of vaped Mixture 3. Mass 91 is fully ^{12}C toluene. Mass 98 is fully ^{13}C toluene.*

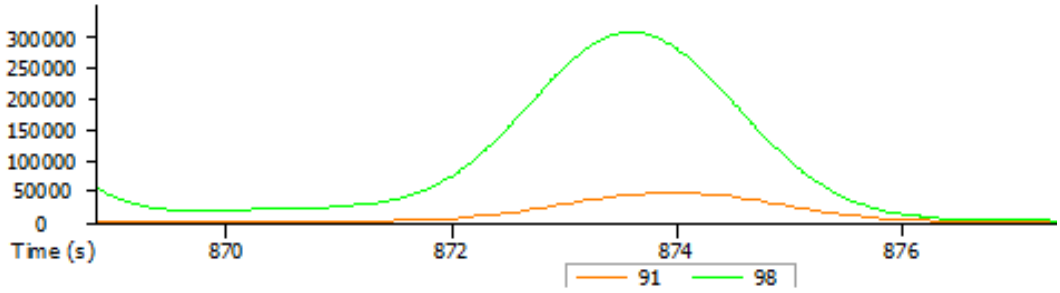

Figure 23. *Extracted ion chromatograph of toluene from GC/MS analysis of vaped Mixture 4. Mass 91 is fully ^{12}C toluene. Mass 98 is fully ^{13}C toluene.*

The base peak of non-labeled toluene has an m/z of 91, which is the largest molecular ion for the non-labeled species. The base peak with an m/z of 91 appears in the samples produced from vaping Mixture 1 (Figure 24a) as well as Mixture 3 (Figure 24c). These

results show that toluene primarily originates from non-labeled GL in these mixtures. The base peak of fully ^{13}C-labeled toluene (m/z = 98) is seen in the samples produced from vaping Mixtures 2 (Figure 24b) and 4 (Figure 24d). These results also support the idea that toluene primarily originates from GL, rather than PG. The peak with an m/z of 65, which is the fragmentation pattern representing the cyclopentadiene cation, is also seen in the samples generated from vaping Mixtures 1 and 3 (Scheme 21). The fully ^{13}C-labeled cyclopentadiene cation (m/z = 70) is also found in the vaporized Mixtures 2 and 4 (Scheme 21). These results also support the idea GL synthesizes more toluene than PG when vaporized in e-cigarettes.

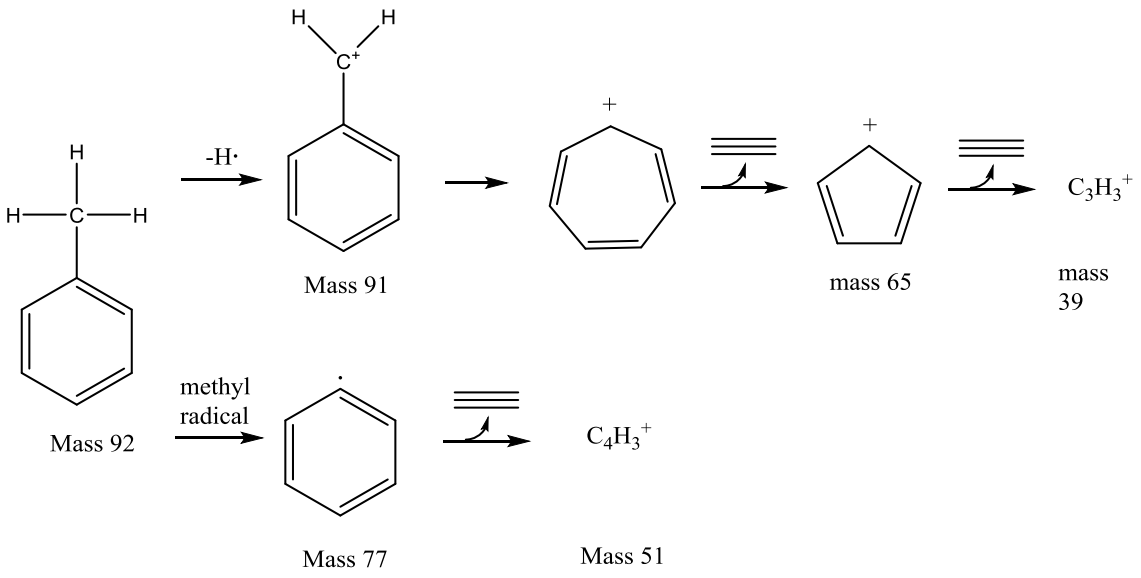

Scheme 21. *Fragmentation of toluene in GC/MS*

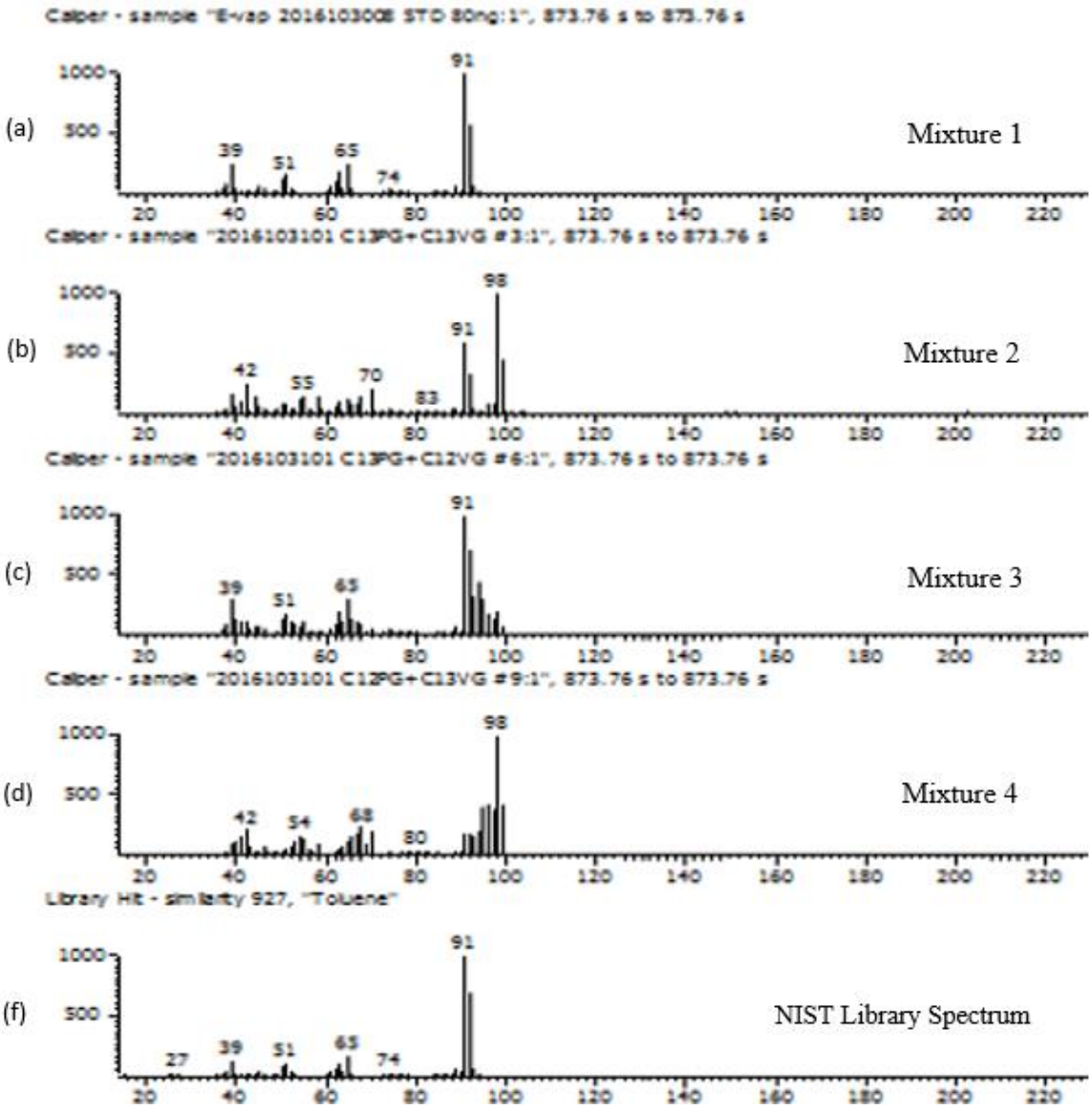

Figure 24. *The mass spectra of toluene produced from vaped Mixtures (a) 1, (b) 2, (C) 3, and (d) 4. The NIST library spectrum for non-labeled toluene is shown in (e). A mass of 91 represents non-labeled toluene and a mass of 98 is fully* ^{13}*C-labeled toluene.*

2.3.4.3. Proposed Mechanism for Toluene and Xylene Formation in the Samples Produced from Vaping Mixtures of Propylene Glycol and Glycerol

Research conducted by Levy et al. proposes the mechanism of toluene and xylene formation by adding methyl radicals to benzene (Scheme 22). Hydrogen atom abstraction on benzene and the addition of a methyl radical produces $C_6H_6 \cdot R$ at high temperatures. This product can further react by addition, or substitution, with methyl radical reactions creating ortho-, para-xylene and toluene respectively (Levy et al., 1954).

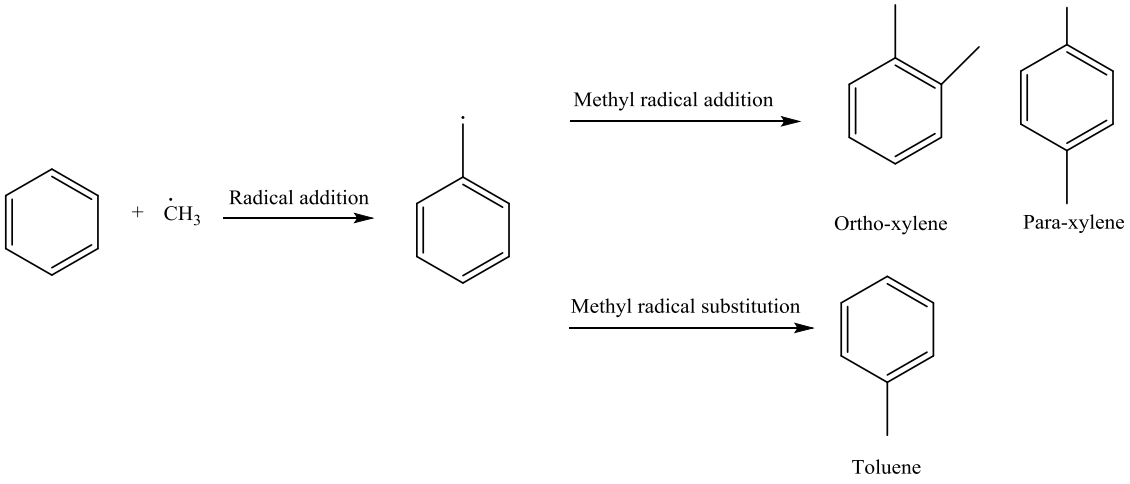

Scheme 22. *The reaction mechanism for the formation of toluene and xylene by addition and substitution of methyl radicals*

Toluene and xylene can be formed by cyclotrimerization of propynes and acetylenes (Scheme 23). Trimerization was previously mentioned to explain the pathways of formation for benzene (Section 3.1.3). Propyne and acetylene are dehydration products of propylene glycol and glycerol, respectively. At the high temperatures experienced in e-

cigarettes during vaping, these two compounds could react with a 1:2 or 2:1 ratio of propyne and acetylene to generate toluene and xylene. Mass spectra show that fully ^{13}C-labeled xylene is the most abundant form produced by vaping Mixture 4 (Figure 25d), while non-labeled xylene is the dominant form in the samples from vaping Mixture 3 (Figure 25c). These results indicate that the primary origin of xylene is GL, rather than PG.

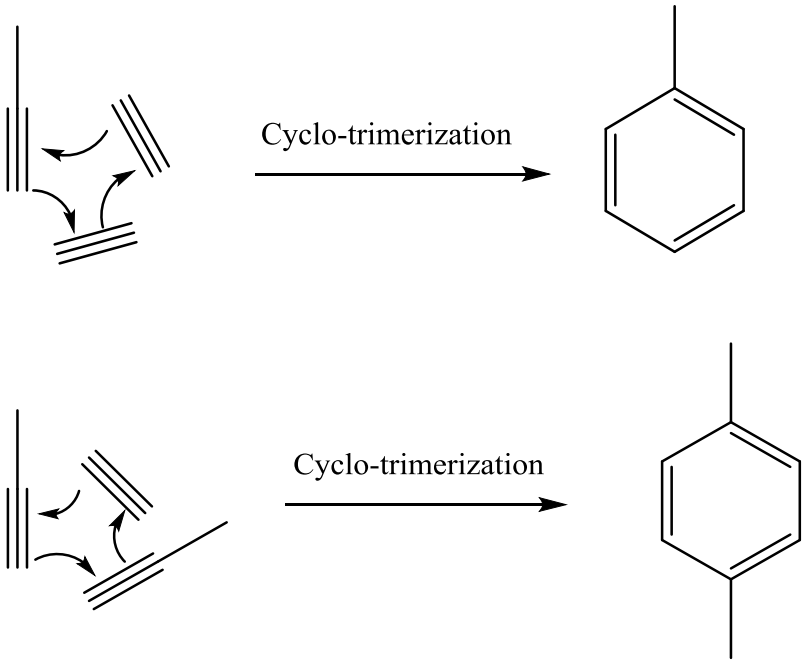

Scheme 23. *The formation reaction mechanisms for toluene and xylene by cyclotrimerization of propynes and acetylenes.*

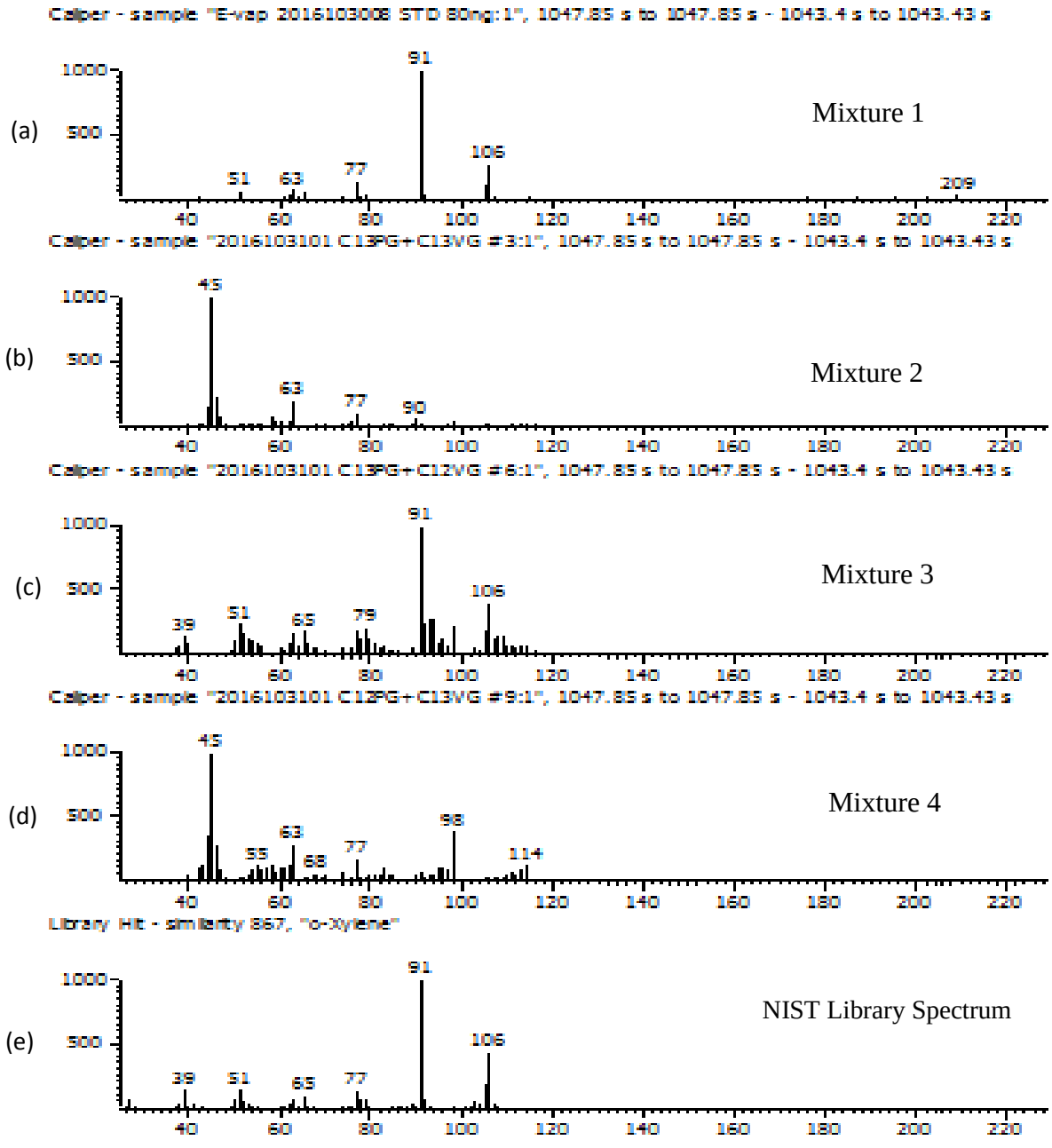

Figure 25. *The mass spectra of xylene produced from vaped mixtures (a) 1, (b) 2, (C) 3, and (d) 4. The NIST library spectrum for non-labeled xylene is shown in (e). A mass of 106 represents non-labeled xylene and a mass of 114 is fully* ^{13}*C-labeled xylene.*

2.3.5. Identification of the Source of Other Chemicals by Isotopic Labeling

Analysis of gas-phase samples produced from vaping isotopically-labeled PG and GL mixtures also identified acrolein, hydroxyacetone, furan and propanal. The molecular ion (M+) peaks of non-labeled acrolein has an m/z of 56. Non-labeled acrolein is seen after vaporizing Mixtures 1 and 3 (Figures 26a and 26c, respectively). The peaks with an m/z of 59, the molecular ion peak representing fully ^{13}C-labeled acrolein are also seen in the samples generated from vaping Mixtures 2 and 4 (Figures 26b and 26d, respectively). These results signify that acrolein originates primarily from GL, rather than from PG.

The base peak of non-labeled hydroxyacetone has an m/z of 43, and the base peak of fully ^{13}C-labeled hydroxyacetone has an m/z of 45. A base peak with an m/z of 45 is seen in the samples produced from vaping the mixtures of both Mixtures 3 and 4 (Figures 27c and 27d, respectively). The highest m/z peak of non-labeled hydroxyacetone is 74. The fully ^{13}C-labeled hydroxyacetone molecular ion (M+) peak has an m/z of 77, and this peak was detected after vaporizing Mixtures 3 and 4. These results indicate that hydroxyacetone originates from both PG and GL.

The greatest m/z value of non-labeled furan is 68, and this is detected from vaped samples generated from vaping both Mixtures 1 and 3 (Figure 28a and 28c, respectively). The fully ^{13}C-labeled furan, which has a molecular ion peak where m/z of 71, is detected in Mixture 4 (Figure 28d). This means that furan mainly comes from GL.

According to the research performed by Jensen et al., propanal is one of the thermal decomposition products of PG. GC/MS analysis of the vaping mixtures confirm this. The largest m/z value for fully ^{13}C-labeled propanal is 61. This peak is detected in the samples produced from the vaporization of Mixture 3 (Figure 29b). While the molecular ion peak with an m/z = 58, representing non-labeled propanal, is detected in samples generated by vaping Mixture 4 (Figure 29a). This result indicates that the origin of propanal is PG, rather than GL.

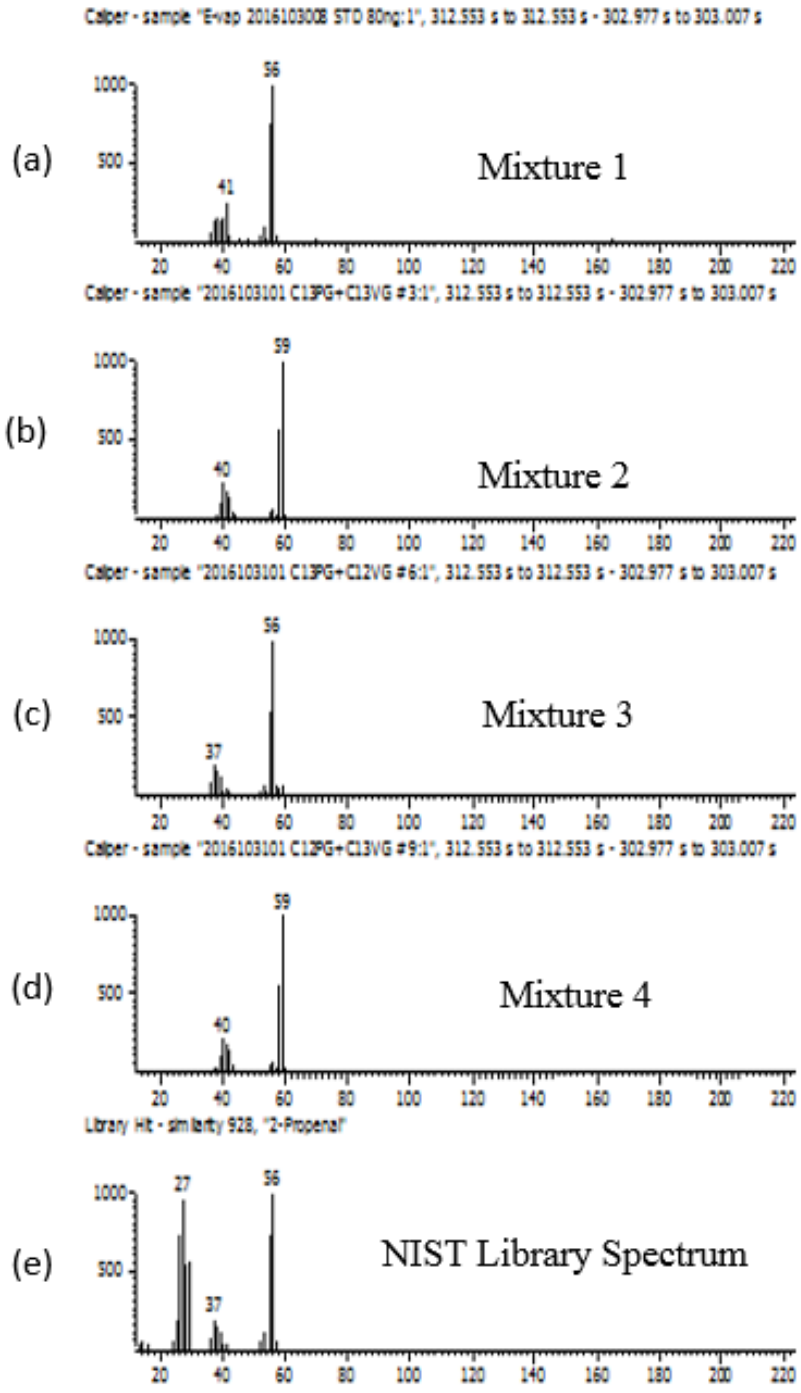

Figure 26. *The mass spectra of acrolein produced from vaped Mixtures (a) 1, (b) 2, (C) 3, and (d) 4. The NIST library spectrum for non-labeled acrolein is shown in (e). A mass of 56 represents non-labeled acrolein and a mass of 59 is fully* ^{13}*C-labeled acrolein.*

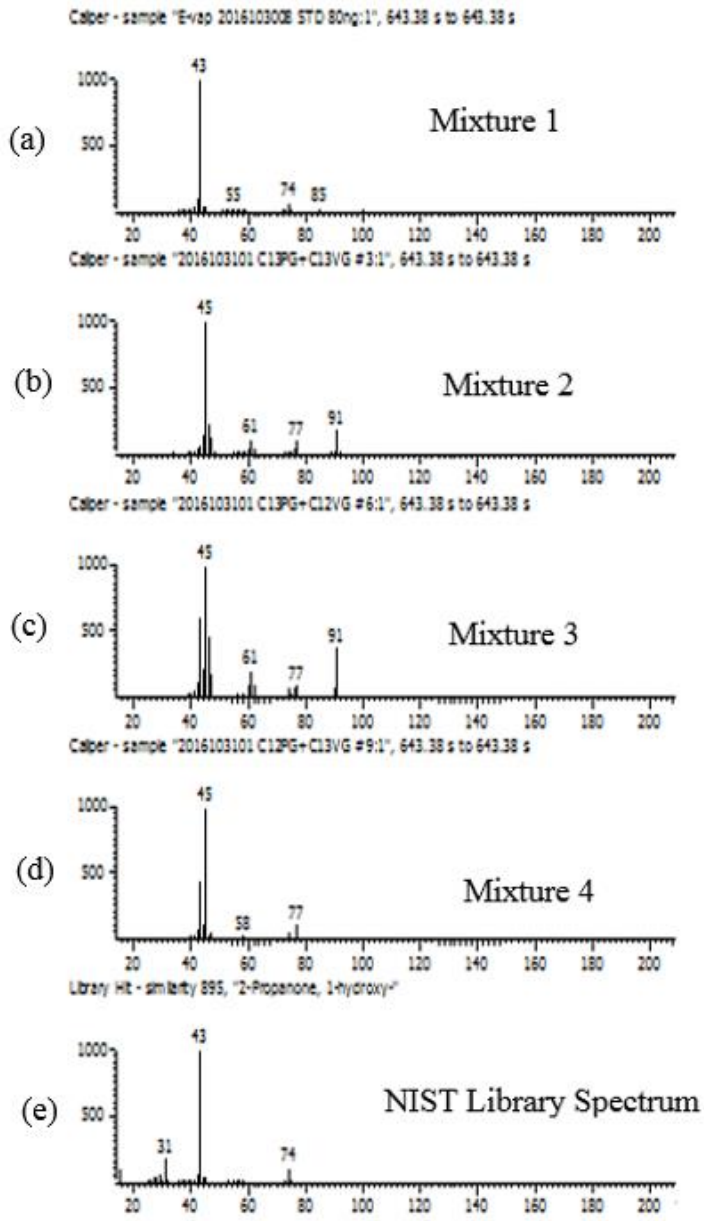

Figure 27. *The mass spectra of hydroxyacetone produced from vaped Mixtures (a) 1, (b) 2, (C) 3, and (d) 4. The NIST library spectrum for non-labeled hydroxyacetone is shown in (e). A mass of 74 represents non-labeled hydroxyacetone and a mass of 77 is fully 13C-labeled hydroxyacetone*

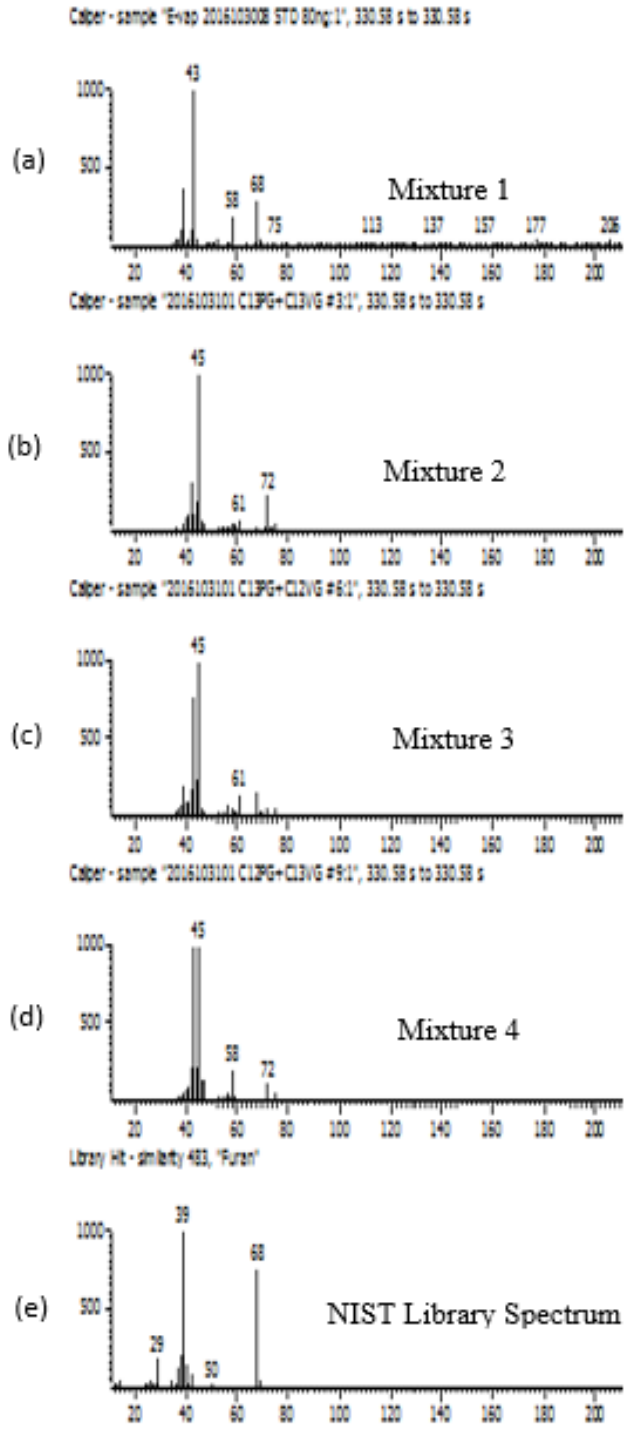

Figure 28. *The mass spectra of furan produced from vaped Mixtures (a) 1, (b) 2, (C) 3, and (d) 4. The NIST library spectrum for non-labeled furan is shown in (e). A mass of 68 represents non-labeled furan and a mass of 72 is fully* ^{13}*C-labeled furan.*

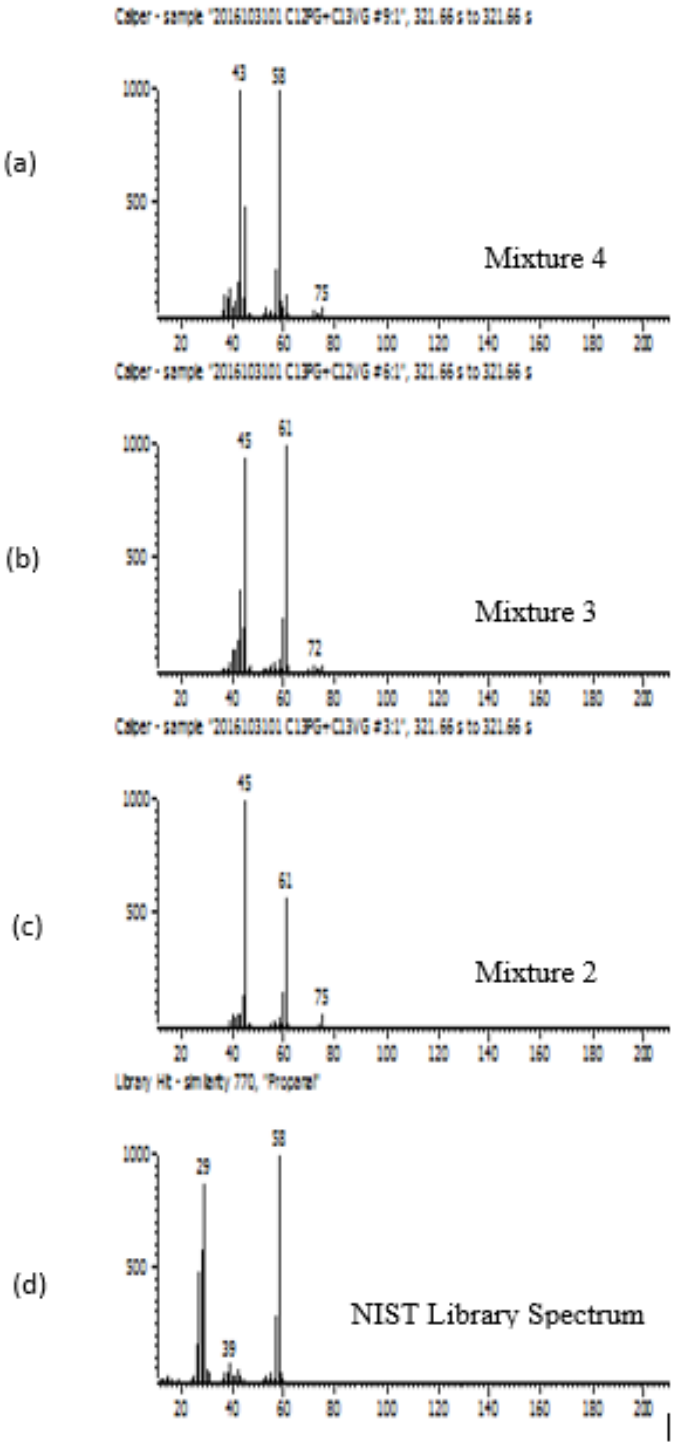

Figure 29. *The mass spectra of propanal produced from vaped Mixtures (a) 4, (b) 3, and (C) 2. The NIST library spectrum for non-labeled propanal is shown in (d). A mass of 58 represents non-labeled propanal and a mass of 61 is fully ^{13}C-labeled propanal.*

2.4. Conclusions

The analysis presented in this section shows that e-cigarettes were capable of producing a variety of known toxicants when e-liquid mixtures were exposed to high operating temperatures. Mixtures of PG and GL were used in this study to replicate the mixtures found in some commercially available e-liquids. To determine the major source (whether PG or GL) of specific harmful products, mixtures of both ^{13}C-labeled and non-labeled PG and GL were exposed to conditions that might be encountered during typical usage of e-cigarettes. With the use of GC/MS analysis, these isotopic labeling experiments provided evidence that benzene, acetaldehyde, 2,3-butanedione, toluene, xylene, acrolein, and furan primarily arose from GL, rather than PG, in the studied mixtures. It was also shown that propanal was mainly derived from PG, rather than GL, and that hydroxyacetone could be formed from both PG and GL. Possible mechanisms for the formation of benzene, 2,3-butanedione, toluene, and xylene formation were also been proposed.

Understanding the origin of toxicants or carcinogens is critical to prevent the inhalation of toxic chemicals during the vaping of e-cigarettes. The results in the preceding sections showed that when 50:50 mixtures of PG and GL were vaped, the majority of the produced benzene, a known carcinogen, originated from GL. Moreover, the results in this chapter indicated that the majority of the toxic chemicals studied were produced by GL, rather than PG, during vaping. While it is may not be a viable option to completely remove GL from e-liquids, the amount of toxic chemicals produced could be minimized by reducing the proportion of GL in e-liquid mixtures.

3. Gas/Particle Partitioning of Nicotine and Flavor Related Chemicals in Electronic Cigarette Liquids at Equilibrium

3.1. Introduction

The aerosol produced by vaping consists of a liquid particle phase and a gas phase. Chemicals in these aerosols will partition between the gas phase and the particulate matter (PM) phase (Pankow, 2017). The aerosols created by vaping e-cigarette liquids are composed of the primary solvents (i.e., propylene glycol (PG), glycerol (GL)), flavor chemicals added to the liquids (e.g., cinnamaldehyde, maltol, menthol), and degradation products of these solvents (e.g., formaldehyde, acetaldehyde, acetone, benzene, 2,3-butanedione, toluene) (Jensen et al., 2017; Pankow, 2017; Pankow et al., 2017; Sleiman et al. 2016). The phase distribution of each chemical in the mainstream aerosols affects the way each chemical interacts with the human body. Volatile compounds that have high or moderate water solubility will tend to be in the gas phase and deposit within the upper respiratory tract. In contrast, compounds with low volatility will tend to stay in the particulate phase and travel into the lower respiratory tract. Therefore, understanding the gas/particle partitioning of chemicals in e-cigarette aerosols is important for both toxicological and analytical chemistry reasons. In this set of experiments, GC/MS analyses of the liquid and gas phases were conducted to evaluate the gas/particle partitioning constant (K_p) for 37 compounds that are relevant to interest to e-cigarette chemistry.

3.2. Materials and Methods

3.2.1. Solution Preparation

A set of 37 target compounds was divided into 3 groups based on vapor pressures values (Appendix J): volatile, moderatly volatile, and less volatile. The vapor pressures at 25 °C (298.15 K) were collected from PubChem and also calculated using the Antoine Equation parameters.

$$\log_{10} P = A - \left(\frac{B}{T+C}\right) \quad (1)$$

A, *B* and *C* are Antoine Equation parameters collected from NIST WebBook. Vapor pressure is represented *p*, and *T* is the room temperature (25 °C.)

The Clausius-Clapeyron equation (3) was also used to estimate the vapor pressures at 298.15 K (the temperature of interest) when the vapor pressures at 20 °C (293.15 K) were known.

$$\ln\left(\frac{P_1}{P_2}\right) = \left(\frac{\Delta H_{\text{vap}}}{R}\right)\left(\left(\frac{1}{T_2}\right) - \left(\frac{1}{T_1}\right)\right) \quad (2)$$

$$p_1 = p_2 e^{\left(\left(\frac{\Delta H_{\text{vap}}}{8.314}\right)\left(\left(\frac{1}{293.15}\right)-\left(\frac{1}{298.15}\right)\right)\right)}$$

The enthalpy of vaporization (ΔH_{vap}) is the molar amount of energy required to transform the species from a liquid to a gas. ΔH_{vap} values were collected from the NIST WebBook (Matthew, et al, 2007). The vapor pressure of the species at 293.15 K is represented by p_2. T_2 is 293.15 K and T_1 is the temperature at which the samples were collected (298.15 K).

The sub-cooled vapor pressures were calculated using Equation 3, below, to determine the vapor pressure when solid compounds dissolve in liquids (Lipkind et al, 2008).

$$\ln\left(\frac{P_{\mathrm{L}}}{P_{\mathrm{S}}}\right) = \left(\frac{\Delta H_{\mathrm{fus}}}{R}\right)\left(1 - \frac{T_m}{T_2}\right) \quad (3)$$

$$p_{\mathrm{L}} = p_{\mathrm{S}} e^{\left(\left(\frac{\Delta H_{\mathrm{fus}}}{8.314}\right)\left(1 - \frac{T_{\mathrm{m}}}{T_2}\right)\right)}$$

The vapor pressure for a pure solid compound is represented by p_s, and T_2 is the target temperature (298.15 K). T_m is the melting point of a compound in kelvin. The enthalpy of fusion (ΔH_{fus}) of a substance is the energy required when a solid substance is transformed into a liquid. ΔH_{fus} for each compound was collected from NIST WebBook.

Solutions of the volatile and medium-volatile compound mixtures were prepared differently from those for the less-volatile compound mixture, as they would be used in different experiments. The volatile and medium-volatile compounds have sufficient volatilities that a small gas sample is adequate in such work (Figure 28); the less-volatile compounds are best studied with active gas generation (Figure 29).

For the 18 volatile and medium volatile compunds, three replicate samples were prepared in 155 mL glass containers. Each glass bottle contained 5 mL of 50:50 PG and GL mixture by volume with the final solution-phase concentrations of each of the 18 target compounds ranging from 0.01 to 1.3 µg/µL based on their volatility and sensitivity in the GC/MS system (Appendix J). Sample mixtures in 155 ml of glass containers were allowed to equilibrate for approximately 3 hours before sample collection.

Less volatile compound mixtures were placed in a 60 mL clear borosilicate VOA vial (Thermo Scientific Inc., Texas) with a 0.125 inch PTFE/silicone septum held in place by a retainer ring inside the cap. The vial contained 25 mL of 50:50 PG and GL mixture and 19 less volatile compounds, the final solution phase concentration of each compound ranged from 1.0 to 9.2 μg/μL. The concentration of each of these compounds is given in Appendix J. Nicotine was included in this group. Solutions were prepared the day preceding the gas sampling.

Separate experiments were also conducted with nicotine by itself. The same type of vial was used as in the less volatile compound mixture experiments. The vial contained 25 mL of a 50:50 PG and GL mixture, and a 1:1 molar ratio mixture of nicotine and ammonia were added to produce a 4 μg/μL nicotine concentration. Solutions were prepared the day preceding the gas sampling.

3.2.2. Sample Collection

3.2.2.1. Sample Collection and Analyses by GC/MS for the Volatile and Medium Volatile Compounds

Three 75 μL gas-phase samples from the headspace of the 2 L standard bottles were collected using 100 μL gas-tight syringes (Hamilton Company Inc., Nevada) and directly injected into the GC/MS (see Figure 30). Similarly, five 75 μL replicates of headspace samples were collected using a 100 μL gas-tight syringe from each of three 155 mL sample mixture bottles and directly injected into the GC/MS (see Figure 30). Each set of trials was performed sequentially from replicate 1 to 3. Three, 75 μL headspace samples

were collected from a mixture of 50:50 PG and GL at the beginning of the experiment to check for any analytical carryover of compounds in the system (blank correction).

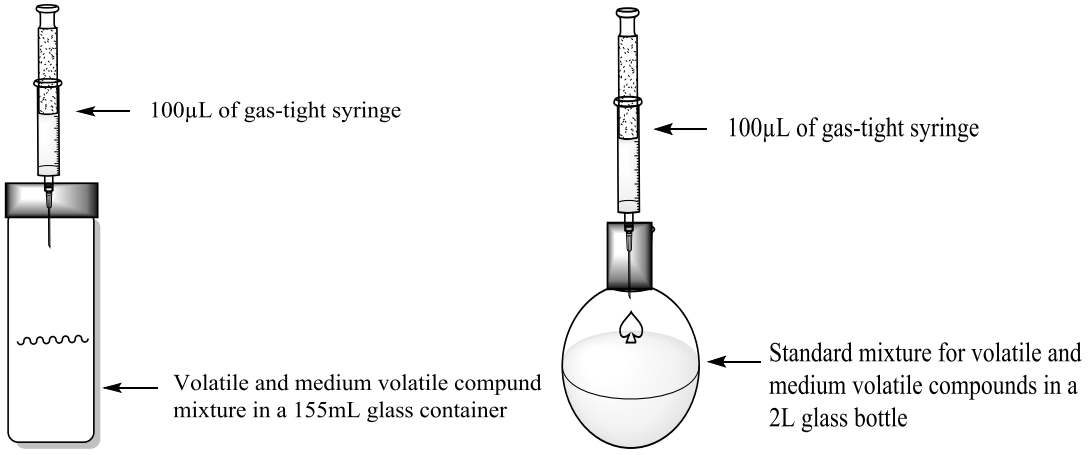

Figure 30*. Headspace gas-phase sample collection apparatus for volatile and medium volatile compounds.*

GC/MS analysis was carried out with an Agilent 7890A GC (Santa Clara, CA) coupled with an Agilent 5975C inert XL EI/CI MSD and operated in electron ionization (70 eV) mode. The GC was outfitted with a Rxi-624Sil MS (Restek Inc., Bellefonte, PA) fused silica capillary GC column (30 m length, 0.25 mm i.d., and 1.4 µm film thickness).

The initial temperature of the GC oven was 40 °C with a hold for 3.5 min. Ramping to 100 °C at a rate of 12 °C/min followed, and then the temperature was increased to 250 °C at a rate of 15 °C/min. The temperature at the inlet injection port was 235 °C with constant helium flow of 1 mL/min. The inlet split ratio was 5:1 with a flow rate of 5 mL/min. The MSD transfer line temperature was 250 °C; the ion source temperature was

220 °C, and the quadrupole temperature was 150 °C. The electron multiplier was set at 1529 V. The mass-to-charge range analyzed was 34-300 m/z.

3.2.2.2. Gas-Phase Sample Collection for the Less Volatile Compounds

A schematic of the low-volatility gas collection apparatus is shown below in Figure 31. A steady flow of 10 mL/min N_2 gas entered the sample container through a 0.32 mm uncoated capillary column which was immersed in the sample mixture to produce bubbles. A stir bar was used in the sample container to maintain solution homogeneity and promote phase equilibration. Gas samples were collected from the sample container through a 0.45 mm uncoated capillary column connected to an ATD cartridge loaded with 100 mg of 35/60 mesh Tenax TA and 200 mg of 60/80 mesh Carbograph 1 TD (Camsco Inc., Houston, TX). A syringe pump (Model NE-1010, New Era Pump Systems Inc., Farmingdale, NY) was used to draw the gas sample through the cartridge. A 1 L Tedlar bag (Model 24633 Supelco Inc., Bellefonte, PA) was connected to a three-way "T" valve at the connection between the ATD cartridge and syringe pump to collect the exhausted gas phase sample from the syringe pump in order to verify sample volume. Prior to sample collection, three 200 mL sample blanks were taken in the same manner used for sample collection but with an empty vial. Five replicates each of three different sample volumes were collected: 200 mL, 100 mL, and 50 mL. Four replicates each of 200 mL and 100 mL samples were collected for the mixture of nicotine and ammonia in 25 mL of PG and GL.

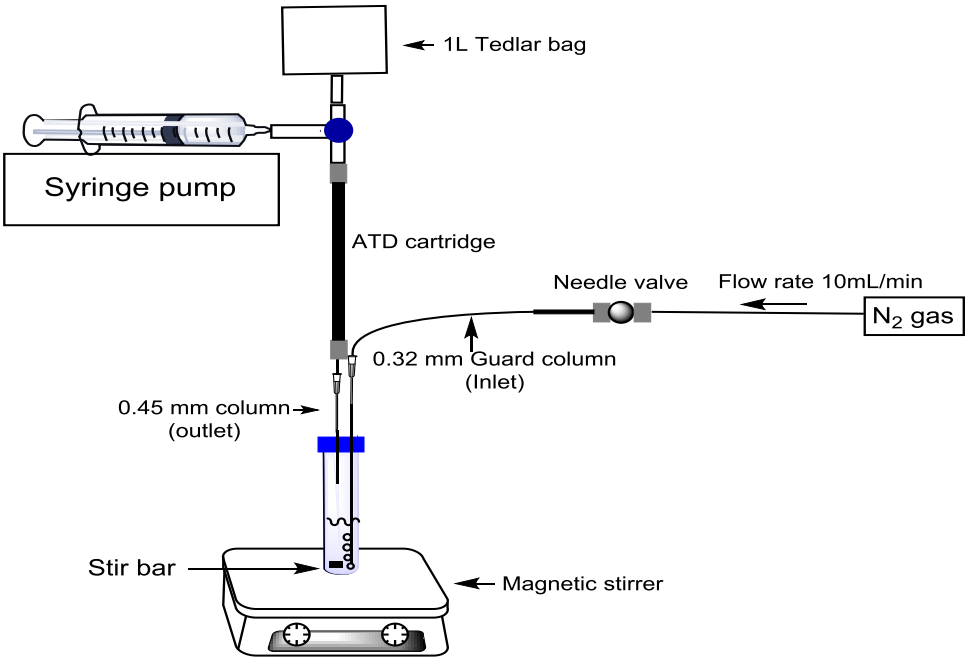

Figure 31. *Headspace gas phase sample collection apparatus for less volatile compounds.*

3.2.2.3. Gas-Phase Sample in ATD Cartridges Analyses by GC/MS for Less Volatile Compounds

All ATD cartridges were desorbed for 10 minutes at 285 °C at a desorption flow of 40 mL/min and an inlet split flow of 25 mL/min. The desorption stream was trapped at -10 °C on an intermediate "Tenax trap". The trap was then thermally desorbed at 295 °C for 4 minutes at 25 psi constant pressure helium and an outlet split flow of 20 mL/min. The non-split portion of the desorption gas stream was passed onto the GC column of the above mentioned Agilent GC/MS system via a heated transfer line (at 225 °C). The initial temperature of the GC oven was 40 °C with a hold for 2 min. Ramping to 100 °C with a

rate of 10 °C/min followed, then the temperature was increased to 280 °C at a rate of 12 °C/min. The temperature of the MSD transfer line was 275 °C, the ion source temperature was 226 °C, and the quadrupole temperature was 150 °C. The electron multiplier was set at 1529 V. The mass-to-charge range analyzed was 34-300 m/z. Eight standard solutions in isopropyl alcohol with concentrations ranging from 1 to 350 ng/µL were prepared. 4 µL of a standard solution was spiked into the inlet end of eight separate cartridges to contain a final mass of 2 to 1400 ng of chemicals in each cartridge. The cartridges were then purged for 10 minutes by a 50 mL/min flow of helium gas and thermally desorbed by a TurboMatrix 650 ATD unit (PerkinElmer, Waltham, MA). Prior to the thermal desorption, each ATD cartridge was amended with 20 ng of fluorobenzene, which served as an internal standard.

3.2.2.4. Liquid Simulants of PM Phase Sample Analyses by GC/MS for Less Volatile Compounds

The Agilent GC/MS detailed in Section 3.2.2.1 was used to analyze the liquid simulants of the PM phase samples for less volatile compounds. An Agilent 7693 autosampler was also used to inject the volume of 1 µL of each liquid sample. Initial temperature of the GC oven was 40 °C with a hold for 2 min. Ramping to 100 °C at a rate of 10 °C/min followed, and then the temperature was increased to 280 °C at a rate of 12 °C /min. The temperature of the front inlet injection port was held at 235 °C. The inlet split ratio was 10:1 with a flow rate of 10 mL/min. The MSD transfer line temperature was 275 °C; the

ion source temperature was 226 °C, and the quadrupole was 150 °C. The electron multiplier was set at 1529 V. The mass-to-charge range analyzed was 34-300 m/z.
Six standard solutions with concentrations ranging from 10 to 900 ng/µL were prepared in isopropyl alcohol (IPA). After the headspace gas sample collections for the less volatile compound mixture, aliquots of 25 µL, 50 µL, and 100 µL of the sample mixture were taken and diluted with enough IPA to make a final volume of 1000 uL in a GC/MS vial (RESTEK, PA). Two replicates of each sample mixture dilution were prepared. The concentrations of dilutions of the sample mixture ranged from 20 to 900 ng/µL. These standards and dilutions of the sample mixture in IPA were analyzed by GC/MS.

3.2.3. Blank Correction

Three blank samples were averaged before the blank correction. All final chemical concentrations were blank corrected. The average chemicals concentration in three blank cartridges was subtracted from the initial concentration of chemicals in a sample cartridge for the blank correction

3.2.4. Calculating the Gas/Particle Partitioning

3.2.4.1. Volatile and Medium Volatile Compounds

Using the calibration standards, calibration curves were made for each chemical allowing the calculation of gas phase concentration ($\mu g/m^3$) for each compound (experiments in Section 3.2.2.1). The total mass in the gas phase for a given compound was subtracted

from its initial mass in the experimental bottle to give the final mass in the PM phase. The concentration in the PM phase (μg/μg) was calculated using Equation (4).

$$\frac{\text{Final mass in PM phase (μg)}}{\text{Sample volume (mL)} \times \text{density of PG/GL mixture } \left(\frac{\text{g}}{\text{mL}}\right) \times 1{,}000{,}000(\mu\text{g/g})} \quad (4)$$

An experimental gas/particle coefficient (K_p) for each compound was calculated using Equation 5 (Pankow, 2017).

$$K_p \left(\frac{\text{m}^3}{\mu\text{g}}\right) = \frac{\text{Concentration in the particle phase } \left(\frac{\mu\text{g}}{\mu\text{g}}\right)}{\text{Concentration in the gas} - \text{phase } \left(\frac{\mu\text{g}}{m^3}\right)} \quad (5)$$

A theoretical gas/particle coefficient (K_p) value for each chemical was calculated using Equation 6 (Pankow, 2017). The activity coefficient was assumed to be 14 for benzene and temporarily assumed to be 1 for other compounds.

$$K_p \left(\frac{m^3}{\mu\text{g}}\right) = \frac{\text{RT}}{10^6 \overline{MW} \zeta_i P_{L,i}^o} \quad (6)$$

In Equation (6), R is the gas constant (8.2×10^5 (m^3-atm)/(mol-K)). T is the temperature in Kelvin, $\overline{\text{MW}}$ is the average molecular weight in the liquid phase (84 g/mol). ζ_i is the mole fraction scale activity coefficient of species i in liquid phase. $p_{L,i}^o$ is the vapor pressure

(atm) of pure liquid *i* at temperature *T*. The sub-cooled vapor pressure is used for solid compounds (Pankow 1994; Pankow 2017).

3.2.4.2. Calculation for the Gas/Particle Partitioning of Less Volatile Compounds

Response factors of each chemical in both gas-phase and particle phase were calculated using standards.

$$\text{Response Factor} = \frac{\dfrac{\text{Peak Area of a chemical}}{\text{Mass of the chemicals in a cartridge (ng)}}}{\dfrac{\text{Peak area of fluorobenzene}}{20\ \text{ng}}} \quad (7)$$

The concentrations of chemicals in the gas-phase were calculated using the equation below.

$$\text{Concentration in the gas-phase } (\mu g/m^3) = \frac{\text{(Peak Area of a chemical / Response Factor)}}{\text{(Peak area of fluorobenzene / 20 ng)}} \text{ / Sample volume (mL)} \times 1000 \quad (8)$$

The concentrations of chemicals in particle phase were calculated using Equation (9), below.

$$\text{Concentration in the particle phase } (\mu g/\mu g) = \frac{\text{(Peak Area of a chemical / Response Factor)}}{\text{(Peak area of 1,2,3-Trichlorobenzene / 0.041 µg)}} \frac{\text{/ Sample volume (mL) /}}{\text{density of PG+GL mixture (1.15g/mL) / 1000}} \quad (9)$$

The gas/particle partitioning coefficient (K_p) for each chemical was calculated using Equation 10 (Pankow, 2004; Pankow, 2017).

$$K_{p,i}\left(\frac{m^3}{\mu g}\right) = \frac{c_{p,i}\left(\frac{\mu g}{\mu g}\right)}{c_{g,i}\left(\frac{\mu g}{m^3}\right)} \quad (10)$$

3.2.4.3. Calculation for the Equilibrium Fraction in the Gas-Phase of Chemicals

The equilibrium fraction in the gas-phase of each species (*i*) was calculated using the equation below.

$$f_{g,i} = \frac{1}{1 + c_{p,i}\mathrm{TPM}} \quad (11)$$

The TPM value used for the calculation was 2.24×10^{8} (Pankow et al., 2017).

3.3. Results and Discussion

3.3.1. Gas/Particle Partitioning Constant (K_p) of Chemicals in the Aerosols Emitted from Vaping E-cigarettes

The theoretical K_p values for each species was calculated based on its activity coefficient (ζ_i) and vapor pressure $p^{\circ}_{L,i}$ using Equation 6. The activity coefficients for polar species such as acetaldehyde, benzaldehyde, and nicotine are expected to be close to 1. In contrast, the activity coefficient of benzene is approximately 14, and the activity coefficients of other non-polar compounds are also greater than 1 (Pankow, 2017). Appendix K provides estimated theoretical K_p values for the 37 compounds. The theoretical K_p value for a compound is dependent on both its activity coefficient and vapor pressure (Equation 6). However, vapor pressure is the primary factor that determines K_p. The experimental log K_p values for16 out of the 37 compounds (including diacetyl, benzene, and nicotine) are close to their theoretical K_p values (Figure 32). The experimental K_p values of non-polar compounds such as toluene, limonene, p-xylene, p-cymene, aromadendrene, and ethyl benzene are smaller than theoretical K_p values if γ values are taken as 1, which is undoubtedly incorrect.

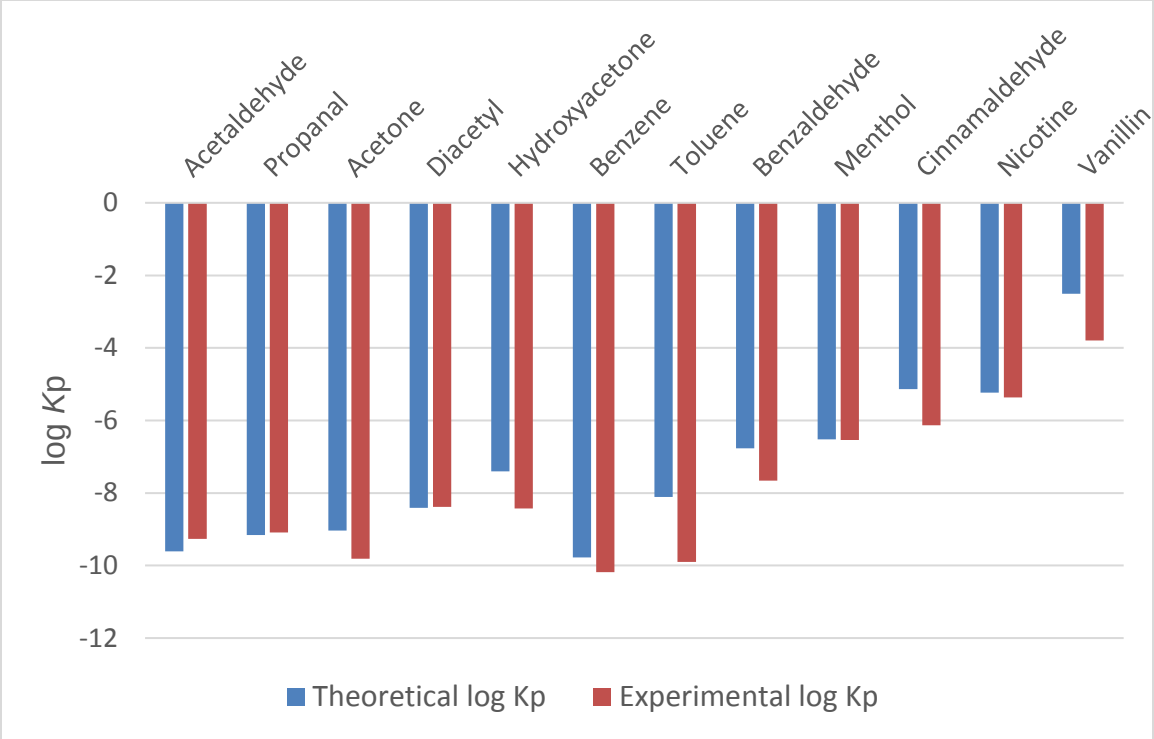

Figure 32. *Theoretical log K_p vs. experimental log K_p*

Nicotine can exist in two different forms in the aerosols emitted from vaping e-liquids: free-base (Nic) and mono-protonated ($NicH^+$) (El-Hellani, Ahmad, et al, 2015; Pankow, 2017). Here, the experimental log K_p values of free-base nicotine were determined (Figure 33). The results indicate that the experimental log K_p of free-base nicotine is close to the theoretical log K_p of nicotine based on its vapor pressure in a pure liquid.

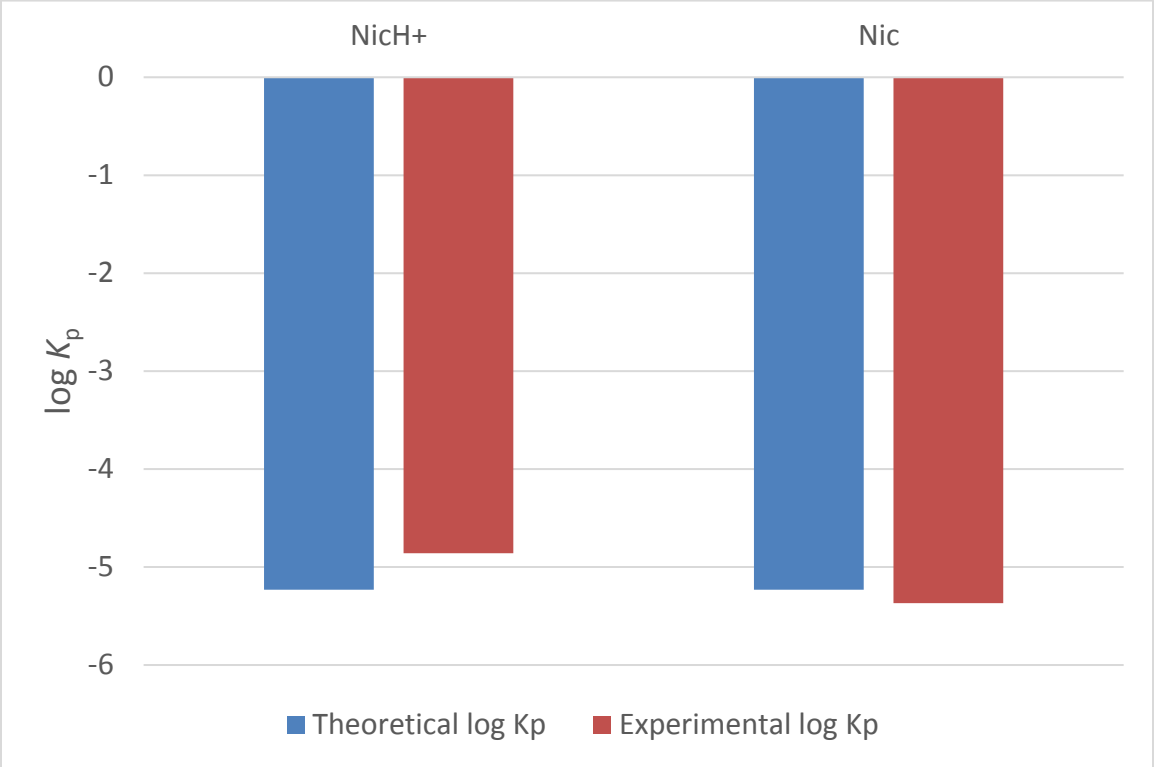

Figure 33. *Comparison of experimental log K_p between nicotine and nicotine with ammonia*

3.3.2. General Trend of Gas/Particle Paritioning Constant (K_p)

A summary of gas/particle partitioning coefficient for the species of interest is given in Figure 34. The more volatile compounds and non-polar compounds in PG and GL mixtures tend to have lower K_p values.

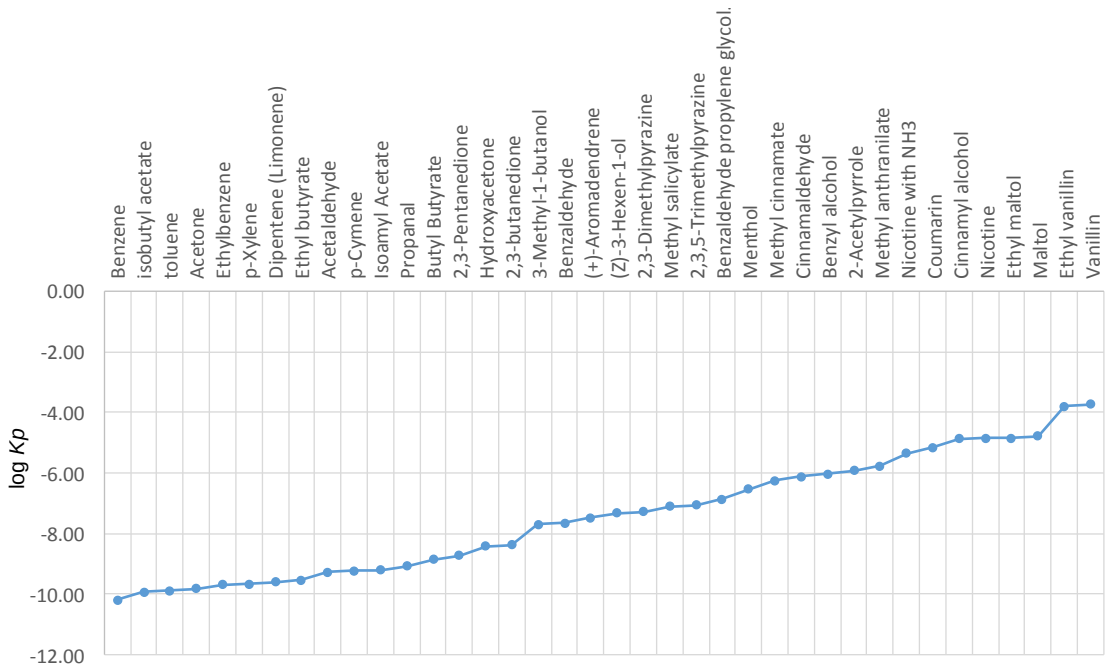

Figure 34. *Experimental log K_p values for compounds*

3.3.3. The Correlation between log $K_{p,i}$ and log Vapor Pressure of Pure Liquid ($p^{\circ}_{L,i}$)

Figure 35 shows the relationship between log $K_{p,i}$ and log $p^{\circ}_{L,i}$. As the log vapor pressure of a compound (i) increases, the log K_p value decreases. This means that as the vapor pressure of a compound increases, the compound is more volatile and more likely to be present in the gas phase at a given TPM value. This trend is observed by the inverse correlation seen in Figure 35. The slope of the trend line of the graph between experimental log $K_{p,i}$ and log $p^{\circ}_{L,i}$ is close to -0.9, which is close to the theoretical value of -1 that would be obtained if all γ values were the same.

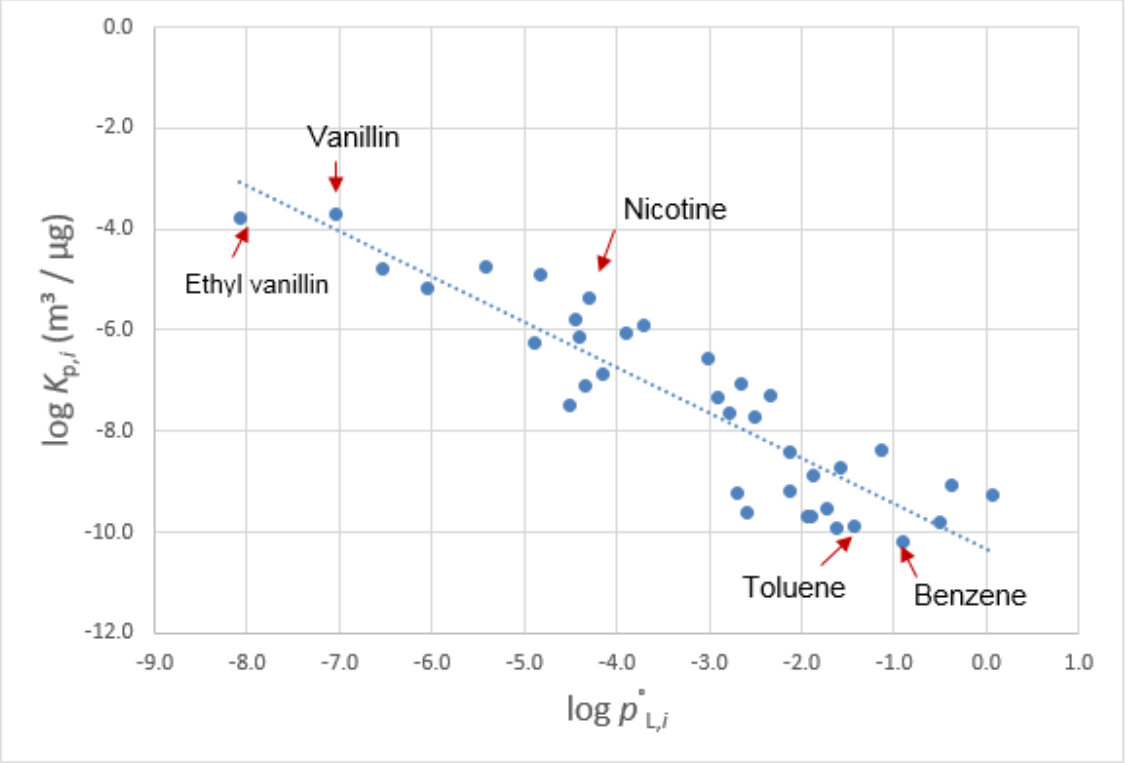

Figure 35. log $K_{p,i}$ versus log $p^{\circ}_{L,i}$

3.3.4. The Relationship between the Fraction of *i* in the Gas-Phase ($f_{g,i}$) and log $p^{\circ}_{L,i}$

Understanding the fraction of *i* in the gas phase ($f_{g,i}$) is important in order to comprehend the effect of the chemical when the chemical is introduced to the human body. When $f_{g,i}$ of a compound is close to 1, most of the compound is in the gas phase (Pankow, 2017). On the other hand, when $f_{g,i}$ of a compound is close to zero, most of the compound is in the particle phase so that deposition in the respiratory tract is limited to where particles deposit (Pankow, 2017). Values for $f_{g,i}$ were calculated using a TPM value of 8.35 (Appendix L). The experimental f_g values of volatile compounds, such as benzene, acetaldehyde, propanal, toluene, are close to one, whereas the experimental f_g values of non-volatile compounds are close to zero as expected (Figure 36).

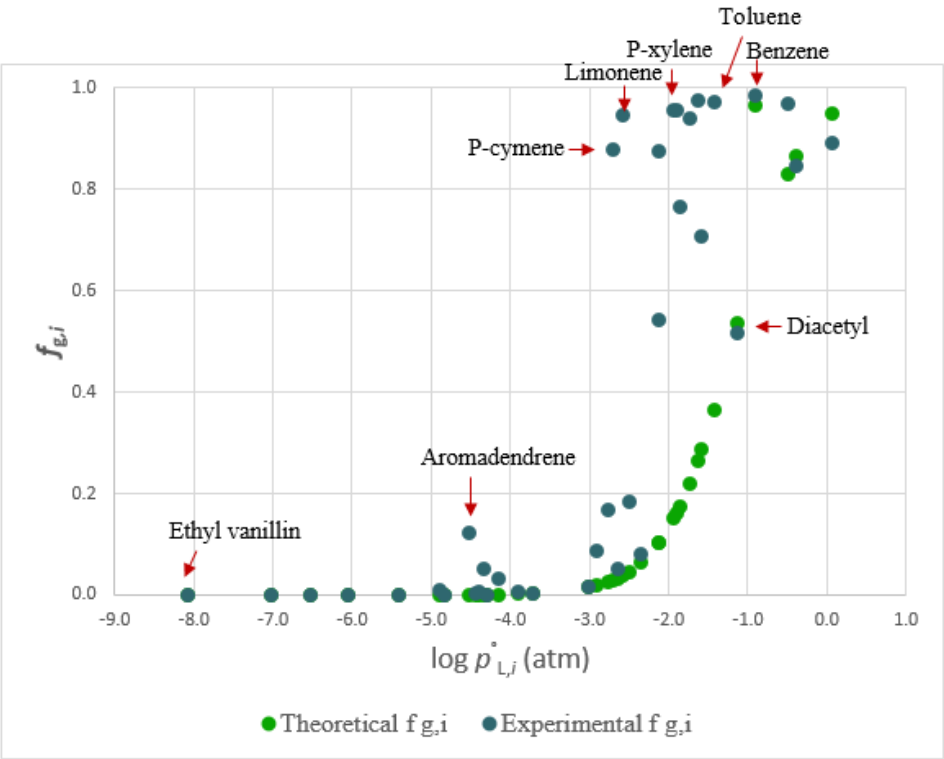

Figure 36. *$f_{g,i}$ versus log $p^{\circ}_{L,i}$ for the 37 tested compounds*

3.4. Conclusions

Understanding the phase distribution of each compound in the aerosols emitted from vaping e-cigarette liquids is crucial to understanding where the compound will deposit when the compound is introduced to the human body. Volatile compounds with small K_p values will reside predominantly in the gas phase. In contrast, less volatile compounds that have large K_p will predominantly reside in the particle phase. The f_g values of volatile compounds including acetaldehyde, propanal, acetone, and benzene are close to "1" for TPM values such as 2.24×10^8, while the f_g values of less volatile compounds are close to zero. Agreement with theory for compounds with known activity coefficient in PG and GL is a good demonstration that theory can be used to predict K_p values for the other compounds.

References

"Acetaldehyde." *Welcome to the NIST WebBook.* National Institute of Standards and Technology, n.d. Web. 13 Mar. 2017.

ATSDR, Toxicological profile for xylene, *U.S Department of Health and Human Services, public health service*, Agency for toxic substance and disease registry.1993

Bawn, C. E. H. "The Stability of Free Radicals."*Transactions of the Faraday Society* 34 (1938): 598-607. Web.

"Benzene." *Welcome to the NIST WebBook.* National Institute of Standards and Technology, n.d. Web. 13 Mar. 2017.

Blitz, MA, MS Beasley, Mj Pilling, and Sh Robertson. "Formation of the Propargyl Radical in the Reaction of (CH2)-C-1 and C2H2: Experiment and Modelling."*Physical Chemistry Chemical Physics* 2.4 (2000): 805-12. Web.

"2,3-Butanidione." *Welcome to the NIST WebBook.* National Institute of Standards and Technology, n.d. Web. 13 Mar. 2017.

Carrero, Alicia, Jose Calles, Lourdes Garcia-Moreno, and Arturo Vizcaine. "Production of Renewable Hydrogen from Glycerol Steam Reforming over Bimetallic Ni-(Cu, Co, Cr) Catalysts Supported on SBA-15 Silica." *Catalysts* 7.2 (2017): 55. Web.

Centers for Disease Control and Prevention (CDC). "Toxic Substances Portal-Toluene." *Centers for Disease Control and Prevention*. Centers for Disease Control and Prevention, 21 Jan. 2015. Web. 09 May 2017.

Centers for Disease Control and Prevention (CDC). Quickstats: Percent Distribution of Cigarette Smoking Status among Adult Current E-Cigarette Users, by

Age Group, National Health Interview Survey, United States, 2015.*Morbidity and Mortality Weekly Report*. October 28, 2016; 65(42):1177.

Chin, Chuang-Wei, et al. "Reducing Byproduct Formation during Conversion of Glycerol to Propylene Glycol."*Industrial &Amp; Engineering Chemistry Research*, vol. 47, no. 18, 2008, pp. 6878–6884.

Corey, C., et al. (2013). Notes from the field: Electronic cigarette use among middle and high school students - United States, 2011–2012. MMWR Morbidity Mortality Weekly Report, 62, 729. http://www.cdc.gov/ mmwr/preview/mmwrhtml/mm6235a6.htm

Ding, Zhongyi, Joseph Chiu, Weihua Jin. Process for Converting Glycerin into Propylene Glycol. Gtc Technology US Lic, assignee. Patent US8394999 B2. 12 Mar. 2013. Print.

Duarte-Davidson, R, Courage, C, Rushton, L, and Levy, L. "Benzene in the Environment: An Assessment of the Potential Risks to the Health of the Population."*Occupational and Environmental Medicine* 58.1 (2001): 2-13. Web.

El-Hellani, Ahmad, et al. "Free-Base and Protonated Nicotine in Electronic Cigarette Liquids and Aerosols." *Chemical Research in Toxicology*, vol. 28, no. 8, 2015, pp. 1532–7.

'Facts about Benzene." *Centers for Disease Control and Prevention*. Center for Disease Control and Prevention, 14 Feb. 2013. Web. 09 May 2017.

Farsalinos, K.E., Romagna, G., Tsiapras, D., Kyrzopoulos, S., Spyrou, A., Voudris, V., 2013a. Impact of flavour variability on electronic cigarette use experience: an internet survey. Int. J. Environ. Res. Public Health 10, 7272e7282.

Fay, Mike. *Toxicological Profile for Xylene*. Atlanta, GA: U.S. Department of Health and Human Setvices, Public Health Service, Agency for Toxic Substance and Disease Registry, 2007. Print.

Fedan, J.S. "Popcorn Worker's Lung: In Vitro Exposure to Diacetyl, an Ingredient in Microwave Popcorn Butter Flavoring, Increases Reactivity to Methacholine."*Toxicology and Applied Pharmacology* 215.1 (2006): Toxicology and Applied Pharmacology, 2006, Vol.215(1). Web.

Geiss, et al. "Correlation of Volatile Carbonyl Yields Emitted by e-Cigarettes with the Temperature of the Heating Coil and the Perceived Sensorial Quality of the Generated Vapours."*International Journal of Hygiene and Environmental Health*, vol. 219, no. 3, 2016, pp. 268–277.

Lipkind, D., Hanshaw, W., & Chickos, J. (2009). Hypothetical Thermodynamic Properties. Subcooled Vaporization Enthalpies and Vapor Pressures of Polyaromatic Heterocycles and Related Compounds. *Journal Of Chemical And Engineering Data*, *54*(10), 2930-2943.

Harrell, Weaver, Loukas, Creamer, Marti, Jackson, . . . Eriksen. (2017). Flavored e-cigarette use: Characterizing youth, young adult, and adult users. *Preventive Medicine Reports, 5*, 33-40.

Hua, My, Henry Yip, and Prue Talbot. "Mining Data on Usage of Electronic Nicotine Delivery Systems (ENDS) from YouTube Videos." *Tobacco Control* 22.2 (2013): 103. Web

"IARC Monographs on the Evaluation of Carcinogenic Risks to Humans." *IARC Monographs-Classifications*. International Agency for Research on Cancer, n.d. Web. 08 May 2017.

"Introducing JUUL – A Real Alternative to Cigarettes." *JUUL*. n.d. Web. 15 May 2017.

Jensen, Robert, Peyton, David H., Abramson, Jonathan, Atkinson, Dean, and Stuart, David.*Thermal Decomposition of Electronic Cigarette Liquids* (2016): ProQuest Dissertations and Theses. Web.

Kandyala, Reena, Sumanth Phani Raghavendra, and Saraswathi Rajasekharan. "Xylene: An Overview of Its Health Hazards and Preventive Measures."*Journal of Oral and Maxillofacial Pathology* 14.1 (2010): 1-5. Web.

"Known and Probable Human Carcinogens." *America Cancer Society*. Amer, n.d. Web. 08 May. 2017.

Kreiss, Gomaa, Kullman, Fedan, Simoes, and Enright. "Clinical Bronchiolitis Obliterans in Workers at a Microwave-Popcorn Plant." *The New England Journal of Medicine* 347.5 (2002): 330-38. Web.

Lachenmeier, Dirk W., Fotis Kanteres, and Jürgen Rehm. "Carcinogenicity of Acetaldehyde in Alcoholic Beverages: Risk Assessment outside Ethanol Metabolism."*Addiction* 104.4 (2009): 533-50. Web.

Laidler, K. J., and M. T. H. Liu. "The Mechanism of the Acetaldehyde Pyrolysis."*Proceedings of the Royal Society of London. Series A, Mathematical and Physical Sciences (1934-1990)* 297.1450 (1967): 365-75. Web.

Levy, M., M. Sterinberg, and M. Szwarc. “The Addition of Methyl Radicals to Benzene.” *Journal of the American Chemical Society* 76.13 (1954): 3439-441. Web.

Liu, Michael T. H., and K. J. Laidler. "Elementary Processes in the Acetaldehyde Pyrolysis."*Canadian Journal of Chemistry*46.4 (1968): 479-90. Web.

Liu, Shao-Quan, and Gordon J. Pilone. "An Overview of Formation and Roles of Acetaldehyde in Winemaking with Emphasis on Microbiological Implications. "*International Journal of Food Science & Technology* 35.1 (2000): 49-61. Web.

Luttrell, William E., Warren W. Jederberg, and Kenneth R. Still. *Toxicology Principles for the Industrial Hygienist*. Fairfax, VA: AIHA, 2008. Print.

Luttrell, and Ngendahimana. "Toxic Tips: Toluene."*Journal of Chemical Health & Safety* 19.3 (2012): 34-35. Web.

Margalith, P.Z. (1981) Flavour Microbiology. Charles C. Thomas Publishers, Springfield, IL.

Mcrobbie, H., Bullen, C., Hartmann-Boyce, J., & Hajek, P. (2014). Electronic cigarettes for smoking cessation and reduction. *Cochrane Database Of Systematic Reviews,12*(12), CD010216.

National Cancer Institute. “Benzene.” National Cancer Institute. N.P., n.d. Web. 08 May. 2017.

"National Adult Tobacco Survey (NATS)." *Centers for Disease Control and Prevention*. Centers for Disease Control and Prevention,01 Aug. 2016. Web. 24 July 2017.

"2011 National Air Toxics Assessment: Assessment Result." *EPA*. Environmental Protection Agency, 26 Dec. 2016. Web 21 May 2017.

Nimlos, Mark R., Blanksby, Stephen J., Johnson, David K., Xianghong Qian, and Himmel, Michael E. "Mechanisms of Glycerol Dehydration."*Journal of Physical Chemistry A* 110.18 (2006): 6145. Web.

Paine, Pithawalla, Naworal, and Thomas. "Carbohydrate Pyrolysis Mechanisms from Isotopic Labeling: Part 1: The Pyrolysis of Glycerin: Discovery of Competing Fragmentation Mechanisms Affording Acetaldehyde and Formaldehyde and the Implications for Carbohydrate Pyrolysis."*Journal of Analytical and Applied Pyrolysis* 80.2 (2007): 297-311. Web.

Pankow, James F. "Calculating Compound Dependent Gas-droplet Distributions in Aerosols of Propylene Glycol and Glycerol from Electronic Cigarettes." *Journal of Aerosol Science* 107 (2017): 9-13. Web.

Pankow, James F., Kilsun Kim, Kevin J. McWhirter, Wentai Luo, Jorge O. Escobedo, Robert M. Strongin, Anna K. Duell, David H. Peyton, and Raymond Niaura. "Benzene Formation in Electronic Cigarettes."*PLOS ONE* 12.3 (2017): PLOS ONE, 2017, Vol.12(3). Web.

Pepper, J., Ribisl, K., & Brewer, N. (2016). Adolescents' interest in trying flavoured e-cigarettes. *Tobacco Control, 25*(Suppl 2), Ii62-ii66.

Prosanov, I. Yu., and Uvarov, N. F. “Electrical Properties of Dehydrated Polyvinyl Alcohol.(Report).”*Physics of the Solid State*, vol. 54, no. 2, 2012, p. 421-24.

Ridley, Matt. "'Quitting Is Suffering': Hon Lik, Life-saving Inventor of the E-cigarette, on Why He Did It."*Spectator* 328.9747 (2015): 20. Web.

Robertson, W. W., E. M. Magee, and F. A. Matsen. "The Formation of Benzene in the Pyrolysis of Acetylene."*Journal of Applied Chemistry* 8.7 (1958): 401-02. Web.

Robinson, R. J., E. C. Hensel, P. N. Morabito, and K. A. Roundtree. "Electronic Cigarette Topography in the Natural Environment." 10.6 (2015): E0129296. Web.

Rossiter, et al. “An Investigation of the Degradation of Aqueous Ethylene Glycol and Propylene Glycol Solutions Using Ion Chromatography.”*Solar Energy Materials*, vol. 11, no. 5, 1985, pp. 455–467.

R. Paul Jensen, Robert M. Strongin, and David H. Peyton. "Solvent Chemistry in the Electronic Cigarette Reaction Vessel." *Scientific Reports* 7 (2017). Web.

Runion, H.E. "Benzene in Gasoline."*Am. Ind. Hyg. Assoc. J.* 36.5 (1975): Am. Ind. Hyg. Assoc. J., 1975, Vol.36(5). Web.

Sakurai, Nakadaira, Hosomi, Eriyama, Hirama, and Kabuto. "ChemInform Abstract: Chemistry of Organosilicon Compounds. 193. Intramolecular Cyclotrimerization of Macrocyclic and Triynes with Group 6 Metal Carbonyls. The Formation of Fulvene and Benzene.” *Chemischer Informationsdienst* 16.17 (1985): No. Web.

Sanchez, Nazly E., Alicia Callejas, Angela Millera, Rafael Bilbao, and Maria U. Alzueta. "Influence of the Oxygen Presence on Polycyclic Aromatic Hydrocarbon (PAH)

Formation from Acetylene Pyrolysis under Sooting Conditions."*Energy & Fuels* 27.11 (2013): 7081-088. Web.

Singh, T., et al. (2016). Tobacco Use Among Middle and High School Students — United States, 2011–2015. *MMWR Morbidity Mortality Weekly Report, 65(14);* 361-367.

Sleiman, Mohamad, Jennifer M Logue, V Nahuel Montesinos, Marion L Russell, Marta I Litter, Lara A Gundel, and Hugo Destaillats. "Emissions from Electronic Cigarettes: Key Parameters Affecting the Release of Harmful Chemicals."*Environmental Science & Technology* 50.17 (2016): 9644-51. Web.

Tang, Weiyong, Robert S Tranter, and Kenneth Brezinsky. "An Optimized Semidetailed Submechanism of Benzene Formation from Propargyl Recombination."*The Journal of Physical Chemistry. A* 110.6 (2006): 2165-75. Web.

Tanielyan, Setrak K., et al. "An Efficient, Selective Process for the Conversion of Glycerol to Propylene Glycol Using Fixed Bed Raney Copper Catalysts."*Organic Process Research &Amp; Development*, vol. 18, no. 11, 2014, pp. 1419–1426.

"Toluene." *Welcome to the NIST WebBook*. National Institute of Standards and Technology, n.d. Web. 13 Mar. 2017.

Tuck, M. W.; Tilley S. N. Process. Patent application PCT/GB2006/ 050181.

U.S. Dapartment of Health and Human Services, "Acetaldehyde."*Report on Carcinogens: Carcinogen Profiles* 12 (2011): 21-4. Print.

U.S. Department of Health and Human Services. The Health Consequences of Smoking-50 Years of Progress: A Report of the Surgeon General. 2014.

Wallace, L A. "Major Sources of Benzene Exposure."*Environmental Health Perspectives* 82 (1989): 165-69. Web.

Weiyong Tang, Tranter, Robert S., and Brezinsky, Kenneth. "Isomeric Product Distribution from the Self-reaction of Propargyl Radicals."*Journal of Physical Chemistry A* 109.27 (2005): 6056-65. Web.

"Xylene." *Welcome to the NIST WebBook*. National Institute of Standards and Technology, n.d. Web. 13 Mar. 2017.

Zhao, Shu, Guo, and Zhu. "Effects of Design Parameters and Puff Topography on Heating Coil Temperature and Mainstream Aerosols in Electronic Cigarettes."*Atmospheric Environment* 134 (2016): 61-69. Web.

Zhou, Ying, Chaoyang Li, Mark A. J. Huijbregts, and M. Moiz Mumtaz. "Carcinogenic Air Toxics Exposure and Their Cancer-Related Health Impacts in the United States." 10.10 (2015): PLOS ONE, Oct 7, 2015, Vol.10(10). Web.

Appendix A. *Benzene and total particulate matter (TPM) generated in e-cigarette aerosols using EVOD. (N.D = not Detected)*

Mixtures	setting (watts)	number of replicates	Benzene produced per volume (ng/L) (±1SD)	Benzene produced per a puff (ng/puff) (±1SD)	Benzene produced per g of e-liquid vaped (µg/g) (±1SD)	The amount of e-liquid used per a puff (mg/puff) (±1SD)	Aerosol log TPM (µg/m³) (±1SD)
PG	13	4	59 ± 20	2.9 ± 1.0	0.40 ± 0.14	7.4 ± 0.1	8.17 ± 0.00
GL	13	4	1600±1300	80 ± 67	6.6 ± 5.4	12 ± 0.5	8.37 ± 0.02
PG+GL	6	3	ND	ND	ND	6.8 ± 0.6	8.13 ± 0.04
	13	3	750±390	38 ± 20	3.2 ± 1.7	12 ± 0.2	8.37 ± 0.01
PG+GL+BA	6	3	ND	ND	ND	6.7 ± 0.6	8.15 ± 0.04
	13	3	5400±2600	270 ± 130	24 ± 12	11 ± 0.1	8.35 ± 0.00
PG+GL+Nic	6	3	9.7±14	0.5 ±0.7	0.08 ± 0.11	6.3 ± 0.3	8.09 ± 0.02
	13	3	5200±3000	260 ± 150	24 ± 14	11 ± 0.2	8.35 ± 0.01
PG+GL+BZ	6	3	21±2.2	1.0 ± 0.1	0.16 ± 0.02	6.6 ± 0.9	8.14 ± 0.06
	13	3	5000±2900	240 ± 140	23 ± 13	10 ± 0.3	8.35 ± 0.01
PG+GL+BZ+Nic	6	3	ND	ND	ND	6.8 ± 0.5	8.13 ± 0.03
	13	3	3300±680	170 ± 35	15 ± 3.3	11 ± 0.4	8.35 ± 0.01

Appendix B. *Benzene and total particute matter (TPM) generated in e-cigarette aerosols using Subtank Nano. (N.D = not Detected)*

Mixtures	setting (watts)	number of replicates	Benzene produced per volume (ng/L) (±1SD)	Benzene produced per a puff (ng/puff) (±1SD)	Benzene produced per g of e-liquid vaped (µg/g) (±1SD)	The amount of e-liquid used per a puff (mg/puff) (±1SD)	Aerosol log TPM (µg/m³) (±1SD)
PG+GL	6	3	ND	ND	ND	0.5 ± 0.5	6.88 ± 0.37
	13	3	ND	ND	ND	8.1 ± 2.1	8.19 ± 0.11
	20	3	ND	ND	ND	17 ± 1.6	8.54 ± 0.04
	25	3	ND	ND	ND	24 ± 1.4	8.68 ± 0.02
PG+GL+BA	6	3	ND	ND	ND	1.2 ± 0.2	7.36 ± 0.07
	13	3	ND	ND	ND	9.8 ± 0.3	8.28 ± 0.02
	20	3	ND	ND	ND	20 ± 4.6	8.59 ± 0.09
	25	2	ND	ND	ND	23 ± 0.8	8.65 ± 0.02
PG+GL+BA+Nic	6	3	ND	ND	ND	0.7 ± 0.4	7.13 ± 0.20
	13	3	ND	ND	ND	9.9 ± 0.9	8.29 ± 0.04
	20	3	ND	ND	ND	19 ± 0.7	8.58 ± 0.02
	25	2	66 ± 25	3.4 ± 1.3	0.11 ± 0.02	31 ± 6.8	8.77 ± 0.10
PG+GL+BZ	6	3	ND	ND	ND	1.6 ± 0.3	7.51 ± 0.07
	13	3	36 ± 0.6	1.6 ± 0.0	0.16 ± 0.01	11 ± 0.4	8.36 ± 0.02
	20	3	75 ± 13	3.4 ± 0.6	0.19 ± 0.03	18 ± 0.7	8.58 ± 0.02
	25	2	101 ± 26	4.6 ± 1.2	0.16 ± 0.01	30 ± 8.9	8.79 ± 0.13
PG+GL+BZ+Nic	6	3	ND	ND	ND	0.8 ± 0.8	7.20 ± 0.36
	13	3	24 ± 2.1	1.2 ± 0.1	0.13 ± 0.01	9.6 ± 0.9	8.28 ± 0.04
	20	3	52 ± 7.7	2.5 ± 0.3	0.14 ± 0.02	19 ± 2.5	8.57 ± 0.06
	25	3	57 ± 5.2	2.7 ± 0.3	0.12 ±0.01	24 ± 1.2	8.68 ± 0.02

Appendix C. *Datum for the overdetermined least squares fits in MATLAB for benzene*

Mass	Caliper Intensity	Relative Peak size
68	0	0
69	0	0
70	0	0
71	0	0
72	3017	0.002789
73	26818	0.024795
74	68206	0.063061
75	22695	0.020983
76	62833	0.058093
77	294515	0.272297
78	1081593	1
79	72958	0.067454
80	1486	0.001374
81	0	0
82	0	0
83	0	0
84	0	0
85	0	0
86	0	0
87	0	0
88	0	0
89	0	0
90	0	0

Equations (A=mass 78, B=mass 79, C=mass 80, D=mass 81, E=mass 82, F=mass 83, G=mass 84)

Mass 75 =A*0.020983+B*0.063061+C*0.024795+D*0.002789+E*0+F*0+G*0

mass 76 =A*0.0580293+B*0.020983+C*0.063061+D*0.024795+E*0.002789+F*0+G*0

Mass 77 =A*0.272297+B*0.0580293+C*0.020983+D*0.063061+E*0.024795+F*0.002789+G*0

Mass 78 =A*1+B*0.272297+C*0.0580293+D*0.020983+E*0.063061+F*0.024795+G*0.002789

Mass 79 =A*0.067454+B*1+C*0.272297+D*0.0580293+E*0.020983+F*0.063061+G*0.024795

Mass 80 =A*0.001374+B*0.067454+C*1+D*0.272297+E*0.0580293+F*0.020983+G*0.063061

Mass 81 =A*0+B*0.001374+C*0.067454+D*1+E*0.272297+F*0.0580293+G*0.020983

Mass 82 =A*0+B*0+C*0.001374+D*0.067454+E*1+F*0.272297+G*0.0580293

Mass 83 =A*0+B*0+C*0+D*0.001374+E*0.067454+F*1+G*0.272297

Mass 84 =A*0+B*0+C*0+D*0+E*0.001374+F*0.067454+G*1

Mass 85 =A*0+B*0+C*0+D*0+E*0+F*0.001374+G*0.067454

mass 86 =A*0+B*0+C*0+D*0+E*0+F*0+G*0.001374

Equations (A=mass 78, C=mass 80, D=mass 81, E=mass 82, G=mass 84)

Mass 75 =A*0.020983+C*0.024795+D*0.002789+E*0+G*0

mass 76 =A*0.0580293+C*0.063061+D*0.024795+E*0.002789+G*0

Mass 77 =A*0.272297++C*0.020983+D*0.063061+E*0.024795+G*0

Mass 78 =A*1+C*0.0580293+D*0.020983+E*0.063061+G*0.002789

Mass 79 =A*0.067454+C*0.272297+D*0.0580293+E*0.020983+G*0.024795

Mass 80 =A*0.001374+C*1+D*0.272297+E*0.0580293+G*0.063061

Mass 81 =A*0+C*0.067454+D*1+E*0.272297+G*0.020983

Mass 82 =A*0+C*0.001374+D*0.067454+E*1+G*0.0580293

Mass 83 =A*0+C*0+D*0.001374+E*0.067454+G*0.272297

Mass 84 =A*0+C*0+D*0+E*0.001374+G*1

Mass 85 =A*0+C*0+D*0+E*0+G*0.067454

mass 86 =A*0+C*0+D*0+E*0+G*0.001374

Appendix D. *Peak area of isotopic species and isotopic distuributions for benzene*

Mixtures	Peak Areas of each mass											
	75	76	77	78	79	80	81	82	83	84	85	86
^{13}C PG +^{12}C GL	361,116	977,733	3,901,388	13,420,030	2,153,576	1,769,109	2,501,942	646,016	884,674	1,515,953	3664.5	1283.2
^{13}C PG +^{12}C GL	571,630	1,393,334	5,403,225	18,547,444	3,935,736	3,228,668	3,735,227	1,925,167	1,843,697	2,413,619	1475.9	813.05
^{13}C PG +^{12}C GL	2,126,445	5,185,391	18,730,511	60,795,701	16,630,756	18,810,417	28,936,711	6,853,933	5,700,027	9,117,155	21405	187.06
^{12}C PG +^{13}C GL	279,123	754,169	2,834,884	8,856,527	3,504,094	6,221,683	9,562,598	7,478,018	11,278,918	23,869,045	782.78	201.26
^{12}C PG +^{13}C GL	281,528	626,112	2,479,970	8,645,263	3,295,764	4,217,860	4,395,573	4,498,383	8,313,757	19,566,672	2125.4	102.25
^{12}C PG +^{13}C GL	651,397	1,735,641	4,306,489	9,897,035	9,068,020	37,757,167	57,165,895	51,139,218	63,176,063	111,785,879	425.07	180.1

Samples	All ^{12} C benzene		$^{13}C_1$ benzene		$^{13}C_2$ benzene		$^{13}C_3$ benzene		$^{13}C_4$ benzene		$^{13}C_5$ benzene		All ^{13}C benzene	
	% of generation	S.D	% of generation	S.D	% of generation	S.D	% of generation	S.D	% of generation	S.D	% of generation	S.D	% of generation	S.D
^{13}C PG +^{12}C GL	54.5	6.9	6.3	1.2	7.4	1.4	16.6	6.1	3.3	1.6	3.3	0.9	8.6	0.8
^{12}C PG +^{13}C GL	11.5	2.3	2.9	1.3	5.0	0.3	12.1	5.0	7.9	1.7	8.9	1.0	51.6	3.7

Samples	All ^{12} C benzene		$^{13}C_2$ benzene		$^{13}C_3$ benzene		$^{13}C_4$ benzene		All ^{13}C benzene	
	% of generation	S.D	% of generation	S.D	% of generation	S.D	% of generation	S.D	% of generation	S.D
^{13}C PG +^{12}C GL	62.8	9.2	8.9	2.4	15.3	7.0	4.1	1.8	8.9	0.5
^{12}C PG +^{13}C GL	19.6	3.9	5.8	0.6	11.3	5.0	10.5	2.1	52.8	2.5

Appendix E. *Datum for the overdetermined least squares fits in MatLab for acetaldehyde*

Mass	Caliper Intensity	relative peak size
38	27	0.001306
39	0	0.000000
40	556	0.026901
41	2,199	0.106396
42	4,616	0.223340
43	12,848	0.621637
44	20,668	1.000000
45	436	0.021095
46	20	0.000968
47	0	0.000000
48	0	0.000000

Equations (A=mass 44, B=mass 45, C=mass 46)

mass 42 = A*0.223340+B*0.106396+C*0.026901

mass 43 = A*0.621637+B*0.223340+C*0.106396

mass 44 = A*1+B*0.621637+C*0.223340

mass 45 = A*0.021095+B*1+C*0.621637

mass 46 = A*0.000968+B*0.021095+C*1

mass 47 = A*0+B*0.000968+C*0.021095

mass 48 = A*0+B*0+C*0.000968

Mixture	Peak Areas (P.A)						
	Mass 42	Mass 43	Mass 44	Mass 45	Mass 46	Mass 47	Mass 47
^{13}C PG +^{12}C GL	51,327,179	144,779,609	246,985,247	79,627,173	113,934,987	646,475	190,615
^{13}C PG +^{12}C GL	55,185,434	156,357,283	269,383,368	107,271,376	161,407,148	1,027,299	278,122
^{13}C PG +^{12}C GL	67,337,249	186,482,327	320,506,754	116,295,551	171,842,227	1,219,838	300,765
^{12}C PG +^{13}C GL	35,487,866	93,671,872	164,839,076	143,365,877	228,532,826	1,692,917	445,522
^{12}C PG +^{13}C GL	46,235,066	132,748,068	229,106,321	153,183,350	243,541,990	2,032,965	470,610
^{12}C PG +^{13}C GL	51,577,711	129,438,612	223,362,209	183,929,987	294,247,154	2,701,622	620,909

Appendix F. *Datum for the overdetermined least squares fits in MATLAB for 2,3,-butanedione (diacetyl)*

Mass	Caliper Intensity	relative peak size
76	14	0.000349
77	14	0.000349
78	0	0.000000
79	20	0.000499
80	17	0.000424
81	21	0.000524
82	18	0.000449
83	14	0.000349
84	0	0.000000
85	19	0.000474
86	40112	1.000000
87	1753	0.043703
88	166	0.004138
89	17	0.000424
90	14	0.000349
91	0	0.000000
92	16	0.000399
93	0	0.000000

Equations (A=mass 86, B=mass 87, C=mass 88, D=mass 89, E=mass 90)

mass 83 = A*0.000349+B*0.000449+C*0.000524+D*0.000424+E*0.000499

mass 84 = A*0.0+B*0.000349+C*0.000449+D*0.000524+E*0.000424

mass 85 = A*0.000474+B*0.0+C*0.000349+D*0.000449+E*0.000524

mass 86 = A*1+B*0.000474+C*0.0+D*0.000349+E*0.000449

mass 87 = A*0.043703+B*1+C*0.000474+D*0.0+E*0.000349

mass 88 = A*0.004138+B*0.043703+C*1+D*0.000474+E*0.0

mass 89 = A*0.000424+B*0.004138+C*0.043703+D*1+E*0.000474

mass 90 = A*0.00349+B*0.000424+C*0.004138+D*0.043703+E*1

mass 91 = A*0.0+B*0.000349+C*0.000424+D*0.004138+E*0.043703

mass 92 = A*0.000399+B*0.0+C*0.000349+D*0.000424+E*0.004138

Appendix G. *Peak area of isotopic species for diacetyl*

Mixtures	Peak Areas									
	mass 83	mass 84	mass 85	mass 86	mass 87	mass 88	mass 89	mass 90	mass 91	mass 92
^{13}C PG +^{12}C GL	9,162	7,501	8,368	29,854,879	3,642,488	3,132,801	9,048,617	5,819,396	29,421	25,945
^{13}C PG +^{12}C GL	21,723	26,732	21,509	82,712,228	11,755,964	11,580,291	33,066,125	25,113,352	213,566	86,684
^{13}C PG +^{12}C GL	27,572	34,265	29,671	94,073,378	12,615,711	9,139,894	25,495,335	14,016,456	157,932	44,400
^{12}C PG +^{13}C GL	16,270	10,567	19,849	3,229,673	12,324,842	4,449,523	6,124,050	71,508,816	214,017	274,348
^{12}C PG +^{13}C GL	17,026	14,124	21,280	12,227,942	40,631,391	13,212,878	15,345,144	147,134,153	550,554	615,578
^{12}C PG +^{13}C GL	34,003	28,200	24,832	12,632,758	40,869,226	10,650,392	23,387,034	162,223,548	716,308	679,489

Appendix H. *Datum for the overdetermined least squares fits in MATLAB for toluene*

Mass	Caliper Intensity	relative peak size
78	1,034	0.001530
79	67	0.000099
80	35	0.000052
81	27	0.000040
82	36	0.000053
83	18	0.000027
84	2,720	0.004024
85	6,309	0.009333
86	7,797	0.011534
87	3,761	0.005564
88	653	0.000966
89	30,687	0.045396
90	12,367	0.018295
91	675,990	1.000000
92	381,783	0.564776
93	27,799	0.041123
94	647	0.000957
95	0	0.000000
96	0	0.000000
97	0	0.000000
98	33	0.000049
99	0	0
100	0	0
101	1	1.479E-06
102	0	0

Equations (A=mass 91, B= mass 92, D=mass 94, E=mass 95, G=mass 97, H=mass 98)

mass 85 = A*0.009333+B*0.004024+D*0.000053+E*0.000040+G*0.000099+H*0.001530

mass 86 = A*0.011534+B*0.009333++D*0.000027+E*0.000053++G*0.000052+H*0.000099

mass 87 = A*0.005564+B*0.011534++D*0.004024+E*0.000027++G*0.000040+H*0.000052

mass 88 = A*0.000966+B*0.005564+D*0.009333+E*0.004024+G*0.000053+H*0.000040

mass 89 = A*0.045396+B*0.000966+D*0.011534+E*0.009333+G*0.000027+H*0.000053

mass 90 = A*0.018295+B*0.045396+D*0.005564+E*0.011534+G*0.004024+H*0.000027

mass 91 = A*1+B*0.018295+D*0.000966+E*0.005564+G*0.009333+H*0.004024

mass 92 = A*0.564776+B*1+D*0.045396+E*0.000966+G*0.011534+H*0.009333

mass 93 = A*0.041123+B*0.564776+D*0.018295+E*0.045396+G*0.005564+H*0.011534

mass 94 = A*0.000957+B*0.041123+D*1+E*0.018295+G*0.000966+H*0.005564

mass 95 = A*0+B*0.000957+D*0.564776+E*1+G*0.045396+H*0.000966

mass 96 = A*0+B*0+D*0.041123+E*0.564776+G*0.018295+H*0.045396

mass 97 = A*0+B*0+D*0.000957+E*0.041123+G*1+H*0.018295

mass 98 = A*0.000049+B*0+D*0+E*0.000957+G*0.564776+H*1

mass 99 = A*0+B*0.000049+D*0+E*0+G*0.041123+H*0.564776

mass 100 = A*0+B*0++D*0+E*0+G*0.000957+H*0.041123

mass 101 = A*0+B*0+D*0.000049+E*0+G*0+H*0.000957

Appendix I. *Peak area of isotopicically labeled Toluene*

Mixtures	Peak Areas																
	85	86	87	88	89	90	91	92	93	94	95	96	97	98	99	100	101
^{13}C PG +GL	1.E+05	2.E+05	7.E+04	1.E+05	4.E+05	2.E+05	9.E+06	5.E+06	1.E+06	1.E+06	9.E+05	5.E+05	4.E+05	8.E+05	3.E+05	3.E+03	0.E+00
^{13}C PG +GL	2.E+05	3.E+05	1.E+05	3.E+05	6.E+05	3.E+05	1.E+07	7.E+06	2.E+06	2.E+06	2.E+06	1.E+06	9.E+05	2.E+06	6.E+05	5.E+03	1.E+01
^{13}C PG +GL	4.E+05	5.E+05	5.E+05	4.E+05	2.E+06	8.E+05	3.E+07	2.E+07	8.E+06	1.E+07	8.E+06	4.E+06	3.E+06	5.E+06	2.E+06	8.E+03	5.E-01
PG+ ^{13}C GL	3.E+05	3.E+04	5.E+04	3.E+04	2.E+05	1.E+05	4.E+06	3.E+06	1.E+06	1.E+06	3.E+06	3.E+06	3.E+06	1.E+07	4.E+06	5.E+04	6.E+04
PG+ ^{13}C GL	7.E+05	3.E+04	8.E+04	3.E+05	2.E+05	1.E+05	5.E+06	3.E+06	2.E+06	1.E+06	2.E+06	3.E+06	3.E+06	2.E+07	7.E+06	1.E+05	1.E+05
PG+ ^{13}C GL	7.E+05	1.E+06	1.E+05	2.E+05	5.E+05	5.E+05	6.E+06	6.E+06	6.E+06	7.E+06	2.E+07	2.E+07	1.E+07	4.E+07	2.E+07	9.E+04	1.E+05

Appendix J. *Chemical Composition in Mixtures for K_p experiment.*

Volatile Compounds		Medium Volatile Compounds		Less volatile compounds	
Chemicals	Concentrations (μg/μL)	Chemicals	Concentrations (μg/μL)	Chemicals	Concentrations (μg/μL)
Acetone	0.01	Acetaldehyde	0.10	benzaldehyde	1.02
Benzene	0.01	Propanal	0.11	2,3-Dimethylpyrazine	1.24
Isobutyl acetate	0.01	3-Methyl-1-butanol	0.78	2,3,5-Trimethylpyrazine	1.18
Toluene	0.01	2,3-Butanedione	0.33	Benzaldehyde propylene glycol acetal	1.12
Ethyl butyrate	0.01	Hydroxyacetone	0.33	(+)-Aromadendrene	1.07
Ethylbenzene	0.01	2,3-Pentanedione	0.16	Benzyl alcohol	3.09
Isoamyl acetate	0.02	(Z)-3-Hexel-1-ol	1.27	2-Acetylpyrrole	2.17
p-Xylene	0.01			Maltol	7.79
Butyl butyrate	0.03			Menthol	2.06
p-Cymene	0.01			Methyl salicylate	1.21
Limonene	0.01			Ethyl maltol	7.72
				Cinnamaldehyde	2.38
				Cinnamyl alcohol	9.23
				Nicotine	4.10
				Methyl anthranilate	2.34
				Methyl cinnamate	2.57
				Vanillin	7.72
				Ethyl vanillin	6.2
				Coumarin	2.06

Appendix K. *Theoretical K_p vs. Experimental K_p*

chemicals	vapor pressure	log vapor pressure	Theoretical		Experimental	
			*K*p	log *K*p	*K*p	log *K*p
Acetaldehyde	1.19E+00	0.07	2.45E-10	-9.61	5.40E-10	-9.27
Propanal	4.17E-01	-0.38	6.98E-10	-9.16	8.14E-10	-9.09
Acetone	3.16E-01	-0.50	9.22E-10	-9.04	1.53E-10	-9.81
Benzene	1.25E-01	-0.90	1.67E-10	-9.78	6.52E-11	-10.19
2,3-butanedione (Diacetyl)	7.47E-02	-1.13	3.89E-09	-8.41	4.18E-09	-8.38
toluene	3.75E-02	-1.43	7.77E-09	-8.11	1.27E-10	-9.90
2,3-Pentanedione	2.63E-02	-1.58	1.11E-08	-7.96	1.84E-09	-8.73
isobutyl acetate	2.34E-02	-1.63	1.24E-08	-7.91	1.19E-10	-9.92
Ethyl butyrate	1.84E-02	-1.73	1.58E-08	-7.80	2.86E-10	-9.54
Butyl Butyrate	1.36E-02	-1.87	2.14E-08	-7.67	1.38E-09	-8.86
Ethylbenzene	1.26E-02	-1.90	2.30E-08	-7.64	2.06E-10	-9.69
p-Xylene	1.16E-02	-1.93	2.50E-08	-7.60	2.10E-10	-9.68
Hydroxyacetone	7.40E-03	-2.13	3.93E-08	-7.41	3.78E-09	-8.42
Isoamyl Acetate	7.37E-03	-2.13	3.95E-08	-7.40	6.45E-10	-9.19
2,3-Dimethylpyrazine	4.54E-03	-2.34	6.41E-08	-7.19	5.16E-08	-7.29
3-Methyl-1-butanol	3.12E-03	-2.51	9.33E-08	-7.03	1.98E-08	-7.70
Dipentene (Limonene)	2.61E-03	-2.58	1.12E-07	-6.95	2.53E-10	-9.60
2,3,5-Trimethylpyrazine	2.27E-03	-2.64	1.28E-07	-6.89	8.44E-08	-7.07
p-Cymene	1.97E-03	-2.70	1.47E-07	-6.83	6.15E-10	-9.21
Benzaldehyde	1.69E-03	-2.77	1.72E-07	-6.77	2.21E-08	-7.66
(Z)-3-Hexen-1-ol	1.24E-03	-2.91	2.35E-07	-6.63	4.73E-08	-7.33
Menthol	9.66E-04	-3.02	3.01E-07	-6.52	2.86E-07	-6.54
2-Acetylpyrrole	1.96E-04	-3.71	1.48E-06	-5.83	1.21E-06	-5.92
Benzyl alcohol	1.24E-04	-3.91	2.35E-06	-5.63	9.04E-07	-6.04
Benzaldehyde propylene glycol acetal	6.97E-05	-4.16	4.17E-06	-5.38	1.38E-07	-6.86
Nicotine	5.00E-05	-4.30	5.82E-06	-5.23	1.37E-05	-4.86
Nicotine with NH3					1.38E-07	-6.86
Methyl salicylate	4.51E-05	-4.35	6.45E-06	-5.19	8.13E-08	-7.09
Cinnamaldehyde	3.95E-05	-4.40	7.37E-06	-5.13	7.34E-07	-6.13
Methyl anthranilate	3.57E-05	-4.45	8.16E-06	-5.09	1.70E-06	-5.77
(+)-Aromadendrene	3.03E-05	-4.52	9.62E-06	-5.02	3.24E-08	-7.49
Cinnamyl alcohol	1.50E-05	-4.82	1.94E-05	-4.71	1.31E-05	-4.88
Methyl cinnamate	1.27E-05	-4.90	2.29E-05	-4.64	5.41E-07	-6.27
Maltol	3.89E-06	-5.41	7.47E-05	-4.13	1.81E-05	-4.74
Coumarin	9.04E-07	-6.04	3.22E-04	-3.49	6.83E-06	-5.17
Ethyl maltol	3.00E-07	-6.52	9.70E-04	-3.01	1.69E-05	-4.77
Vanillin	9.32E-08	-7.03	3.12E-03	-2.51	1.98E-04	-3.70
Ethyl vanillin	8.45E-09	-8.07	3.44E-02	-1.46	1.60E-04	-3.80

Appendix L. *Theoretical and Experimental* $f_{g,i}$ *vs. log* $p^{\circ}_{L,i}$

chemicals	log $p^{\circ}_{L,i}$	Theoretical $f_{g,i}$	Experimental $f_{g,i}$
Acetaldehyde	0.1	9.48E-01	8.92E-01
Propanal	-0.4	8.65E-01	8.46E-01
Acetone	-0.5	8.29E-01	9.67E-01
Benzene	-0.9	9.64E-01	9.86E-01
2,3-butanedione	-1.1	5.34E-01	5.17E-01
toluene	-1.4	3.65E-01	9.72E-01
2,3-Pentanedione	-1.6	2.88E-01	7.08E-01
isobutyl acetate	-1.6	2.64E-01	9.74E-01
Ethyl butyrate	-1.7	2.20E-01	9.40E-01
Butyl Butyrate	-1.9	1.73E-01	7.65E-01
Ethylbenzene	-1.9	1.62E-01	9.56E-01
p-Xylene	-1.9	1.51E-01	9.55E-01
Hydroxyacetone	-2.1	1.02E-01	5.42E-01
Isoamyl Acetate	-2.1	1.02E-01	8.74E-01
2,3-Dimethylpyrazine	-2.3	6.51E-02	7.96E-02
3-Methyl-1-butanol	-2.5	4.57E-02	1.84E-01
Dipentene (Limonene)	-2.6	3.84E-02	9.46E-01
2,3,5-Trimethylpyrazine	-2.6	3.36E-02	5.03E-02
p-Cymene	-2.7	2.94E-02	8.79E-01
Benzaldehyde	-2.8	2.53E-02	1.68E-01
(Z)-3-Hexen-1-ol	-2.9	1.86E-02	8.63E-02
Menthol	-3.0	1.46E-02	1.54E-02
2-Acetylpyrrole	-3.7	3.01E-03	3.69E-03
Benzyl alcohol	-3.9	1.89E-03	4.92E-03
Benzaldehyde propylene glycol acetal	-4.2	1.07E-03	3.15E-02
Nicotine	-4.3	7.67E-04	1.04E-03
Nicotine + NH3			3.26E-04
Methyl salicylate	-4.3	6.92E-04	5.21E-02
Cinnamaldehyde	-4.4	6.05E-04	6.05E-03
Methyl anthranilate	-4.4	5.47E-04	2.62E-03
(+)-Aromadendrene	-4.5	4.64E-04	1.21E-01
Cinnamyl alcohol	-4.8	2.30E-04	3.41E-04
Methyl cinnamate	-4.9	1.95E-04	8.19E-03
Maltol	-5.4	5.98E-05	2.46E-04
Coumarin	-6.0	1.39E-05	6.53E-04
Ethyl maltol	-6.5	4.60E-06	2.64E-04
Vanillin	-7.0	1.43E-06	2.26E-05
Ethyl vanillin	-8.1	1.30E-07	2.79E-05